

SUPPRESSIVE EFFECT OF CREPIDATIN ON STEMNESS OF LUNG CANCER CELLS



Miss Narumol Bhummaphan

A Dissertation Submitted in Partial Fulfillment of the Requirements  
for the Degree of Doctor of Philosophy in Biomedical Sciences

Inter-Department of Biomedical Sciences

Graduate School

Chulalongkorn University

Academic Year 2018

Copyright of Chulalongkorn University

ฤทธิ์ของสารเครพิดาตินในการยับยั้งการแสดงลักษณะของการเป็นเซลล์ต้นกำเนิดของเซลล์มะเร็ง  
ปอด



วิทยานิพนธ์นี้เป็นส่วนหนึ่งของการศึกษาตามหลักสูตรปริญญาวิทยาศาสตรดุษฎีบัณฑิต  
สาขาวิชาชีวเวชศาสตร์ สหสาขาวิชาชีวเวชศาสตร์  
บัณฑิตวิทยาลัย จุฬาลงกรณ์มหาวิทยาลัย  
ปีการศึกษา 2561  
ลิขสิทธิ์ของจุฬาลงกรณ์มหาวิทยาลัย

Thesis Title SUPPRESSIVE EFFECT OF CREPIDATIN ON STEMNESS OF  
LUNG CANCER CELLS  
By Miss Narumol Bhummaphan  
Field of Study Biomedical Sciences  
Thesis Advisor Associate Professor PITHI CHANVORACHOTE, Ph.D.  
Thesis Co Advisor Professor Regine Schneider-Stock, Ph.D.

---

Accepted by the Graduate School, Chulalongkorn University in Partial Fulfillment  
of the Requirement for the Doctor of Philosophy

..... Dean of the Graduate School  
( )

DISSERTATION COMMITTEE

..... Chairman  
(Professor APIWAT MUTIRANGURA, Ph.D.)

..... Thesis Advisor  
(Associate Professor PITHI CHANVORACHOTE, Ph.D.)

..... Thesis Co-Advisor  
(Professor Regine Schneider-Stock, Ph.D.)

..... Examiner  
(Assistant Professor TEWIN TENCOMNAO, Ph.D.)

..... Examiner  
(Assistant Professor CHATCHAI CHAOTHAM, Ph.D.)

..... External Examiner  
(Associate Professor Chanitra Thuwajit (Toraksa), Ph.D.)

นฤมล ภูมมาพันธุ์ : ฤทธิ์ของสารเครพิตาดินในการยับยั้งการแสดงลักษณะของการเป็นเซลล์ต้นกำเนิดของเซลล์มะเร็งปอด. ( SUPPRESSIVE EFFECT OF CREPIDATIN ON STEMNESS OF LUNG CANCER CELLS) อ.ที่ปรึกษาหลัก : รศ. ภก.ดร.ปิติ จันทร์วรโชติ, อ.ที่ปรึกษาร่วม : ศ. ดร.เรจิน่า ชไนเดอร์ สตีอก

เซลล์มะเร็งต้นกำเนิดถูกจัดว่าเป็นกลุ่มของเซลล์ที่พบได้น้อยในกลุ่มของมะเร็งแต่กลับเป็นกลุ่มที่ผลักดันให้เกิดการดำเนินการของมะเร็ง การกลูกลามของมะเร็งและการื้อยาของกลุ่มโรคมะเร็งหลายชนิด การศึกษาค้นคว้าสารกลุ่มใหม่ที่สามารถหยุดคุณลักษณะของการเป็นเนื้องอกและการเป็นเซลล์มะเร็งต้นกำเนิดได้ถือได้ว่าเป็นการพัฒนาที่ก้าวหน้าในการจำกัดการเกิดซ้ำของมะเร็ง งานวิจัยนี้แสดงให้เห็นฤทธิ์ของสารในกลุ่ม bibenzyl สองตัวที่แยกมาได้จาก *Dendrobium pulchellum* ที่มีความสามารถในการหยุดการดำเนินการของการเป็นเซลล์มะเร็งต้นกำเนิดทั้ง โครโซที่ออกซินและเครพิตาดิน แสดงการยับยั้งการแสดงออกของการเป็นเซลล์มะเร็งต้นกำเนิดโดยทำการศึกษาโดยใช้กลุ่มประชากรที่อุดมไปด้วยเซลล์มะเร็งต้นกำเนิดและการลดการเนื้องอกการเป็นมะเร็งต้นกำเนิด โดยทั้งโครโซที่ออกซินและเครพิตาดินต่างส่งผลกระทบต่อการแสดงออกของโปรตีนสำคัญที่เกี่ยวข้องกับการแสดงออกของการเป็นเซลล์มะเร็งต้นกำเนิด จากการศึกษาทดลองพบว่าโครโซที่ออกซินสามารถลดการทำงานของ Src/Akt signal และการลดระดับของโปรตีน Sox2 ที่เป็นตัวควบคุมเซลล์มะเร็งต้นกำเนิด โดยการค้นพบของเราในครั้งนี้ได้มีการกำหนดเป้าหมายใหม่ของสารโครโซที่ออกซินที่มีต่อเซลล์มะเร็งต้นกำเนิดโดยการควบคุมทาง Src / Akt และ Sox2 ซึ่งอาจนำไปใช้ในการรักษามะเร็งได้ ในเวลาเดียวกัน สารเครพิตาดินถูกพบว่ามีประสิทธิภาพสูงสุดในการฆ่าเซลล์มะเร็งปอดของมนุษย์ โดยสารเครพิตาดินถูกกำหนดให้เป็นยาเป้าหมายสำหรับเซลล์ต้นกำเนิดมะเร็งปอด เช่นเดียวกับโครโซที่ออกซิน เครพิตาดินก็สามารถลดการแสดงออกของการเป็นเซลล์มะเร็งต้นกำเนิดในกลุ่มประชากรที่อุดมไปด้วยเซลล์มะเร็งต้นกำเนิดโดยการทดสอบการเนื้องอกในการเกิดเซลล์มะเร็งต้นกำเนิดได้เมื่อเทียบกับยาซิสพลาติน โดยเครพิตาดินสามารถลดการกำเนิดของเซลล์มะเร็งต้นกำเนิดในปอดได้อย่างเห็นได้ชัดโดยทำการวิเคราะห์จากโปรตีนที่บ่งชี้การเป็นเซลล์มะเร็งต้นกำเนิดหลายชนิด นอกจากนี้เครพิตาดินยังสามารถยับยั้งการเปลี่ยนแปลงจาก epithelial ให้กลายเป็นมีเซนไคม์เซลล์ได้และยับยั้งการรุกรานของเซลล์มะเร็งต้นกำเนิด โดยสารนี้ยังยับยั้งการเป็นเซลล์ต้นกำเนิดในเซลล์มะเร็งปอดที่ได้มาจากมนุษย์ นอกจากนี้เรายังได้ยืนยันผลของเครพิตาดินที่มีผลต่อเซลล์ต้นกำเนิดที่ก้าวร้าวเช่นเดียวกับที่รุกรานในเซลล์มะเร็งปอดซึ่งได้รับการรักษาจากเครพิตาดินและซิสพลาติน ซึ่งถูกวิเคราะห์โดยการใช้ chorioallantoic membrane (CAM) โดยผลการทดลองได้บ่งชี้ว่า สารเครพิตาดินนั้นสามารถลดขนาดของก้อนมะเร็งปอดได้อย่างมีนัยสำคัญเมื่อเทียบกับกลุ่มที่ได้รับการรักษาด้วยซิสพลาติน การค้นพบครั้งนี้ถือว่าเป็นค้นพบทางเภสัชวิทยาที่สำคัญในการที่ศึกษาสร้างกลไกพื้นฐานของสารโครโซที่ออกซินและเครพิตาดินที่ต่อผลการควบคุมการแสดงฟีโนไทป์ที่มีลักษณะของการเป็นเซลล์มะเร็งต้นกำเนิด ดังนั้นผลจากการศึกษาครั้งนี้จะให้ข้อมูลเชิงลึกที่สำคัญที่ช่วยในการตรวจสอบและพัฒนาสารจากธรรมชาติทั้งสองชนิดคือโครโซที่ออกซินและเครพิตาดินเพื่อเป็นยาเป้าหมายต่อการรักษาโรคมะเร็ง

จุฬาลงกรณ์มหาวิทยาลัย  
CHULALONGKORN UNIVERSITY

สาขาวิชา ชีวเวชศาสตร์

ปีการศึกษา 2561

ลายมือชื่อนิสิต .....

ลายมือชื่อ อ.ที่ปรึกษาหลัก .....

ลายมือชื่อ อ.ที่ปรึกษาร่วม .....

# # 5787852820 : MAJOR BIOMEDICAL SCIENCES

KEYWORD: lung cancer, cancer stem cells, chrysotoxine, crepidatin, CSC-rich population, epithelial to mesenchymal transition

Narumol Bhummaphan : SUPPRESSIVE EFFECT OF CREPIDATIN ON STEMNESS OF LUNG CANCER CELLS. Advisor: Assoc. Prof. PITHI CHANVORACHOTE, Ph.D. Co-advisor: Prof. Regine Schneider-Stock, Ph.D.

Cancer stem cells (CSCs) have been perceived as rare populations driving cancer progression, metastasis, and drug resistance in leading cancers. The discovery of new compounds that attenuates CSCs' properties is crucial for enabling advances in novel therapeutics to limit recurrence. We have reported the CSC-suppressing activity of chrysotoxine and crepidatin, two bibenzyl compounds isolated from *Dendrobium pulchellum*. Both chrysotoxine and crepidatin displayed suppression in CSC-like phenotypes, as determined in CSC-rich populations and primary CSCs in 3D culture and extreme limiting dilution assay. Individual treatment of chrysotoxine and crepidatin also affected the expression of CSC markers and associated proteins concomitantly decreased known CSCs markers. Importantly, chrysotoxine was shown to suppress active Src/Akt signal and intern depleted Sox2-mediated CSC. Our findings indicate a novel CSC-targeted role of chrysotoxine and its regulation by Src/Akt and Sox2, which may be exploited for the cancer treatment. At the same time, crepidatin showed the highest potency to kill human lung cancer cells. Crepidatin was accomplished as a drug targeting model for lung cancer stem cells. Crepidatin also suppressed CSC-like phenotypes, as determined by CSC-rich populations in 3D culture, clonogenic assay and extreme limiting dilution assay, when compared to cisplatin. The treatment of crepidatin showed dramatic suppression in the CSCs in lung cancer cells, as verified by several CSC phenotype assessments and CSC markers. In addition, crepidatin also suppressed epithelial to mesenchymal transition (EMT) markers and inhibited migratory behavior of CSCs. Importantly, we confirmed the CSC-targeted activity of crepidatin in CSC-rich primary lung cancer cells. The compound dramatically inhibited the formation of tumor spheres of primary lung cancer cells. Finally, we confirmed the effect of crepidatin on the aggressive stem-like and invasive phenotype in lung cancer cells, where in vivo growth and aggressiveness of crepidatin and cisplatin treated cells were analyzed using the chorioallantoic membrane (CAM) assay. The results revealed that crepidatin significantly reduced tumor growth in lung cancer cells, when compared to nontreated cells, whereas the tumor sizes have been significantly increased in cisplatin treatment. These findings document a novel pharmacological action and establishes the underlying mechanism of chrysotoxine and crepidatin in negatively regulating CSC-like phenotypes and sensitizing resistant cancer cells. Therefore, the findings from this study would provide important insights that facilitate the further investigation and development of the two natural compounds, chrysotoxine and crepidatin, for CSC-targeted approaches.

Field of Study: Biomedical Sciences

Academic Year: 2018

Student's Signature .....

Advisor's Signature .....

Co-advisor's Signature .....

## ACKNOWLEDGEMENTS

This accomplishment could not be achieved without the great guidance and encouragement from my thesis advisor, committee members, academic staffs, my colleagues and my family.

I would like to express my deepest appreciation and special thanks to my thesis advisors, Associate Professor Dr. Pithi Chanvorachote, who not only carefully planned out and intensively advised me through my Ph.D. years, but also gave me the worth opportunity to study and developed the skill of thinking and knowledge. His guidance helped me in all the time of research and writing of this thesis. I could not have imagined having a better advisor and mentor for my Ph.D study. I also would like to express my sincere gratitude to co-advisor, Professor Regine Schneider - Stock who kindly gave me invaluable intellectual advices, encouragement and gave me an opportunity for expanding laboratory intellectual and skills.

I would like to acknowledge Professor Dr. Apiwat Mutirangura, Associate Professor Dr. Boonchoo Sritularak, Assistant Professor Dr. Chatchai Chaotham, Assistant Professor Dr. Varisa Pongrakhananon for their generous and invaluable help to complete my manuscript and dissertation. Furthermore, I would like to thanks to the committee members Assistant Professor Tewin Tencomnao and Associate Professor Chanitra Thuwajit for their help in improving and gave a valuable and insightful comments for my dissertation. I also would like to give special thanks to my laboratory members both in Thailand and in Germany for their assistance and making the tough working hours seemed easy. I would like to thank their beautiful friendships and I will keep our precious memories forever. My deepest gratitude goes to my dear family for love and support not only during my degree seeking, but throughout my life. Without their encouragement and understanding, I would not have finished this course.

This dissertation is dedicated to my parents for giving birth to me and supporting me spiritually throughout my life. and my sister for her continuous support and encouragement.

Finally, my gratefulness is expressed to Royal Golden Jubilee Ph.D. program (Grant No. PHD/0033/2558) for their grant support.

Narumol Bhummaphan

## TABLE OF CONTENTS

	Page
.....	iii
ABSTRACT (THAI).....	iii
.....	iv
ABSTRACT (ENGLISH).....	iv
ACKNOWLEDGEMENTS.....	v
TABLE OF CONTENTS.....	vi
LIST OF TABLES.....	x
LIST OF FIGURES.....	xiii
CHAPTER I INTRODUCTION.....	3
CHAPTER II LITERATURE REVIEW.....	7
1. Lung cancer.....	7
2. Cancer stem cells (CSCs).....	11
3. Characteristics of CSCs.....	12
4. Cancer stem cell markers.....	14
4.1 CD133.....	14
4.2 CD44.....	14
4.3 ABCG2.....	15
5. CSC transcription factors.....	17
5.1 Sox2.....	17
5.2 Oct4.....	17
5.3 Nanog.....	18

6. Epithelial-to-mesenchymal transition (EMT) .....	18
7. EMT markers .....	20
7.1 E-cadherin.....	20
7.2 Vimentin.....	21
7.3 Snail .....	21
7.4 Slug .....	21
8. The link between cancer stemness and EMT.....	22
9. Tyrosine kinase signaling pathways in CSCs .....	24
9.1 Epidermal growth factor receptor .....	24
9.2 Vascular endothelial growth factor (VEGF).....	25
9.3 Src kinase family.....	25
10. Dendrobium pulchellum.....	26
11. Chrysotoxine .....	27
12. Crepidatin .....	27
13. Chrysotobibenzyl.....	28
14. Cisplatin .....	29
CHAPTER III MATERIALS AND METHODS.....	31
1. Cell culture .....	31
2. Plant material.....	31
3. Cytotoxicity assay .....	32
4. Nuclear staining assay.....	33
5. Wound healing assay .....	33
6. Spheroids formation assay.....	34
7. Extreme limiting dilution assay (ELDA).....	34



8. Water-soluble tetrazolium salt (WST) assay.....	35
9. Western blot analysis.....	35
10. Clonogenic assay.....	36
11. 3D-CSC migration assay .....	37
12. NanoString nCounter Gene Expression Assay .....	37
13. Chick chorioallantoic membrane (CAM) assay.....	38
14. Enriched primary non-small cell lung cancer stem cells assay.....	38
15. Statistical analysis.....	39
CHAPTER IV RESULTS.....	44
1. Cytotoxicity analysis.....	44
1.1 Effect of chrysotoxine, crepidatin, and chrysotobibenzyl on human lung cancer and normal cells.....	44
2. The effects of chrysotoxine on the stem cell-like characteristics of lung cancer cells. 61	
3. The effects of chrysotoxine on the stem cell markers of lung cancer cells. ....	70
4. The effects of chrysotoxine on Sox2 via Src-Akt signaling cascade in lung cancer cells.....	72
5. The effect of chrysotoxine on epithelial-mesenchymal transition (EMT) in lung cancer cells.....	74
6. Cytotoxic effect of crepidatin on human lung cancer cells.....	77
7. The effects of crepidatin on the stem cell-like characteristics of lung cancer cells. 79	
8. The effects of crepidatin on the stem cell-like characteristics of lung cancer cells. 87	
9. The effect of crepidatin on apoptosis in lung cancer cells comparing to cisplatin.....	90

10. The effect of crepidatin and cisplatin on CSC-like phenotype on lung cancer cells. ....	92
11. The effects of crepidatin and cisplatin on the stem cell markers of lung cancer cells. 97	
12. The effects of crepidatin on the stem cell migratory behavior of lung cancer cells. 100	
13. The effects of crepidatin on mRNA expression profile which targeted to CSC-like phenotypes in lung cancer cells.....	103
14. The effect of crepidatin on tumor growth and angiogenesis in vivo using chick chorioallantoic membrane (CAM) assay.....	108
15. The effect of crepidatin on primary human lung cancer cells. ....	111
16. The effect of crepidatin on the induction of CSC-induced apoptosis and sensitization of chemotherapy-induced apoptosis in human lung cancer cells. ....	113
CHAPTER V DISCUSSION AND CONCLUSION.....	115
APPENDIX TABLE OF EXPERIMENTAL RESULTS.....	132
REFERENCES.....	157
VITA.....	176

## LIST OF TABLES

	Page
Table 1 Statistics of the top three leading cancer type within the past 20 years in U.S. male. ....	9
Table 2 Statistics of the top three leading cancer type within the past 20 years in U.S. male. ....	10
Table 3 CSC markers for distinct solid tumor types .....	16
Table 4 IC <sub>50</sub> of chrysotoxine, crepidatin, and chrysotobibenzyl on human lung cancer H460 and H23 and human normal keratinocyte HaCaT cells.....	50
Table 5 Dysregulated genes in H460 treated with crepidatin 24 h compared to control cells.....	107
Table 6 Cytotoxicity of chrysotoxine on H460 cells .....	132
Table 7 Cytotoxicity of chrysotoxine on H23 cells .....	132
Table 8 Cytotoxicity of chrysotoxine on HaCaT cells.....	133
Table 9 Cytotoxicity of crepidatin on H460 cells .....	133
Table 10 Cytotoxicity of crepidatin on H23 cells.....	134
Table 11 Cytotoxicity of crepidatin on HaCaT cells.....	134
Table 12 Cytotoxicity of chrysotobibenzyl on H460 cells.....	135
Table 13 Cytotoxicity of chrysotobibenzyl on H23 cells.....	135
Table 14 Cytotoxicity of chrysotobibenzyl on HaCaT cells .....	136
Table 15 The effect of chrysotoxine exposure on H460 cell migration .....	136
Table 16 The effect of crepidatin exposure on H460 cell migration .....	137
Table 17 The effect of chrysotobibenzyl exposure on H460 cell migration .....	138
Table 18 The effect of chrysotoxine suppresses on H460 CSC-rich population .....	139

Table 19 The effect of chrysotoxine suppresses on H23 CSC-rich population.....	140
Table 20 Cytotoxicity of chrysotoxine on H460 CSC-rich population .....	141
Table 21 Cytotoxicity of chrysotoxine on H23 CSC-rich population .....	141
Table 22 The effect of chrysotoxine on CSC markers in H460 cells .....	142
Table 23 The effect of chrysotoxine on CSC markers in H23 cells .....	142
Table 24 The effect of chrysotoxine on Src/Akt/Sox2 regulating mechanism in H460 cells .....	143
Table 25 The effect of chrysotoxine on Src/Akt/Sox2 regulating mechanism in H23 cells .....	143
Table 26 The effect of chrysotoxine on EMT markers in H460 cells .....	144
Table 27 Cytotoxicity of crepidatin on H460 cells .....	144
Table 28 Cytotoxicity of crepidatin on H23 cells .....	145
Table 29 Cytotoxicity of crepidatin on H292 cells .....	145
Table 30 Cytotoxicity of crepidatin on A549 cells .....	146
Table 31 The effect of crepidatin suppresses on H460 CSC-rich population.....	147
Table 32 The effect of crepidatin suppresses on A549 CSC-rich population.....	148
Table 33 Cytotoxicity of crepidatin on H460 CSC-rich population .....	149
Table 34 Cytotoxicity of crepidatin on A549 CSC-rich population .....	149
Table 35 The effect of crepidatin on CSC markers in H460 cells .....	150
Table 36 The effect of crepidatin on CSC markers in A549 cells .....	150
Table 37 The effect of crepidatin on EMT markers in H460 cells .....	151
Table 38 Cytotoxicity of cisplatin on H460 cells .....	151
Table 39 Cytotoxicity of cisplatin on A549 cells .....	152
Table 40 Effect of crepidatin suppression colony formation in H460 by clonogenic assay .....	152

Table 41 Effect of cisplatin suppression colony formation in H460 by clonogenic assay.....	152
Table 42 Effect of crepidatin suppression colony formation in A549 by clonogenic assay.....	153
Table 43 Effect of cisplatin suppression colony formation in A549 by clonogenic assay.....	153
Table 44 Effect of crepidatin on stem cell 3D-migration in H460 cells.....	154
Table 45 Effect of crepidatin on stem cell 3D-migration in A549 cells.....	155
Table 46 Cytotoxicity in combination treatment in H460 cells.....	156
Table 47 Cytotoxicity in combination treatment in A549 cells.....	156



## LIST OF FIGURES

	Page
Figure 1 Self-renewal characteristic of CSCs modified from <a href="http://www.wikiwand.com">http://www.wikiwand.com</a> by Bhummaphan N. ....	13
Figure 2 Chemotherapeutic resistance of CSCs modified from (Baccelli & Trumpp, 2012) by Bhummaphan N. ....	13
Figure 3 Basics of epithelial-mesenchymal transition (EMT) and EMT markers, modified from (Angadi & Kale, 2015) by Bhummaphan N. ....	20
Figure 4 The cancer stem cells metastatic cascades modified from (Chaffer & Weinberg, 2011) by Bhummaphan N. ....	23
Figure 5 Chemical structure of chrysotoxine modified from (Chanvorachote et al., 2013) by Narumol N. ....	27
Figure 6 Chemical structure of crepidatin modified from (Chanvorachote et al., 2013) by Narumol N. ....	28
Figure 7 Chemical structure of chrysotobibenzyl modified from (Chanvorachote et al., 2013) by Narumol N. ....	29
Figure 8 Chemical structure of Cisplatin modified from <a href="https://biology.stackexchange.com">https://biology.stackexchange.com</a> by Bhummaphan N. ....	30
Figure 9 Cytotoxic effect of chrysotoxine on human lung cancer H460 and H23 cells. ....	46
Figure 10 Cytotoxic effect of crepidatin on human lung cancer H460 and H23 cells. ....	47
Figure 11 Cytotoxic effect of chrysotobibenzyl on human lung cancer H460 and H23 cells. ....	48
Figure 12 Cytotoxic effect of chrysotoxine, crepidatin, and chrysotobibenzyl on human normal keratinocyte HaCaT cells. ....	50
Figure 13 Effect of chrysotoxine on apoptotic and necrotic cell death. ....	52

Figure 14 Effect of crepidatin on apoptotic and necrotic cell death.....	54
Figure 15 Effect of chrysotobibenzyl on apoptotic and necrotic cell death.....	55
Figure 16 Effect of chrysotoxine, crepidatin, and chrysotobibenzyl on lung cancer cell migration.....	60
Figure 17 The effect of chrysotoxine suppresses CSC-like phenotypes in CSC-rich population.....	65
Figure 18 The effect of chrysotoxine suppresses CSC-like phenotypes in CSC-rich population.....	67
Figure 19 The effect of chrysotoxine suppresses viability in CSC-rich population.....	68
Figure 20 The effect of chrysotoxine on the capability for generating spheroids.....	70
Figure 21 Effect of chrysotoxine on CSC markers in H460 and H23 cells. ....	71
Figure 22 Effect of chrysotoxine on Src/Akt/Sox2 mechanism in H460 and H23 cells. ....	74
Figure 23 Effect of chrysotoxine on EMT markers. ....	76
Figure 24 Cytotoxic effect of crepidatin on various human lung cancer.....	79
Figure 25 The effect of crepidatin suppresses CSC-like phenotypes in CSC-rich population.....	82
Figure 26 The effect of crepidatin suppresses CSC-like phenotypes in CSC-rich population.....	84
Figure 27 The effect of crepidatin suppresses viability in CSC-rich population.....	85
Figure 28 The effect of crepidatin on the capability for generating spheroids. ....	87
Figure 29 Effect of crepidatin on CSC markers in H460 and A549 cells. ....	88
Figure 30 Effect of crepidatin on EMT markers. ....	89
Figure 31 Cytotoxic effect of cisplatin on human lung cancer.....	91
Figure 32 Effect of crepidatin and cisplatin on apoptotic markers on human lung cancer H460 and A549 cells.....	92

Figure 33 Effect of crepidatin suppresses CSC-like phenotypes in H460 cells.....	94
Figure 34 Effect of crepidatin suppresses CSC-like phenotypes in A549 cells.....	95
Figure 35 The effect of crepidatin and cisplatin on the capability for generating spheroids.....	96
Figure 36 Effect of crepidatin and cisplatin on CSC markers on human lung cancer H460 and A549 cells.....	98
Figure 37 Effect of crepidatin and cisplatin on EMT markers on human lung cancer H460 and A549 cells.....	99
Figure 38 Effects of crepidatin on the stem cell migratory behavior of lung cancer cells.....	101
Figure 39 Effects of crepidatin on the stem cell migratory behavior of lung cancer cells.....	102
Figure 40 Transcriptional analysis revealed different expression profile in crepidatin and cisplatin treated in H460 cells.....	107
Figure 41 In vivo growth and aggressiveness of crepidatin and cisplatin treated cells in H460 and A549 compared to control in the chorioallantoic membrane (CAM) xenograft assay.....	111
Figure 42 The effect of crepidatin on enriched primary human lung CSC.....	112
Figure 43 Cytotoxic effect of crepidatin in combination treatment with cisplatin on human lung cancer H460 and A549 cells.....	114
Figure 44 Schematic diagram illustrates the effect of chrysotoxine and crepidatin in negatively regulating CSC-like phenotypes in inhibiting EMT and sensitizing resistant cancer cells to apoptosis.....	131



## LIST OF ABBREVIATIONS

ABCG2, ATP-binding cassette sub family G2

Akt, protein kinase B

ALDH, Aldehyde dehydrogenase-1

CAM, chick chorioallantoic membrane

CSCs, cancer stem cells

DMSO, dimethylsulfoxide

EGFR, Epidermal growth factor receptor

ELDA, extreme limiting dilution assay

EMT, epithelial to mesenchymal transition

FBS, fetal bovine serum

GAPDH, Glyceraldehyde 3-phosphate dehydrogenase

HRP, horseradish peroxidase

MAPK, Mitogen-activated protein kinase

MTT, 3-(4, 5-dimethylthiazol-2-yl)-2, 5-diphenyltetrazolium bromide

NSCLC, non-small cell lung cancer

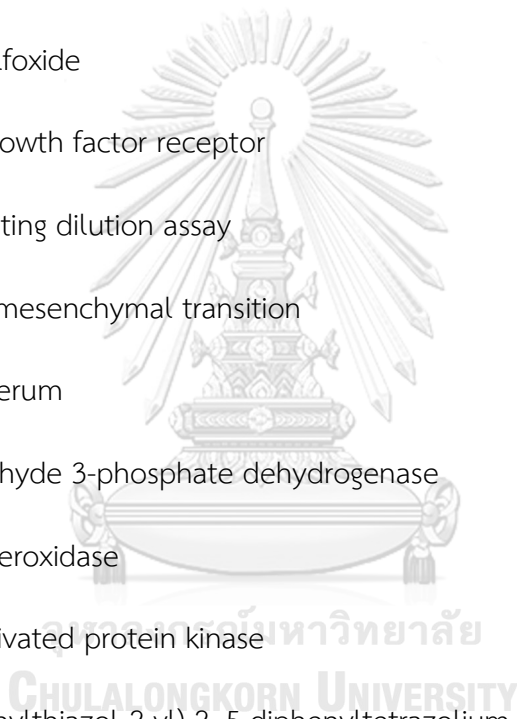
PBS, phosphate-buffered saline

PI, propidium iodide

ROS, reactive oxygen species

SCID, severe combined immune-deficient

SCLC, small cell lung cancer



TCF/LEF, T-cell factor/lymphoid enhancing factor

TF, transcription factors

VEGF, vascular endothelial growth factor

WST1, water soluble tetrazolium 1.



## CHAPTER I

### INTRODUCTION

Recently, researches in the field of cancer have shown that within the malignant tumor as well as in the blood of advanced stage cancer patients, there are special cancer cells called cancer stem cells (CSCs) (Bao, Ahmad, Azmi, Ali, & Sarkar, 2013; Vinogradov & Wei, 2012). CSC was first discovered in 1997 by which isolated and identified the subpopulation of cancer having high tumorigenic potential and stem-cell like phenotypes (Bonnet & Dick, 1997). CSCs may generate tumors through the stem cell processes of self-renewal and differentiation into multiple cell types (Lobo, Shimono, Qian, & Clarke, 2007; Ricci-Vitiani et al., 2007; S. K. Singh et al., 2003). This subpopulation is distinguished from other cancer populations by specific CSC markers such as cell surface protein CD133 (Bao et al., 2013; Li, 2013; Rappa, Fodstad, & Lorico, 2008). Such cells are proposed to persist in tumors as a distinct population and cause relapse and metastasis by giving rise to new tumors (Hanahan & Weinberg, 2011).

Moreover, researchers accepted that these CSCs account for most aggressive behaviors of the disease including chemotherapeutic resistance, metastasis, and cancer relapse (Hanahan & Weinberg, 2011; Y. Zhang et al., 2012). CSCs have been shown to maintain their stemness through the sustained level of several transcription factors as well as the stem cell-related signals (Han, Shi, Gong, Zhang, & Sun, 2013; A.

Liu, Yu, & Liu, 2013). CSCs have been identified in a wide variety of cancers. Recent studies have shown that the CSCs presenting in the lung cancer may facilitate the malignancy and progression of the disease. Lung cancer has been recognised among the top most common cancers and account for high rate of cancer-related death (Alamgeer, Peacock, Matsui, Ganju, & Watkins, 2013; Eramo, Haas, & De Maria, 2010; O'Brien, Pollett, Gallinger, & Dick, 2007; Ricci-Vitiani et al., 2007). Interestingly, there is strong evidence showing that aggressive phenotypes of lung cancer depend on the presence of CSCs.

Regarding controlling mechanism for CSCs. The regulatory pathways of CSC are found to be due to the function pluripotent transcription factors including Sox2, Oct4, and Nanog (Jeter et al., 2011; Kashyap et al., 2009; Pan, Chang, Scholer, & Pei, 2002; Shi & Jin, 2010). These genes have been found to be linked many core transcriptional networks which responsible for the regulation of stem cell self-renewal and pluripotency. Among the stemness transcription factors, Sox2 is suggested to be the most important transcription factor to controlling CSC characteristics. Sox2 has been identified as a key regulator of the self-renewal capability of CSCs (Herreros-Villanueva et al., 2013; S. Singh et al., 2012). Sox2 is overexpress in various cancers and associate with malignant progression and poor prognosis. Especially, Sox2 is a pivotal prognostic marker with correlated to clinical-pathologic characteristics in lung cancers (Karachaliou, Rosell, & Viteri, 2013; Lundberg et al., 2016; Weina & Utikal, 2014). Moreover, Sox2 and Oct4 cooperative to activate gene transcription by binding at non-

palindromic sequence and promote to the activating of regions of cancer stem cell related genes (Boumahdi et al., 2014; A. Liu et al., 2013; Pan et al., 2002; Shi & Jin, 2010; S. Singh et al., 2012).

Moreover, epithelial to mesenchymal transition (EMT) is a process which epithelial cells lose their epithelial phenotype to become mesenchymal phenotype and has been closely associated with acquisition of aggressive behaviors of cancer cells (Luo et al., 2013). EMT is controlled by a set of transcription factors (TF) including SNAI1/Snail1, SNAI2/Snail2 (also called as Slug), KLF8, and Twist. Importantly, molecular links between EMT-TF and self-renewal capacity of CSC suggesting that EMT could be orchestrate with CSC phenotype to play critical role in metastatic cascade (Kalluri & Weinberg, 2009; Y. Wang, Shi, Chai, Ying, & Zhou, 2013). In addition, some evidence suggests that cells that undergo EMT gain stem cell-like properties, thus giving rise CSCs. EMT facilitates the generation of CSCs with the mesenchymal traits required for dissemination as well as self-renewal properties needed for initiating secondary tumors (Ishiwata, 2016; C.-Y. Liu, Lin, Tang, & Wang, 2015; Voulgari & Pintzas, 2009).

The concept that CSCs is a major factor driving cancer cell aggressiveness and metastasis has led to investigations of the novel therapeutic strategies as well as drugs targeting the CSCs.

The compounds isolated from the Thai orchids have been shown their cytotoxicity in various cancers including lung, liver, stomach and colon cancers.

Accumulative evidences have proved that orchids are the promising source of bioactive compounds for anti-cancer drug discovery and development. Chrysotoxine and crepidatin, a bibenzyl compound were found in *Dendrobium pulchellum* (Li et al., 2013). These compounds were gained increase interest due to their promising pharmacological activities. In previous studies revealed that chrysotoxine had potential as neuroprotective compounds with antioxidant activity which can be used in the treatment of Parkinson's disease (J.-X. Song et al., 2012; J. X. Song et al., 2010). Furthermore, both chrysotoxine and crepidatin increase antioxidant activity, crepidatin had found to induce apoptosis through the direct induction of intracellular ROS, attenuate growth of lung cancer cells in anchorage-independent condition and facilitate anoikis. In addition, both chrysotoxine and crepidatin also were found to be inhibited metastasis in lung cancer; however, the mechanism is still unknown (Chanvorachote et al., 2013; Chaotham, Pongrakhananon, Sritularak, & Chanvorachote, 2014). Since the effect of chrysotoxine and crepidatin on CSC regulation had not been clarified, the present study aimed to investigate the effect of chrysotoxine and crepidatin on CSC phenotypes as well as underlying molecular mechanism. The findings from this study would provide the important insights that facilitate the further investigation and development of chrysotoxine and crepidatin for CSC-targeted approaches.

## CHAPTER II

### LITERATURE REVIEW

#### 1. Lung cancer

Cancer has always been the major health problem with a dominant cause of death in worldwide. The American Cancer Society compiled cancer-associated data and analyzed the data to estimate cancer statistics for every year. Siegel and colleagues estimated new cancer cases and cancer deaths for ten leading cancer types in both gender population of the United States in 2018, and results reflect that up to 121,680 male patients are estimated to be diagnosed with lung and bronchus-related cancer. This can be accounted for approximately 14% of the new cancer cases in males, and up to 112,350 (13%) in U.S. females (Siegel, Miller, & Jemal, 2018).

Ranking within the top three most diagnosed cancer is lung cancer, where this type is continuously the major cause of death in both genders. Table 1 and 2 showed the statistics of the top three leading cancer type within the past 20 years, differentiated by genders, in the United States (Siegel et al., 2018). According to the information, the top three leading cancer types in male are colorectal, lung and bronchus, and prostate cancer, whereas in female are colorectal, lung and bronchus, and breast cancer. Although lung and bronchus were not ranked the highest estimated cases to be diagnose in both genders, but however, the top causes of death are

always diagnosed to be lung and bronchus (Siegel et al., 2018). This urged the scientists to focus more on lowering the statistics of lung cancer patients.

Lung cancer has been divided into two major groups, including of small cell lung cancer (SCLC) and non-small cell lung cancer (NSCLC). The most common type of cancer is NSCLC, which is found in approximately 85% of the overall lung cancer patients. The poor survival rate in lung cancer patients is due to late diagnosis, which means the cancer has already spread to other sites within the patient's body. In addition, lung cancer was recognized as one of the most important human cancers due to its high metastasis, drug resistance, and mortality rate (E. S. Kim, 2016; Rafiemanesh et al., 2016; Shanker, Willcutts, Roth, & Ramesh, 2010). Patients diagnosed with lung cancer tend to have higher relapse rates, where cancer stem cells (CSCs) have been pointed out to be the cause of these intractable. For the past ten years, remarkable progresses have been uncovered in the treatment of cancer. However, the low success rate among lung cancer patients may be due to difficulties in chemo-resistance and relapses (Alamgeer, Peacock, Matsui, Ganju, & Watkins, 2013; Eramo, Haas, & De Maria, 2010; S. Singh et al., 2012; Templeton, Miyamoto, Babu, Munshi, & Ramesh, 2014).



**Table 1** Statistics of the top three leading cancer type within the past 20 years in U.S. male.

	Male					
	Estimated New Cases			Estimated Deaths		
Year/Cancer Type	Prostate (%)	Lung & Bronchus (%)	Colorectal (%)	Lung & Bronchus (%)	Colorectal (%)	Prostate (%)
1994 (Boring, 1994)	32	16	32	33	13	10
1999 (Landis, 1999)	29	15	29	31	13	10
2004 (Jemal, 2004)	33	13	33	32	10	10
2009 (Siegel, 2009)	25	15	25	30	9	9
2018 (Siegel, 2018)	19	14	9	26	9	8

**Table 2** Statistics of the top three leading cancer type within the past 20 years in U.S. male.

	Female					
	Estimated New Cases			Estimated Deaths		
Year/Cancer Type	Breast (%)	Lung & Bronchus (%)	Colorectal (%)	Lung & Bronchus (%)	Breast (%)	Colorectal (%)
1994 (Boring, 1994)	32	13	13	23	18	11
1999 (Landis, 1999)	29	13	11	23	16	8
2004 (Jemal, 2004)	32	12	11	25	15	9
2009 (Siegel, 2009)	27	14	10	26	15	10
2018 (Siegel, 2018)	30	13	7	25	13	8

## 2. Cancer stem cells (CSCs)

Cancer stem cells (CSCs), or tumor-initiating cells, are a small subpopulation of propagating cancer cells within a tumor (Bao, Ahmad, Azmi, Ali, & Sarkar, 2013; Vinogradov & Wei, 2012). The concept of cancer stem cells was first established by Bonnet & Dick in the year 1997. In the past, it was reviewed that any somatic cell could become cancerous after receiving many series of sequential mutation throughout a period of time. Nevertheless, mature somatic cells usually have a short life span, therefore, the probability of a successful mutation within the life span of one cell would be very low (Bonnet & Dick, 1997). The main characteristics of CSC include the deregulation of self-renewal, as well as the formation of tumors and indefinite proliferation (Chiou et al., 2010; Lobo, Shimono, Qian, & Clarke, 2007). CSCs and normal stem cells share the characteristics of hallmark, as both have the ability to self-renewal and can produce differentiated progeny. However, normal stem cells differ in the high regulation of differentiation and self-renewal process. According to the similarities between CSCs and stem cells, there are three possible hypotheses of original of CSCs, including a stem cell undergoes mutation, a progenitor cells undergoes mutation, and differentiated cell further undergoes other mutations, ultimately resulting in a reversion back to a stem-like state. In all three possible hypotheses, the resultants CSCs found to lose the ability to regulate their own cell division (Crocker & Allan, 2008; Gil, Stembalska, Pesz, & Sasiadek, 2008; Reya, Morrison, Clarke, & Weissman, 2001).

### 3. Characteristics of CSCs

CSCs are an unambiguous population of tumor cells, which consists of multiple features that are vital for formation of tumor. CSCs have the ability of self-renewal and are considered immortal and crucial in the maintenance of tumor cells (Chiou et al., 2010; S. Singh et al., 2012). CSCs are pluripotent and have the capability to procreate tumor cells with different phenotypes. This enables the cultivation of the primary tumor and evolution of subsequent new tumors (Gil et al., 2008; Hanahan & Weinberg, 2011). CSCs contain ability to differentiate to be other cell type, called tumor heterogeneity which facilitates cell growth and survival in distant region. These CSCs properties are thought to be cause of aggressive phenotype in cancer including chemotherapeutic resistance, metastasis, and cancer relapse (Hanahan & Weinberg, 2011; Y. Zhang et al., 2012). CSCs have been shown to maintain their stemness through the sustained level of several transcription factors as well as the stem cell-related signals. Recent studies have shown that the CSCs presenting in the lung cancer may facilitate the malignancy and progression of the disease. Recently, reports have shown that CSCs are becoming less responsive towards chemotherapeutic treatments (Leon, MacDonagh, Finn, Cuffe, & Barr, 2016). In addition, clinical data suggested that lung cancer patients with a high level of CSC markers are associated with lower recurrence-free survival (Suzuki et al., 2012; Yu, Ramena, & Elble, 2012).

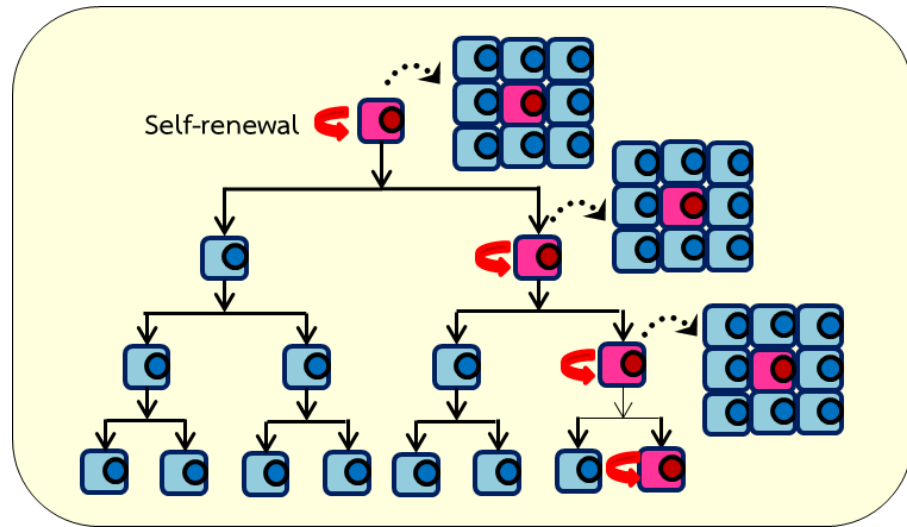


**Figure 1** Self-renewal characteristic of CSCs modified from <http://www.wikiwand.com> by Bhummaphan N.

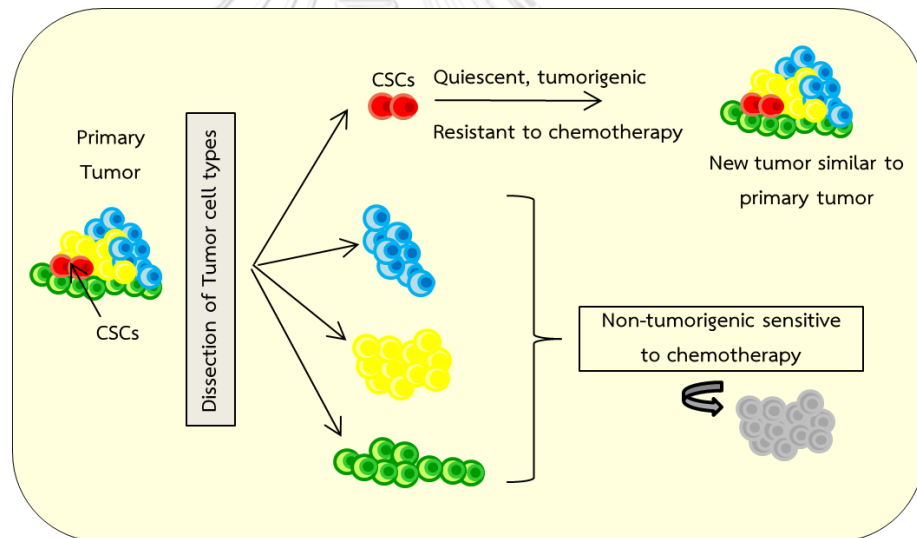


**Figure 2** Chemotherapeutic resistance of CSCs modified from (Bacelli & Trumpp, 2012) by Bhummaphan N.

## 4. Cancer stem cell markers

### 4.1 CD133

Cluster of differentiation-133 (CD133, prominin-1, PROM-1), a penta-span membrane protein, has been implicated as a marker for stemness in solid tumors. Correlation of the expression of CD133 and the CSC phenotype have been reported in pancreatic adenocarcinoma, hepatocellular carcinoma, prostate, neural and renal cancers (Li, 2013; Rappa, Fodstad, & Loricco, 2008). Furthermore, following immunohistochemical analysis of tumor samples, CD133 were found to be the marker to distinguish the stemness in lung cancer and colorectal cancer. Models of severe combined immune-deficient (SCID) mice showed that subsequent transplantation of CD133<sup>+</sup> cells cultured from the tumors into generated tumor xenografts demonstrated identical phenotypes, when compared to the original tumor (NAGATA et al., 2011; Ren, Sheng, & Du, 2013).

### 4.2 CD44

CD44, a cell surface glycoprotein, is responsible for a majority of cellular processes, including cell growth and differentiation, cellular movement, angiogenesis and release of protease enzyme from cell membrane (Jing et al., 2015). Once activated by heterodimerization with growth factor receptors, CD44 subsequently activates PI3K-AKT and MAPK pathways. CD44 has been recognized as a marker for lung CSCs. Furthermore, cells that are CD44-positive exhibit elevated tumorigenicity in

transplantation, heightened capacity to resist to chemotherapy, and higher expression of the stem cell transcription factors, Oct-4 and Sox2 (Leung et al., 2010).

#### 4.3 ABCG2

ABCG2 is the member of ABC family that is consist of transmembrane proteins. ABCG2 gene is located in chromosome 4q22, which consists of 15 introns and 16 exons which contain 655 amino acids (72 kDa). As a half-transporter, the ABCG2 is predominantly localization at the plasma membranes, where is required to activate the function.

Side population phenotype has been defined by the capability to efflux the Hoechst 33342 fluorescent dye from cell, which has been identified as a characteristic trait of stem cells. Previous reports proved that ABCG2 was a molecular determinant culpable for the SP phenotype. The expression of ABCG2 conserves the features of stem cells from a wide variety of sources, which includes the pancreas, testis, lung, brain, prostate, heart, muscle, cornea and conjunctiva, and embryo. In addition, high levels of ABCG2 were determined in a variety of cancers, which includes carcinomas of the lung, colon, breast, melanoma, and ovarian. The ABCG2 expression level is also established in tumors with high pathological grade and the poor prognosis of patient outcome (An & Ongkeko, 2009; Fatima, Zhou, & Sorrentino, 2012; Wee et al., 2016).

**Table 3** CSC markers for distinct solid tumor types

Breast	Colon	Glioma	Liver	Lung	Melanoma	Ovarian	Pancreatic	Prostate
ALDH1A1	ALDH1A1 1	CD15	CD13	ALDH1A1 1	ALDH1A1	CD24	ALDH1A1	ALDH1A1 1
CD24	ABCB5	CD90	CD24	ABCG2	ABCB5	CD44	ABCG2	CD44
CD90	CD133	CD133	CD44	CD133	CD20	CD117	CD133	CD133
CD133	CD24	$\alpha_6$ - integrin	CD90	CD44	CD133	CD133	CD24	CD166
Hedgehog	CD26	Nestin	CD13 3	CD117	CD217		CD44	$\alpha_2\beta_1$ - integrin
$\alpha_6$ - integrin	CD29			CD90			CXCR4	$\alpha_6$ - integrin
	CD44						Nestin	TroP2
	CD66						C-Met	
	$\beta$ - catenin							
	LGR5							



## 5. CSC transcription factors

Sox2, Oct4, and Nanog are genes which are responsible for the encode of transcription factors involved in the regulation of CSCs. These genes are liable for the major transcriptional network that oversees the regulation of self-renewal and pluripotency of stem cells.

### 5.1 Sox2

Sox2, a member of the SOX family transcription factors, consists of three essential domains, including a N-terminal domain, a high-mobility group (HMG) domain, and a transactivation domain. The expression of Sox2 is found in various cancers and also expressed in stem populations in the lung, pancreas, and stomach. In addition, the overexpression of Sox2 have been reported to elevate cell proliferation via cyclin D3 induction. In contrast, the knockdown of Sox2 results in cell cycle arrest and inhibition of cell growth. Furthermore, the silencing of Sox2 may inhibit cellular proliferation in lung squamous cell carcinoma cells (Herreros-Villanueva et al., 2013; S. Singh et al., 2012; Weina & Utikal, 2014).

### 5.2 Oct4

Oct4 is transcription factor that is crucial for the maintenance of pluripotency. Overexpression of Oct4 can be found in recurring tissues of the prostate cancer. Bioinformatic analysis exhibit the overexpression of Oct4 in different types of solid tumor, when compared to corresponding normal tissues. Oct4 works synergistically with Sox2, among other factors, in the regulation of transcription. Sox2 and Oct4 can

both promote genes involved with pluripotency, and inhibit genes involved in differentiation (Kashyap et al., 2009; Pan, Chang, Scholer, & Pei, 2002).

### 5.3 Nanog

Nanog expression is found in various cancers, including lung cancer, prostate cancer, and head and neck carcinoma. Nanog mRNA was shown to be expressed in both pluripotent mouse and human stem cell lines. Nanog is capable of exerting multiple functions through the transcription of regulatory activities. Nanog regulates the cell cycle and proliferation via direct binding to the cyclin D1 promoter. The induction of Nanog generates the upregulations of CD133 and ALDH1A1 in prostate cancer cell lines, which are well-known cancer stem cell markers. Moreover, Nanog is capable of inducing CSC-like features in primary p53-deficient mature mouse astrocytes (Y. Du et al., 2013; Jeter et al., 2011; Kashyap et al., 2009).

## 6. Epithelial-to-mesenchymal transition (EMT)

Epithelial-to-mesenchymal transition, or EMT, is a multistep process of cellular biochemical changes from squamous epithelial cell morphology into spindle-like mesenchymal phenotype. The process of EMT naturally occurs during embryonic development where the epithelial precursors transdifferentiate to complete gastrulation or to form neural crest. These morphogenesis processes require the differentiated epithelial cells to regain their migrative fibroblastic phenotypes in order to travel a long distance to build other tissues (X. Liu & Fan, 2015; Voulgari & Pintzas, 2009). Recently increasing evidence has been reported that EMT also occurs in

metastatic cancer cells as one of the most important mechanisms to escape anoikis and facilitate cell movement. In contrast, it was reported that an inhibition of EMT process leads to a reduction on cell viability caused by the down-regulation of the survival pathways and the up-regulation of the apoptotic pathways (Taddei, Giannoni, Fiaschi, & Chiarugi, 2012; Yilmaz & Christofori, 2009).

The characteristics of EMT consists of morphological changes from cobblestone-shaped epithelial like cells to spindle-shaped mesenchymal like cells, loss of cell-to-cell adhesion and acquisition of metastatic ability, as well as increased expression of the mesenchymal markers, such as Vimentin and N-cadherin, and decreased expression of the epithelial marker E-cadherin. The E-cadherin transcription are associated with the Snail, Slug, and Vimentin transcription factors (Lamouille, Xu, & Derynck, 2014; Son & Moon, 2010; Voulgari & Pintzas, 2009).

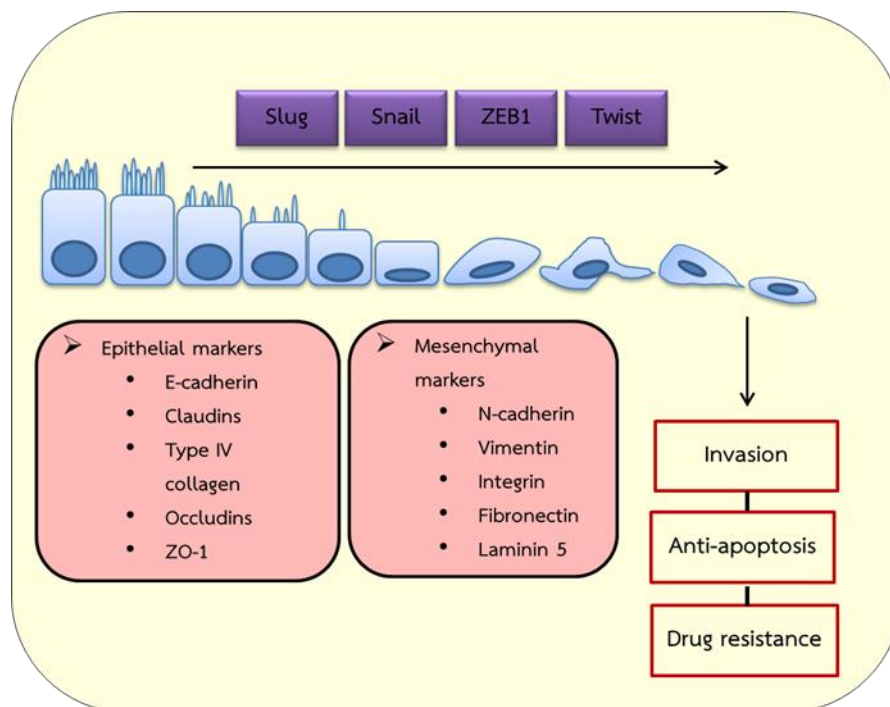


**Figure 3** Basics of epithelial-mesenchymal transition (EMT) and EMT markers, modified from (Angadi & Kale, 2015) by Bhummaphan N.

## 7. EMT markers

### 7.1 E-cadherin

E-cadherin is the major molecular component in establishing stable epithelial cell-cell adhesions including desmosome, adherent's junction, and tight junction. These intercellular junctions allow communication between cells, restrict mobility of the epithelial tissue, and preserve the apico-basal polarization. The down-regulation of E-cadherin leads to the propagation of epithelial cell architecture by disrupting the apico-basal polarization and promoting the front-rear polarization supporting the migratory phenotype (Hollestelle et al., 2013; Lamouille et al., 2014).

## 7.2 Vimentin

Vimentin is an intermediate filament found in most mesenchymal cells and is required for migration. Vimentin can tolerate high stress of the traction force during cellular movements. The expression of Vimentin has been found to correlate with EMT incidence and cancer progression. Thus, Vimentin was also claimed as a cytoskeleton maker for EMT process (Kokkinos et al., 2007; Satelli & Li, 2011).

## 7.3 Snail

Snail is a protein that in humans, encoded by the *SNAI1* gene. Snail is a family of transcription factors that nurtures the inhibition of the E-cadherin adhesion molecule to regulate EMT during embryonic development. Moreover, the metastasis of lung cancer has been most reported with the requirement of Snail family protein up-regulation. Since Snail family members function as transcriptional repressor of EMT-related protein including E-cadherin and also have been reported to be able to regulate the apoptosis as a resistance to paclitaxel, Adriamycin and radiotherapy by inhibiting p53-mediated apoptosis (Shih & Yang, 2011; Y. Wang, Shi, Chai, Ying, & Zhou, 2013).

## 7.4 Slug

Slug is a protein encoded by the *SNAI2* gene, which also encodes a member of the Snail superfamily of C2H2-type zinc finger transcription factors. Slug acts as a transcriptional agent that binds to E-box motifs, and may also suppress E-cadherin transcription in many cancer cells. Slug is involved in EMT process and

possess anti-apoptotic activity. Previous studies showed that Slug is required for the metastasis of the transformed in many cancer cells. Slug is a necessary mediator of Twist-induced EMT and metastasis. Twist needs to induce Slug to suppress the epithelial branch of the EMT, then, together, Twist and Slug function to promote EMT and metastasis (Medici, Hay, & Olsen, 2008; Shih & Yang, 2011; Voulgari & Pintzas, 2009).

### 8. The link between cancer stemness and EMT



Emerging studies propose that cells that undergo EMT acquire stem cell-like properties, thus, give rise to CSCs. EMT facilitates the generation of CSCs with the mesenchymal traits required for dissemination, as well as self-renewal properties required for instigating secondary tumors (Shih & Yang, 2011; Y. Wang et al., 2013). In immortalized human mammary epithelial cells, the induction of EMT by ectopic expression of Snail, Twist or exposure to TGF- $\beta$  leads to an increased potential to form tumor spheres and enriched with CD44<sup>high</sup>/CD24<sup>low</sup> markers in breast cancer cells. In addition, in ovarian cancer cells, Snail and Slug effectively mediate cell survival and are involved in the acquisition of CSC-like with indirectly increase the activation of a self-renewal program by up-regulating Nanog, HDAC1, TCF4, KLF4, HDAC3 and GPC3. Furthermore, it can induce expression of other pluripotent activators, including Oct4, BMI1 and Nestin, as well as increase the number of cells with CD44<sup>high</sup>/CD117<sup>high</sup>, which are ovarian CSC markers. In addition, Slug and Sox9 can harmoniously regulate the mammary stem cell state. Co-expression of Slug and sox9 increase self-renewal ability

and generate CSCs (Wenjun Guo et al.; Luanpitpong et al., 2016). In addition, ZEB1 has the ability to confer stem cell-like properties, which results in strengthening the relationship between EMT and stemness. Once conferred, this property is considered twice as dangerous for the patient, due to the ability of carcinoma cells to enter the bloodstream as well as also support them with properties of stemness by virtue of which these cells have increased tumorigenic and proliferative potential (Ishiwata, 2016; Kalluri & Weinberg, 2009; Kashyap et al., 2009).

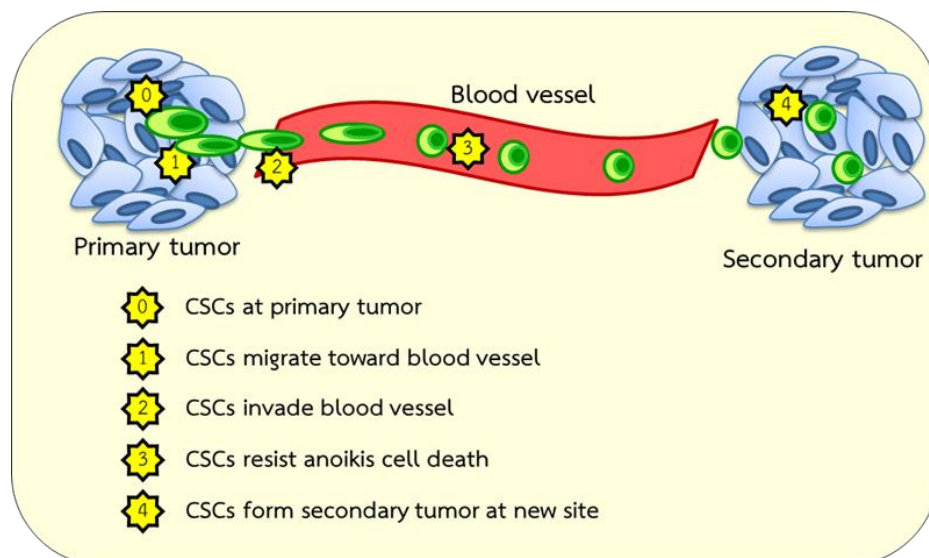


**Figure 4** The cancer stem cells metastatic cascades modified from (Chaffer & Weinberg, 2011) by Bhummaphan N.

## 9. Tyrosine kinase signaling pathways in CSCs

There are multiple CSC models have been proposed as mechanism for tumor. Nevertheless, Tyrosine kinase receptor, Wnt, Hedgehog, and Notch pathways are considered important CSCs' regulators.

Tyrosine kinases are important mediators of the signaling cascade, where their key roles are determination of diverse biological processes, including growth, differentiation, metabolism and apoptosis, in response to external and internal stimuli. Emerging studies have suggested the role of tyrosine kinases in the pathophysiology of cancer. Although tyrosine kinases are tightly regulated in normal cells, but mutation, overexpression and autocrine paracrine stimulation may lead to the transformation of functions, ultimately leading to malignancy. Since angiogenesis is a major event in cancer growth and proliferation, the application of tyrosine kinase inhibitors as a target for anti-angiogenesis may be recommended as a new outlook in cancer therapy (Z. Du & Lovly, 2018; Hubbard & Miller, 2007; Paul & Mukhopadhyay, 2004).

### 9.1 Epidermal growth factor receptor

Epidermal growth factor receptor (EGFR) family is a family that related with tyrosine kinase receptor. Many cancers are upregulated EGFR with inducing various transcription factors. A study in mice showed that a loss of signaling of EGFR family resulted in embryonic lethality with defection in organs, including the lungs, skin, heart, and brain, whereas excessive EGFR signaling is related to the



development of a vast variety of solid tumor. The EGFR family are reported in various human cancers and their unrestrained signaling may be an important element in the development and malignancy of these tumors (Sasaki, Hiroki, & Yamashita, 2013; Seshacharyulu et al., 2012; Yewale, Baradia, Vhora, Patil, & Misra, 2013).

### 9.2 Vascular endothelial growth factor (VEGF)

Vascular endothelial growth factor, or VEGF, is a signal protein produced by cells that nourishes the formation of blood vessels. Moreover, VEGF is a subfamily of growth factors, the platelet-derived growth factor family of cystine-knot growth factors. VEGF is crucial for many signaling proteins that are involved in vasculogenic and angiogenesis. Overexpression of VEGF may lead to a state of disease, where solid cancers absolutely cannot grow with a limited size and without an adequate blood supply, therefore, cancers would increase the expression of VEGF for growing and metastasizing (Carmeliet, 2005; Goel & Mercurio, 2013; Sia, Alsinet, Newell, & Villanueva, 2014).

### 9.3 Src kinase family

Src kinase is a family of non-receptor tyrosine kinases which is associate with many cellular pathways and membrane proteins. The phosphorylation of Src at tyrosine residues is found in stimulating of migration, EMT and CSC markers. A number of substrates have been discovered for the over expression may contribute to the progression of cellular transformation and oncogenic activity. The activation of Src via

phosphorylation at Y416 has been shown to activate Akt via phosphorylation at Ser473, which is an important mediator for cell survival and proliferation. Studies have implicated that the Sox2 pluripotent transcription factor also plays a part in maintaining the characteristics of stem cell, where Sox2 is regulated by the Src-Akt activity (Lundberg et al., 2016; S. Singh et al., 2012). Thus, Src would be the great target for CSCs treatment.

## 10. *Dendrobium pulchellum*



*Dendrobium pulchellum*, is an orchid which is naturally native be found in Southeast Asia such as Thailand, Malaysia, Vietnam, Nepal, and Bhutan. *Dendrobium pulchellum* can be acknowledged from large white flower petals with remnants of purple and yellow pigments. Previous study found that a MeOH extract was prepared from the stem of this orchid was found to possess cytotoxic effects against human lung cancer cells. Subsequent chemical investigation of the extract precipitated the isolation of four known bibenzyls, named chrysotobibenzyl, chrysotoxine, crepidatin, and moscatilin (Chanvorachote et al., 2013).

## 11. Chrysotoxine

Chrysotoxine, a bibenzyl compound isolated from the orchid *Dendrobium pulchellum*. Past reports revealed that chrysotoxine has the ability to induce apoptosis through the direct induction of intracellular reactive oxygen species (ROS), attenuate the growth of lung cancer cells in an anchorage-independent condition, as well as facilitate anoikis (J.-X. Song et al., 2012; J. X. Song et al., 2010). However, the effect of chrysotoxine on CSC regulation has not been clarified.

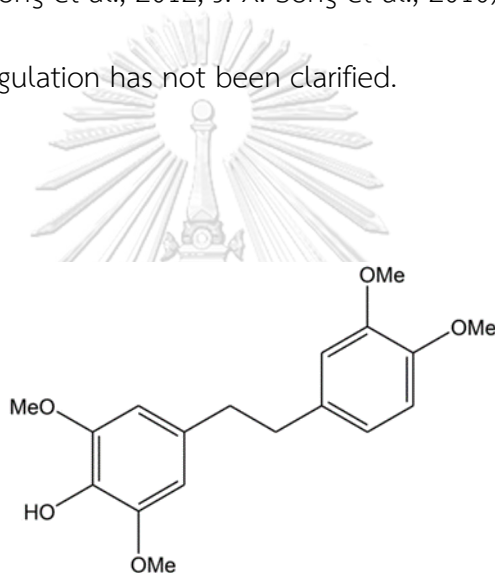


**Figure 5** Chemical structure of chrysotoxine modified from (Chanvorachote et al., 2013) by Narumol N.

## 12. Crepidatin

Crepidatin, a bibenzyl compound was found in *Dendrobium pulchellum* (Majumder & Chatterjee, 1989). This compound was gained increase interest due to its promising pharmacological activities. In previous study revealed that crepidatin had potential to induce apoptosis through the direct induction of intracellular ROS, reduce

growth of lung cancer cells in anchorage-independent condition, and facilitate anoikis (Chanvorachote et al., 2013). In addition, crepidatin was found to be inhibited metastasis in lung cancer; however, the mechanism is still unknown. Nevertheless, the effect of crepidatin on CSC regulation had not been made clear.

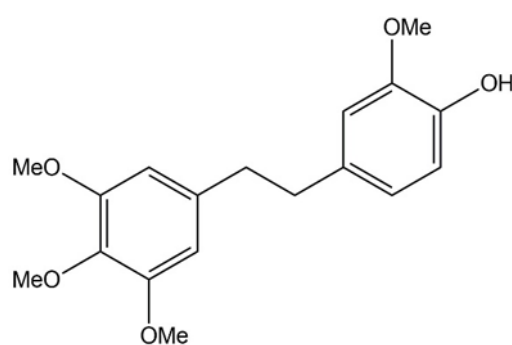


**Figure 6** Chemical structure of crepidatin modified from (Chanvorachote et al., 2013) by Narumol N.

### 13. Chrysotobibenzyl

Chrysotobibenzyl is also a derivative from bibenzyl compound, which was isolated from the orchid *Dendrobium pulchellum*. Past reports revealed that chrysotobibenzyl was able to attenuate the migratory behavior in lung cancer cell. However, the underlying mechanism for such anti-metastasis has not yet been investigated (Chanvorachote et al., 2013).

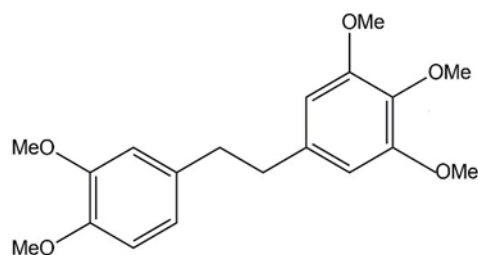


**Figure 7** Chemical structure of chrysotobibenzyl modified from (Chanvorachote et al., 2013) by Narumol N.

#### 14. Cisplatin

Cisplatin or also called *cis*-diamminedichloroplatinum(II), is a metallic (platinum) coordination compound which is a yellow crystalline powder. The mechanism of Cisplatin is related to interfere with DNA replication and attenuate proliferating cells.

Cisplatin is a chemotherapy medication which often used for NSCLC patients. Cisplatin always used with one other drug such as gemcitabine with vinorelbine or paclitaxel. Cisplatin combination chemotherapy is used of treatment of many cancers. Although cisplatin can kill many cancer cells, but the majority of cancer patients will eventually relapse with cisplatin-resistant disease. Many mechanisms of cisplatin resistance have been proposed including changes in cellular uptake and efflux of the drug, inhibition of apoptosis and increased DNA repair (Dasari & Tchounwou, 2014).

In addition, recently, Cisplatin found to be resisted to cancer treatment via increasing anoikis resistance and induce CSC enrichment in various cancers. Previous

studies Cisplatin also promoted transcriptional upregulation of PIK3CA, and cause of activating in PI3K/AKT signaling in resistant cells. In vivo study confirmed drug-resistant tumors displayed the enhanced expressions of CSC transcription factors in cisplatin treated cells. Therefore, a novel perspective in development of new drug for chemotherapy resistance and combination with cisplatin treatment may provide a promising approach for the treatment of patients with NSCLC (Shafee et al., 2008; Thakur & Ray, 2017; L. Wang et al., 2017).

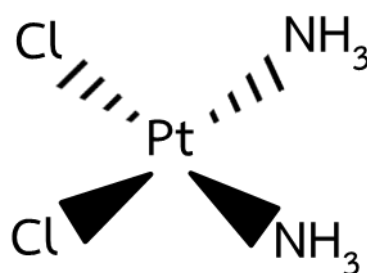


**Figure 8** Chemical structure of Cisplatin modified from <https://biology.stackexchange.com> by Bhummaphan N.

## CHAPTER III

### MATERIALS AND METHODS

#### 1. Cell culture

The human non-small cell lung cancer cell lines, NCI-H460, NCI-H23, NCI-H292 and NCI-A549, and human keratinocyte HaCaT cells were obtained from the American Type Culture Collection (Manassas, VA, USA). NCI-H460, NCI-H23, NCI-H292 were cultivated in Roswell Park Memorial Institute (RPMI) 1640 medium supplemented with 10% fetal bovine serum (FBS), 2 mM L-glutamine, and 100 U/ml penicillin and streptomycin, while A549 and HaCaT cells were cultivated in Dulbecco's Modified Eagle Medium (DMEM) supplemented with 10% fetal bovine serum (FBS), 2 mM L-glutamine, and 100 U/ml penicillin and streptomycin. Cell cultures were maintained in a 37°C humidified incubator with 5% CO<sub>2</sub>. Cells were routinely passaged at preconfluent density using a 0.25% trypsin solution with 0.53 mM EDTA. RPMI 1640 medium, FBS, L-glutamine, penicillin/streptomycin, phosphate-buffered saline (PBS), trypsin, and EDTA were purchased from GIBCO (Grand Island, NY).

#### 2. Plant material

Chrysotoxine, crepidatin, and chrysotobibenzyl were isolated from the stems of *Dendrobium pulchellum* and its purity was evaluated using HPLC and NMR spectroscopy. The compound with > 98% purity was used in the present study. In this experiment, all compounds were dissolved in DMSO as a master stock solution, which

was further diluted with cell culture medium for working concentration. The final concentration of DMSO was used in all experiments less than 0.1%, which is no toxicity to the cells.

### 3. Cytotoxicity assay

For analyzing cytotoxicity assay, H460, H23, H292, A549, and HaCaT were seeded onto 96-well plates at a density of  $1 \times 10^4$  cells/well and allowed to adhere by incubation overnight. Cells then were treated with various concentrations of chrysotoxine, crepidatin, and chrysotobibenzyl for 48 h and then analyzed for cell viability using the 3-(4, 5-dimethylthiazol-2-yl)-2, 5-diphenyltetrazolium bromide (MTT) assay. Cells were incubated with 500  $\mu\text{g/ml}$  of MTT for 4 h at 37 °C and the intensity of formazan product, after solubilization in 100  $\mu\text{l}$  DMSO were measured at 570 nm using a microplate reader (Anthros, Durham, NC, USA). Relative cell viabilities were calculated by dividing the absorbance of the treated cells by that of the control cells. The half-maximal inhibition concentration ( $\text{IC}_{50}$ ) were determined from four independent experiments using the GraphPad Prism 5.0 software (La Jolla, CA).

$$\text{Percent cell viability} = \frac{\text{A570 of treatment group}}{\text{A570 of control group}} \times 100$$



#### 4. Nuclear staining assay

Hoechst 33342 (Molecular Probes Inc., Eugene, OR) and PI (Molecular Probes Inc.) co-staining were used to determine the level of apoptotic and necrosis cell death. After treatments at indicated time, cells were stained with 10  $\mu\text{M}$  of Hoechst and 5  $\mu\text{g/mL}$  of PI for 30 min at 37  $^{\circ}\text{C}$  and then cells were visualized and imaged by fluorescence microscope (Nikon Eclipse Ts2).

#### 5. Wound healing assay

Cell migration was evaluated using wound healing assays. H460 were cultured in 96-well plate in 20,000 cells in each well for 24 h and wound space were created by micropipette tip. Then, media was removed and washed one time with PBS. The monolayer cells were incubated with non-toxic concentration of chrysotoxine, crepidatin, and chrysotobibenzyl (0-50  $\mu\text{M}$ ) and allowed to migrate for 24 h, 48h. The photos of cell migration were taken under a phase contrast microscope (Nikon Eclipse Ts2), and were measured wound space using Image J. The percentage of change in the wound space was calculated as follows.

$$\text{Change in wound space} = \frac{\text{Average space at time (0 h - 24, 48 h)} \times 100}{\text{Average space at time 0 h}}$$

## 6. Spheroids formation assay

Cells were seeded approximately  $2.5 \times 10^3$  cells/well onto a 24-well ultralow attachment plate in 0.8% methylcellulose-based serum-free medium supplemented with 20 ng/ml epidermal growth factor, basic fibroblast growth factor, and 4 mg/ml insulin for 7 days. Then primary spheroids were resuspended as single cells and were reseeded again  $2.5 \times 10^3$  cells/well onto a 24-well ultralow attachment plate. Secondary spheroids were allowed to form for 14 days and spheroid formation.

For single three-dimension (3D) spheroid-formation assay, H460, H23 and A549 cells were allowed to form primary and secondary spheroids as detailed above. At day 14 of secondary spheroid formation, they were dissociated into a single spheroid of the same size and each spheroid was then were treated with a noncytotoxic and  $IC_{50}$  concentrations of chrysotoxine and crepidatin (0–25  $\mu$ M). Phase-contrast images of the secondary spheroids were taken at day 0, 3 and 7 after chrysotoxine and crepidatin treatment under a phase-contrast microscope (Nikon Eclipse Ts2).

## 7. Extreme limiting dilution assay (ELDA)

Extreme limiting dilution assay (ELDA) used in this study was slightly modified from previous described. H460, H23 and A549 cells were plated and allowed to adhere by incubation overnight. Cells then were treated with nontoxic and  $IC_{50}$  concentrations of chrysotoxine, crepidatin, and cisplatin for 48 h and then cells were replated again in totally decreasing numbers from 200 cells/well to 1 cell/well in 200  $\mu$ l onto a 96-well ultralow attachment plate and cultured for 14 days, whereupon the number of

wells containing spheres for each cell plating density (number of positive cultures) were counted and recorded. Spheroid formation with treated cells were calculated in all wells compared to control.

#### **8. Water-soluble tetrazolium salt (WST) assay**

H460, H23 and A549 cells were seeded onto a 24-well ultralow attachment plate approximately  $2.5 \times 10^3$  cells/well using RPMI serum-free medium. The primary spheroids were allowed to form for 7 days. At day 7, primary spheroids were then resuspended into single cells using 1 mM EDTA and were reseeded at  $2.5 \times 10^3$  cells/well onto a 24-well ultralow attached plate and cultured for 14 days to form secondary spheroids. At day 14, the CSC-rich population were treated with the chrysotoxine and crepidatin (0-50  $\mu$ M) for 48 h and were analyzed for cell viability using the WST assay. The harvested cells were incubated with 10% WST for 2 h at 37°C and the intensity of the formazan product were measured at 450 nm using a plate reader. Cell viability were calculated from OD readings and were represented as percentages with respect to the non-treated control value.

#### **9. Western blot analysis**

Treated cells and nontreated control cells were plated and incubated as above experiments. After that, cells were washed with 1X PBS and lyzed on ice for 45 min with lysis buffer containing 20 mM Tris-HCl (pH 7.5), 1% Triton X-100, 150 mM NaCl, 10% glycerol, 1 mM  $\text{Na}_3\text{VO}_4$ , 50 mM NaF, 100 mM PMSF and cocktail protease inhibitor

mixture (Roche Molecular Biochemical, Indianapolis, IN, USA). The protein lysates were analyzed for protein content using BCA protein assay kit from Pierce Biotechnology (Rockford, IL, USA). Equal amounts of denatured protein samples (60  $\mu$ g) were loaded onto 10% SDS-PAGE in 1X Tris/Glycine/SDS buffer before transferring onto to 0.45- $\mu$ m nitrocellulose membranes in 1X Tris/Glycine buffer for 2 h (Bio-Rad, Hercules, CA, USA). Transferred membranes were blocked for 1 h in 5% nonfat dry milk in TBST (25 mM Tris-HCl, pH 7.5, 125 mM NaCl, and 0.05% Tween 20) and were incubated overnight with specific primary antibodies against CD133, CD44, ABCG2, Sox2, Vimentin, Snail, Slug, E-cadherin, p-Src, Src, p-Akt, Akt, PARP, gamma-H2AX and GAPDH. Membranes were washed three times with TBST and were incubated with appropriate horseradish peroxidase (HRP)-labeled secondary antibodies for 2 h at room temperature. The immune complexes were detected by Super Signal West Pico chemiluminescent substrate (Pierce Biotechnology) and were exposed to film.

#### **10. Clonogenic assay**

For analyzing clonogenic assay, H460 and A549 were seeded and allowed to adhere by incubation overnight. Cells then were treated with nontoxic and  $IC_{50}$  concentrations of crepidatin and cisplatin for 48 h. After indicated time, cells were counted and re-plated in a low number with 250 cells in 6-well plate in medium. After 10 days of growth, cells were washed with 1X PBS, fixed with methanol and stained with crystal violet. Then, colonies were counted by Image Pro Plus6 program.

### 11. 3D-CSC migration assay

The secondary spheroids were dissociated into a single spheroid which had the similar size as described above. Then each spheroid was treated with the crepidatin in indicated concentration for 7 days and then each spheroid was re-plated on 24 well plate and evaluated every 24, 48, 72, and 96 h. After 96 h, each spheroid was stained with calcein AM to clarify cell viability and PI dye to determine apoptotic of cells. Photos were captured, and migratory area were calculated in all treated spheres compared to control.

### 12. NanoString nCounter Gene Expression Assay

Treated cells and nontreated control cells were plated and incubated as above experiments. After that, cells were washed with 1X PBS and solubilized at  $1 \times 10^7$  cells/ml in lysis buffer with phosphatase inhibitors at 2–8 °C for 30 min and were preceded according to manufacturer's protocol. Briefly, Total RNA were extracted by using Trizol reagent according to the manufacturer's instruction. Cells were homogenized in 1 ml of Trizol reagent and then centrifuged at 15,000 rpm for 10 min for dissociation of nucleoprotein complexes. Supernatants were transferred to a new eppendorf tube and precipitated the total RNA by adding 500  $\mu$ l of isopropanol, followed by centrifugation at 15,000 rpm for 10 min. RNA pellets were washed once with 100 % ethanol and dried at room temperature for 10-15 min before dissolving in

RNase free water, then, the total RNA were analyzed using NanoString nCounter Gene Expression.

### **13. Chick chorioallantoic membrane (CAM) assay**

H460 and A549 cells were seeded in 100 mm dish for 24 h, then, cells were pretreated with crepidatin and cisplatin for 48 h at  $IC_{50}$  concentrations. After 48 h, cells were counted the viable cells  $1 \times 10^6$  / CAM and subject to CAM assay. A small window was made in the shell on day 1 of chick embryo development under aseptic conditions. Then, pretreated cells were mixed with growth factor with Matrigel in a total volume of 30  $\mu$ l and allowed to solidify for 1 h. Then, Matrigel grafts were placed on top of the CAM and eggs were resealed and returned to the incubator for 72 hours until day 14 (n = 7 chicken embryos per cell line). Blood vessels of CAM models were captured at day 3, 4, and 5 of xenograft. After that, Matrigel grafts with surrounding CAM were harvested from each embryo and fixed with 4% paraformaldehyde for 24 hours and embedded in paraffin. Serial sections (6  $\mu$ m) were stained with hematoxylin and eosin. Slides were digitally scanned using the NanoZoomer.

### **14. Enriched primary non-small cell lung cancer stem cells assay**

Enriched primary non-small cell lung cancer stem cells were obtained from Promab Biotechnologies, Inc. (Richmond, CA, USA). Cells were cultivated in Cancer stem cell media premium (Cat. No. 20101) and supplemented with 10% fetal bovine serum (FBS), 2 mM L-glutamine, and 100 U/ml penicillin and streptomycin. Then, enriched primary lung cancer stem cells were incubated with chrysotoxine and

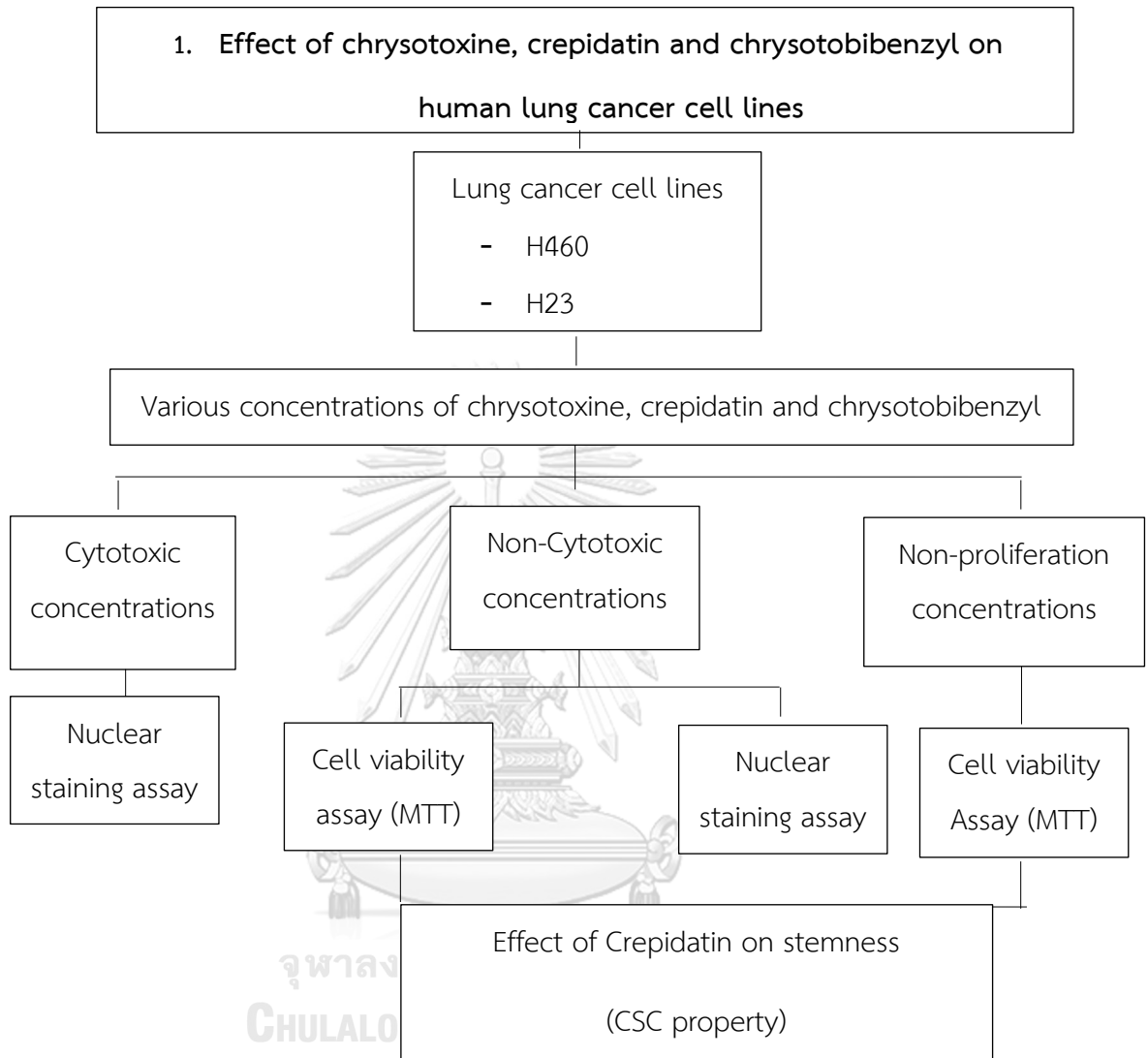
crepidatin for 48 h. After chrysotoxine and crepidatin treatment, cells were captured under a phase-contrast microscope (Nikon Eclipse Ts2).

### 15. Statistical analysis

Data were shown as the mean  $\pm$  S.D., derived from at least three independent experiments. Statistical analysis was performed by one-way ANOVA and student's *t* test and followed by multiple comparison test. The statistical analysis was performed using GraphPad software with the statistical significance were considered at *P* value less than 0.05.

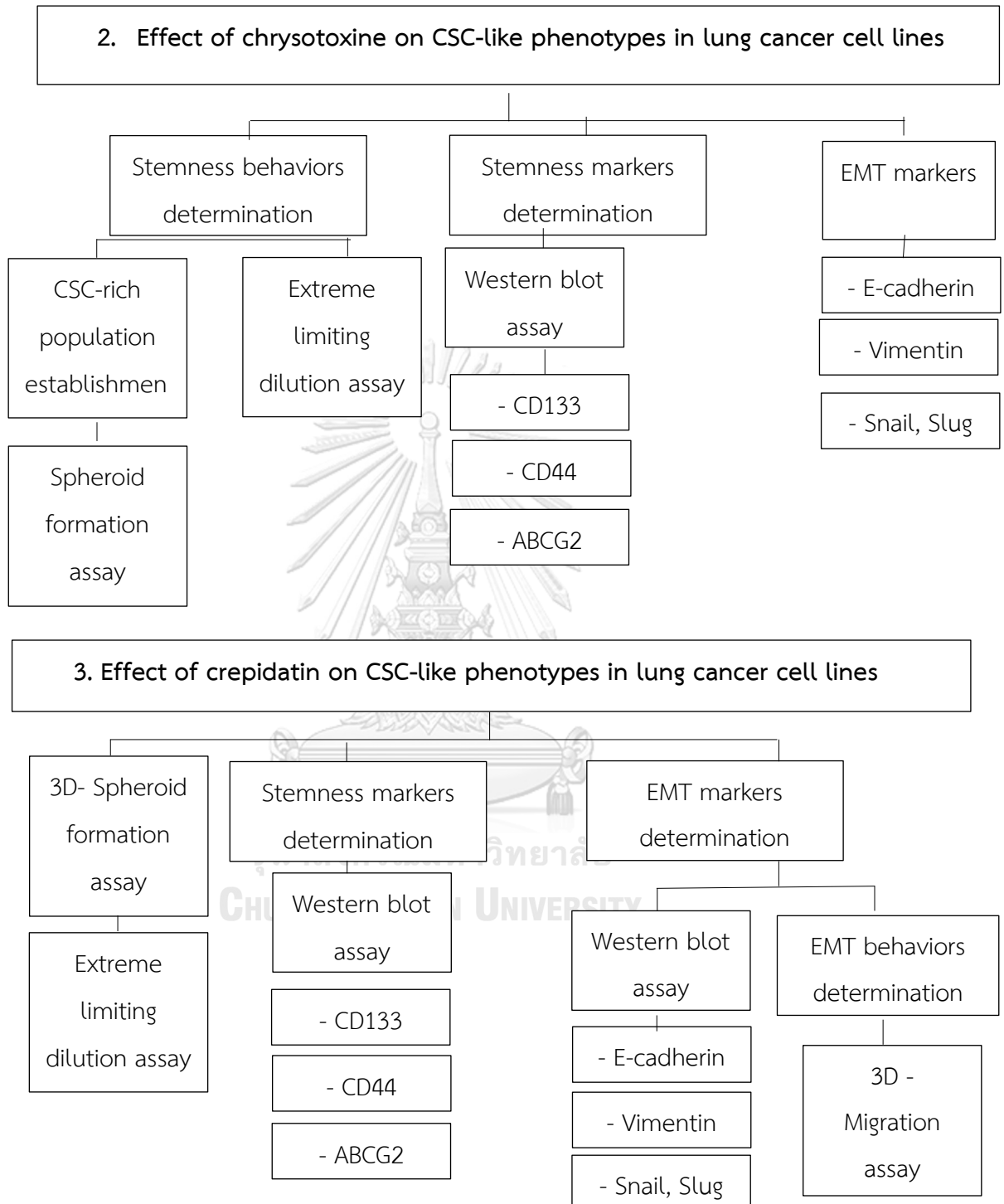


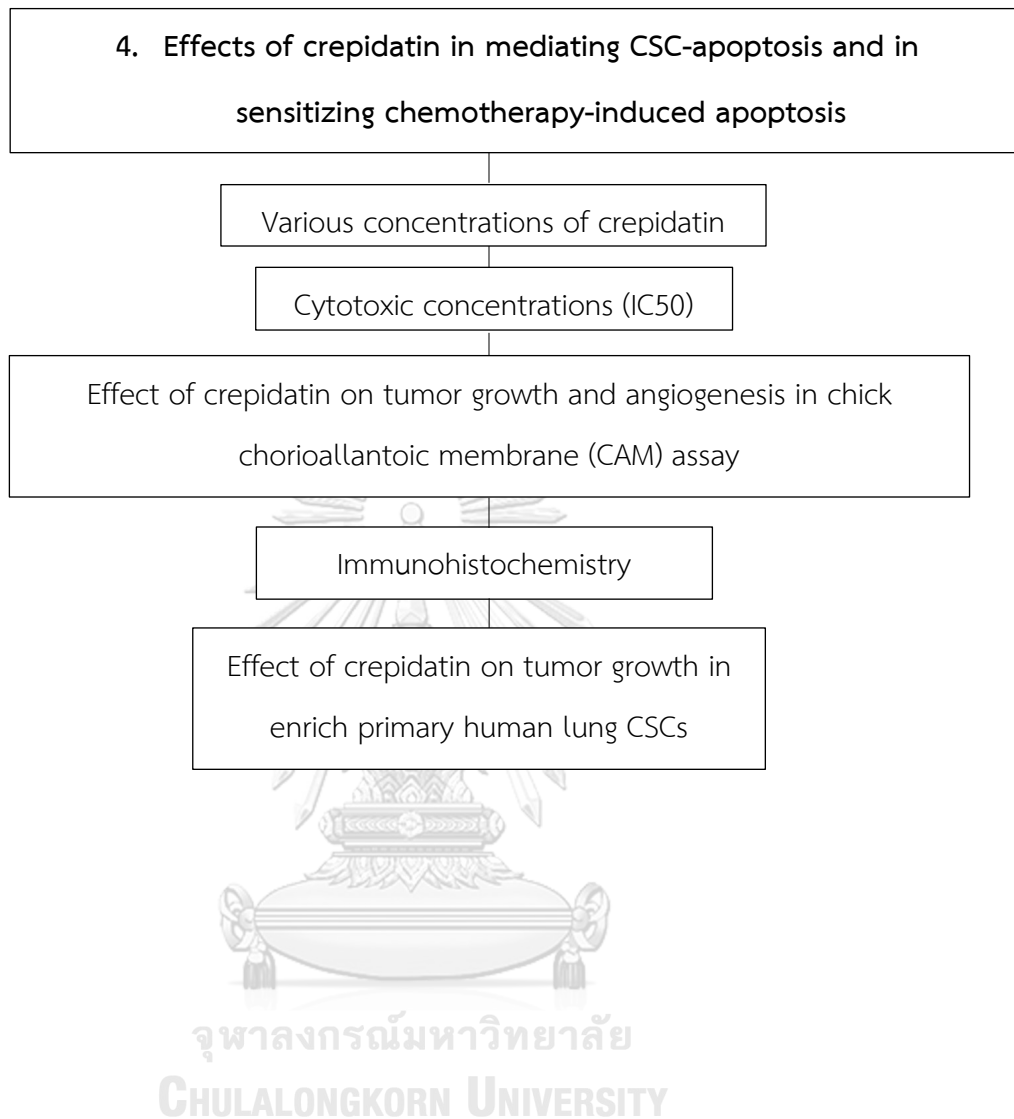
## Research Design

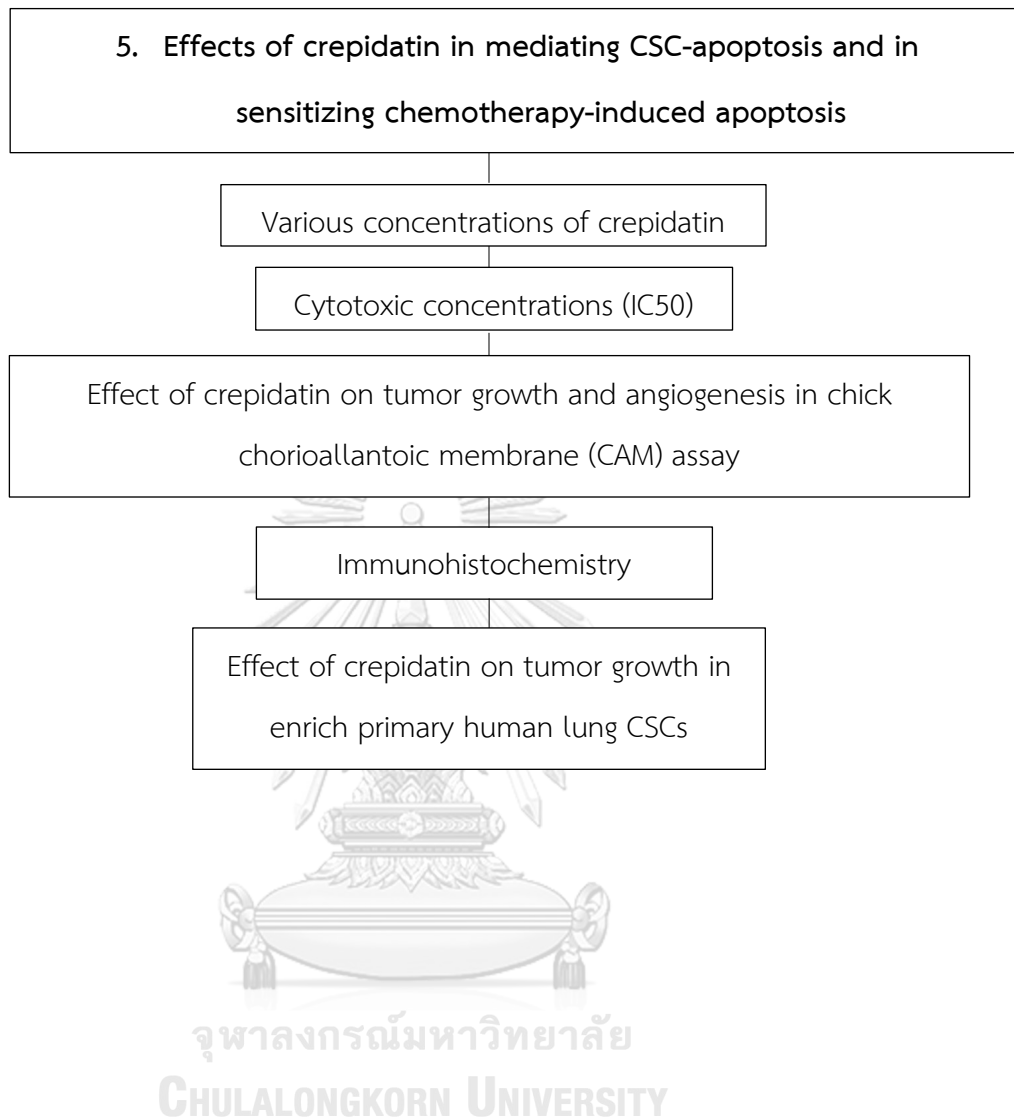




## Research Design (Conc.)







## CHAPTER IV

### RESULTS

Part 1. Evaluation the effect of chrysotoxine, crepidatin, and chrysotobibenzyl on stemness of lung cancer and normal cells.

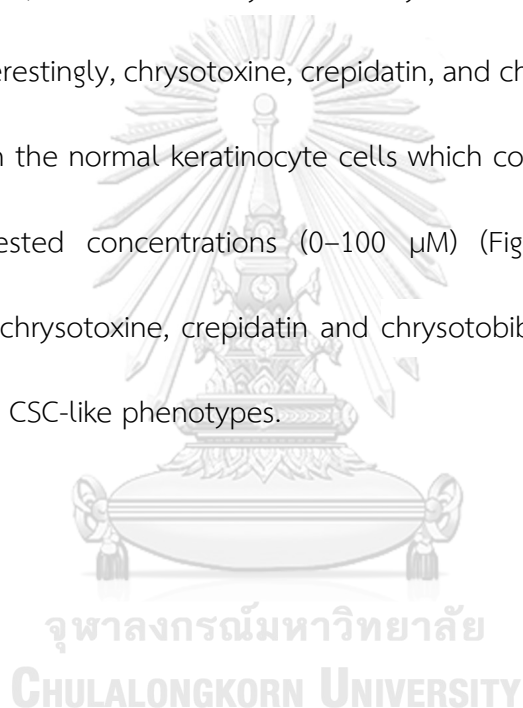
#### 1. Cytotoxicity analysis

##### 1.1 Effect of chrysotoxine, crepidatin, and chrysotobibenzyl on human lung cancer and normal cells.

Prior to determine the effect of chrysotoxine, crepidatin and chrysotobibenzyl on CSC's properties, the appropriate non-cytotoxic concentrations were evaluated. To study the effect of these compounds, human NSCLC H460 and H23 cells were treated with various concentrations of compound (0, 1, 5, 10, 20, 50 and 100  $\mu\text{M}$ ) for 48 h and then their cell viability was determined by the MTT viability assay. Chrysotoxine was found to be nontoxic at concentrations below 20  $\mu\text{M}$  in both H460 and H23 cells, with no significantly decreased cell viability or increased apoptosis/necrotic cell death, whereas significantly reduced cell viability and an increased level of apoptosis was noted at 50  $\mu\text{M}$  (Figure 9 and Figure 13A). The derived  $\text{IC}_{50}$  values of chrysotoxine were approximately 78.34  $\mu\text{M}$  for H460 cells and 92.47  $\mu\text{M}$  for H23 cells.

In addition, crepidatin was found to be non-toxic at concentrations below 10  $\mu\text{M}$  in H460 and  $\text{IC}_{50}$  value of crepidatin on H460 has been found at 29.1  $\mu\text{M}$  whereas in H23 cells, non-toxic of crepidatin was found at concentration below 100  $\mu\text{M}$  and the  $\text{IC}_{50}$  value of crepidatin on H23 were found at 89.86  $\mu\text{M}$ . However, there were no

significant decreased cell viability or increased apoptosis nor necrotic cell death, whereas a significantly reduced cell viability and increased level of apoptosis was found at 25  $\mu\text{M}$  and 100  $\mu\text{M}$  in H460 and H23 cells accordingly (Figure 10 and Figure 13B). Finally, chrysotobibenzyl was found to be non-toxic at concentrations below 100  $\mu\text{M}$  in H460 and  $\text{IC}_{50}$  value of chrysotobibenzyl on H460 has been found at  $\geq 100$   $\mu\text{M}$  whereas in H23 cells, non-toxic of chrysotobibenzyl was found at concentration  $\geq 100$   $\mu\text{M}$  (Figure 11). Interestingly, chrysotoxine, crepidatin, and chrysotobibenzyl showed no cytotoxic effect on the normal keratinocyte cells which contained normal stem cells (HaCaT) at all tested concentrations (0–100  $\mu\text{M}$ ) (Figure 12). Thus, non-toxic concentrations of chrysotoxine, crepidatin and chrysotobibenzyl were further tested for their effects on CSC-like phenotypes.



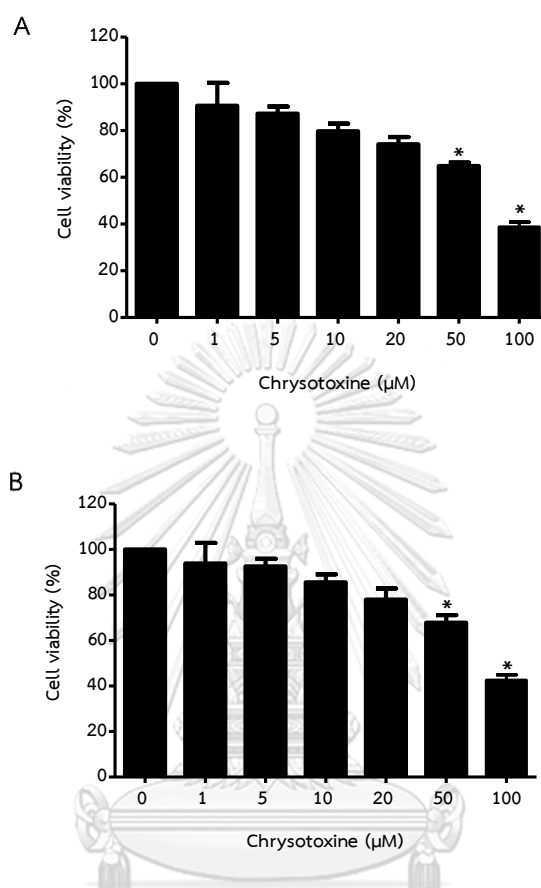


**Figure 9** Cytotoxic effect of chrysotoxine on human lung cancer H460 and H23 cells. (A) H460, and (B) H23 cells were treated with various concentrations of chrysotoxine (0–100 μM) for 48 h and then the cell viability was determined by the MTT assay, relative to the viability of untreated cells set as 100%. The data is presented as mean  $\pm$  SD (n=3).

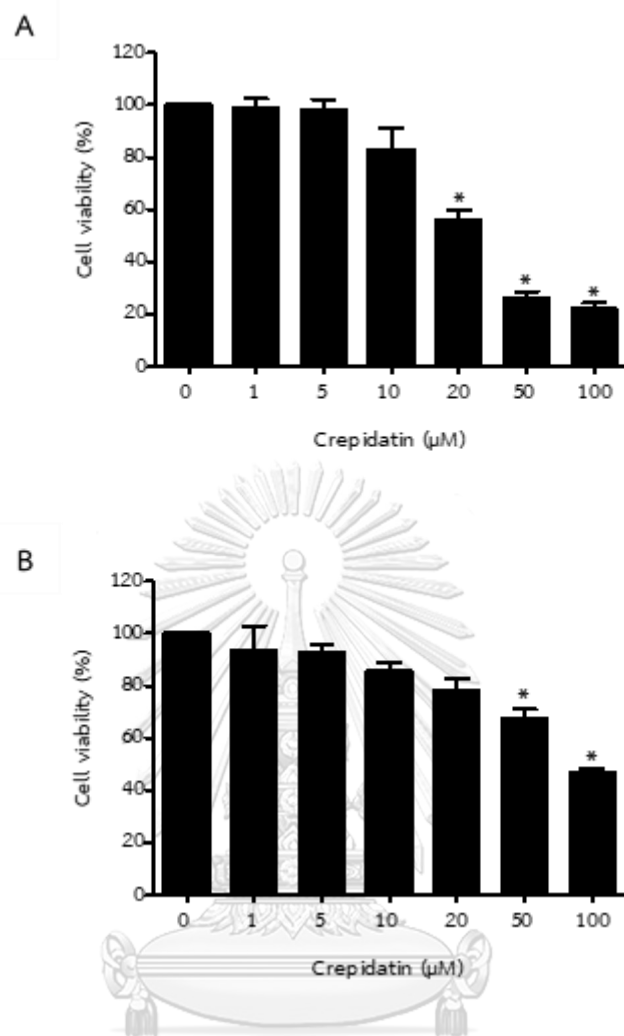
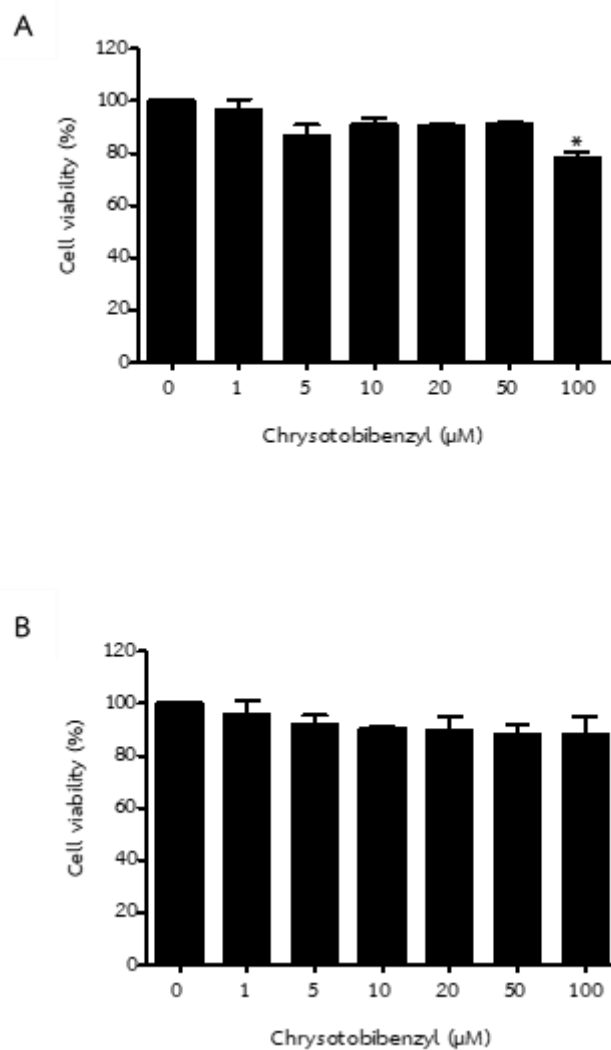


**Figure 10** Cytotoxic effect of crepidatin on human lung cancer H460 and H23 cells.

(A) H460, and (B) H23 cells were treated with various concentrations of crepidatin (0–100  $\mu\text{M}$ ) for 48 h and then the cell viability was determined by the MTT assay, relative to the viability of untreated cells set as 100%. The data is presented as mean  $\pm$  SD (n=3).



CHULALONGKORN UNIVERSITY

**Figure 11** Cytotoxic effect of chrysotobibenzyl on human lung cancer H460 and H23 cells.

(A) H460, and (B) H23 cells were treated with various concentrations of chrysotobibenzyl (0–100  $\mu\text{M}$ ) for 48 h and then the cell viability was determined by the MTT assay, relative to the viability of untreated cells set as 100%. The data is presented as mean  $\pm$  SD (n=3).



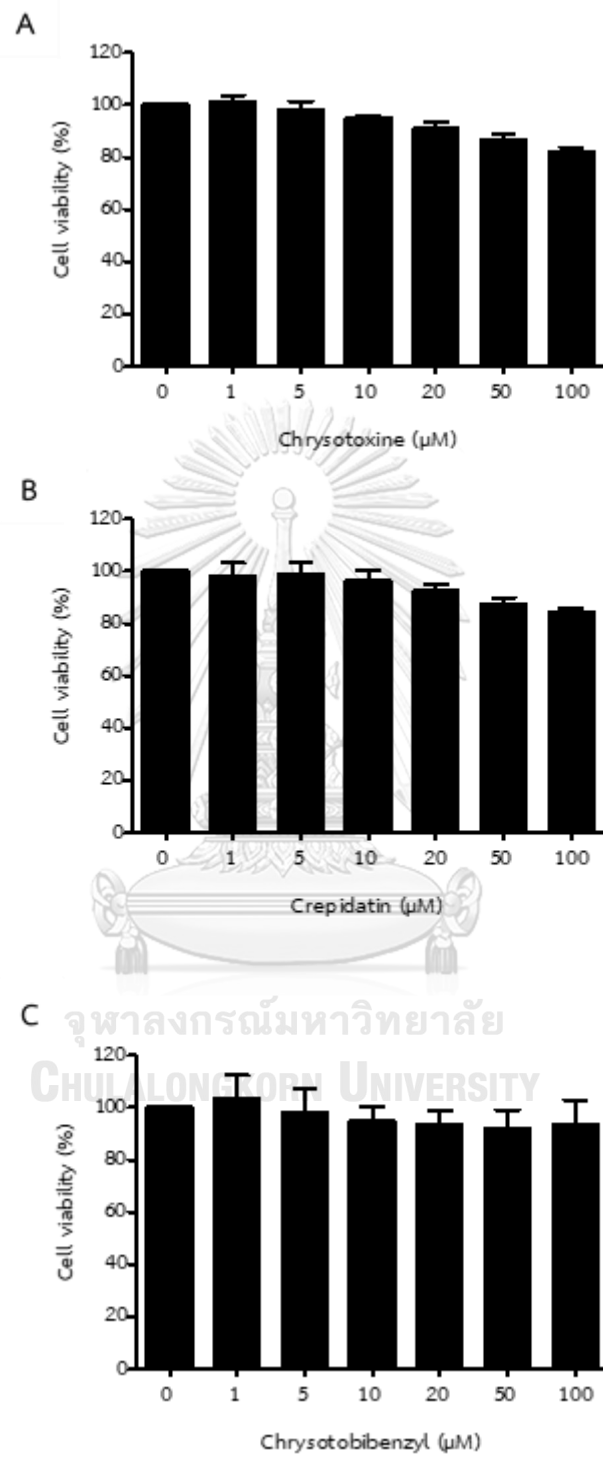


**Figure 12** Cytotoxic effect of chrysotoxine, crepidatin, and chrysotobibenzyl on human normal keratinocyte HaCaT cells.

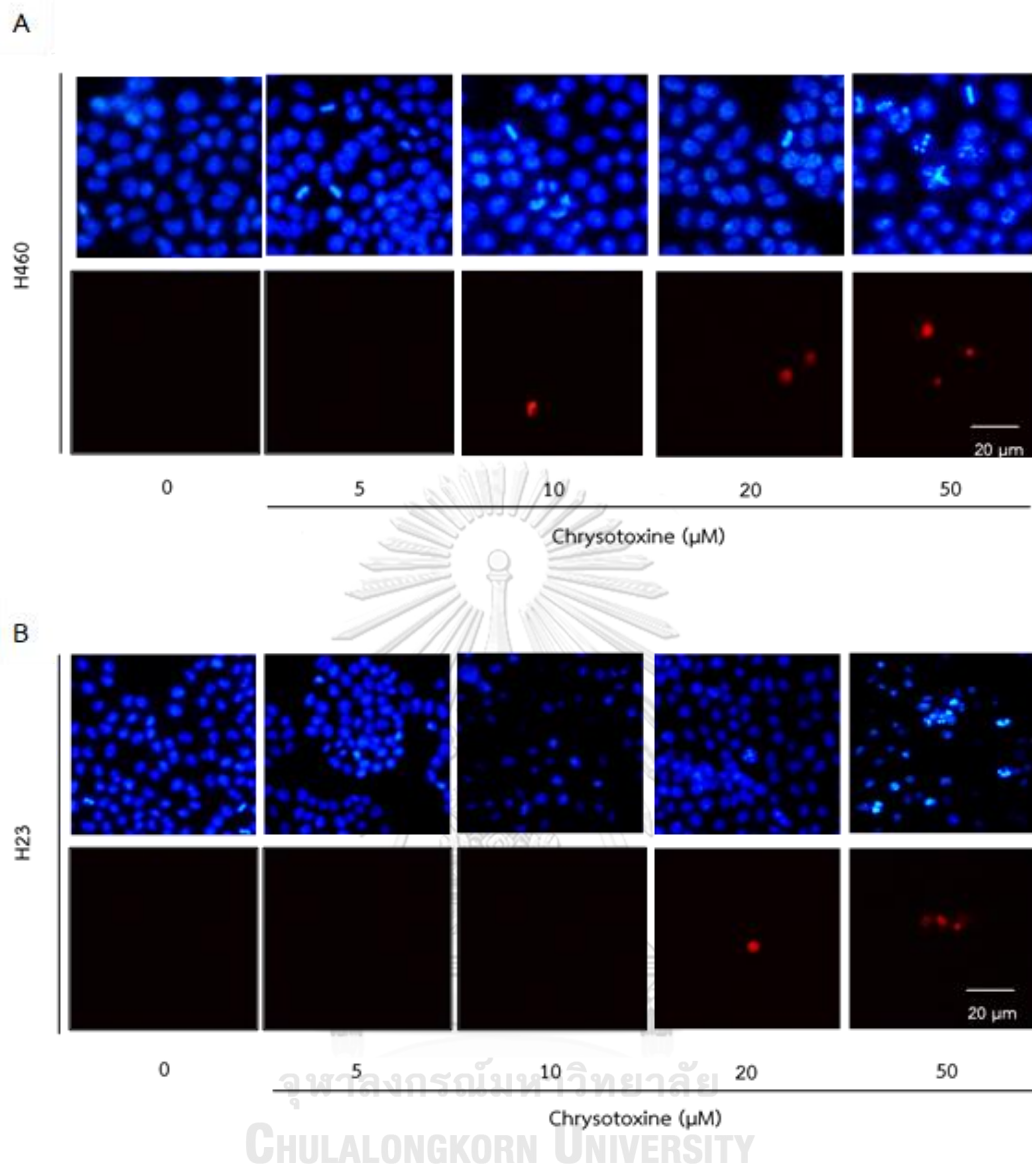
(A) chrysotoxine, (B) crepidatin, and (C) chrysotobibenzyl were treated with various concentrations (0–100  $\mu$ M) in HaCaT cells for 48 h and then the cell viability was determined by the MTT assay, relative to the viability of untreated cells set as 100%.

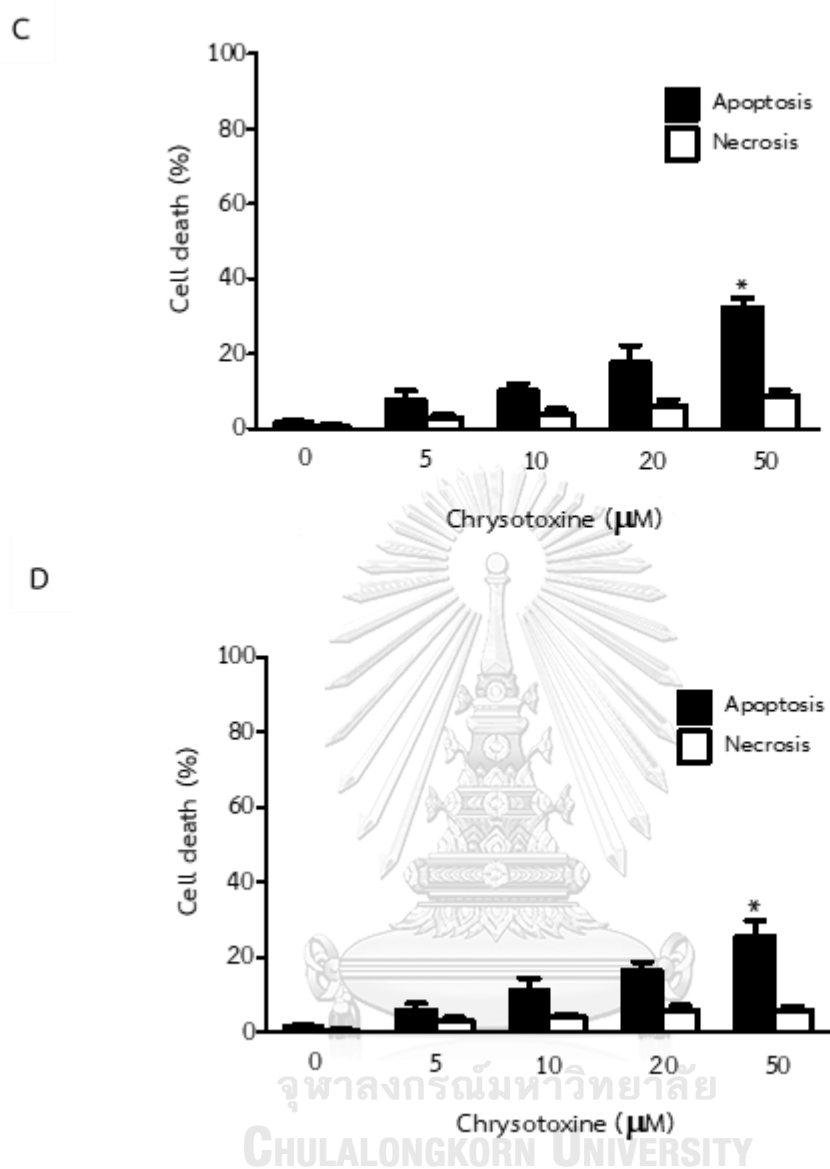
The data is presented as mean  $\pm$  SD (n=3).

**Table 4** IC<sub>50</sub> of chrysotoxine, crepidatin, and chrysotobibenzyl on human lung cancer H460 and H23 and human normal keratinocyte HaCaT cells.

Treatment	H460	H23	HaCaT
chrysotoxine	78.34	92.47	$\geq 100$
crepidatin	29.31	89.86	$\geq 100$
chrysotobibenzyl	$\geq 100$	$\geq 100$	$\geq 100$

CHULALONGKORN UNIVERSITY

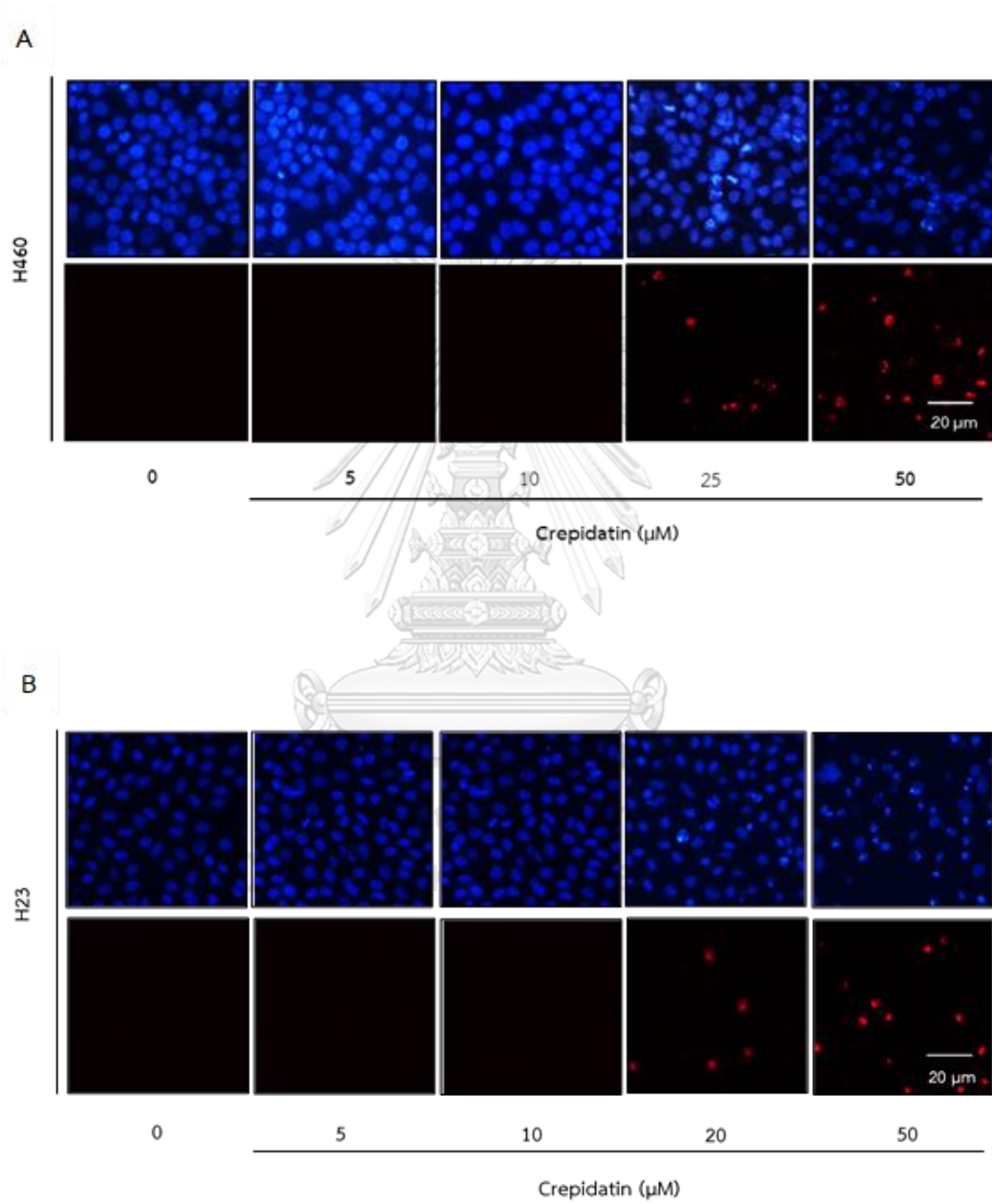




**Figure 13** Effect of chrysotoxine on apoptotic and necrotic cell death.

(A) and (C) H460 and (B) and (D) H23 were treated with various concentrations chrysotoxine for 48 h. The level of apoptotic and necrotic cell death was evaluated at the same time using Hoechst 33342/PI costaining and is shown relative to that of the

untreated control cells. All plots show the mean  $\pm$  SD ( $n = 3$ ). \*  $P < 0.05$  vs. untreated cells.



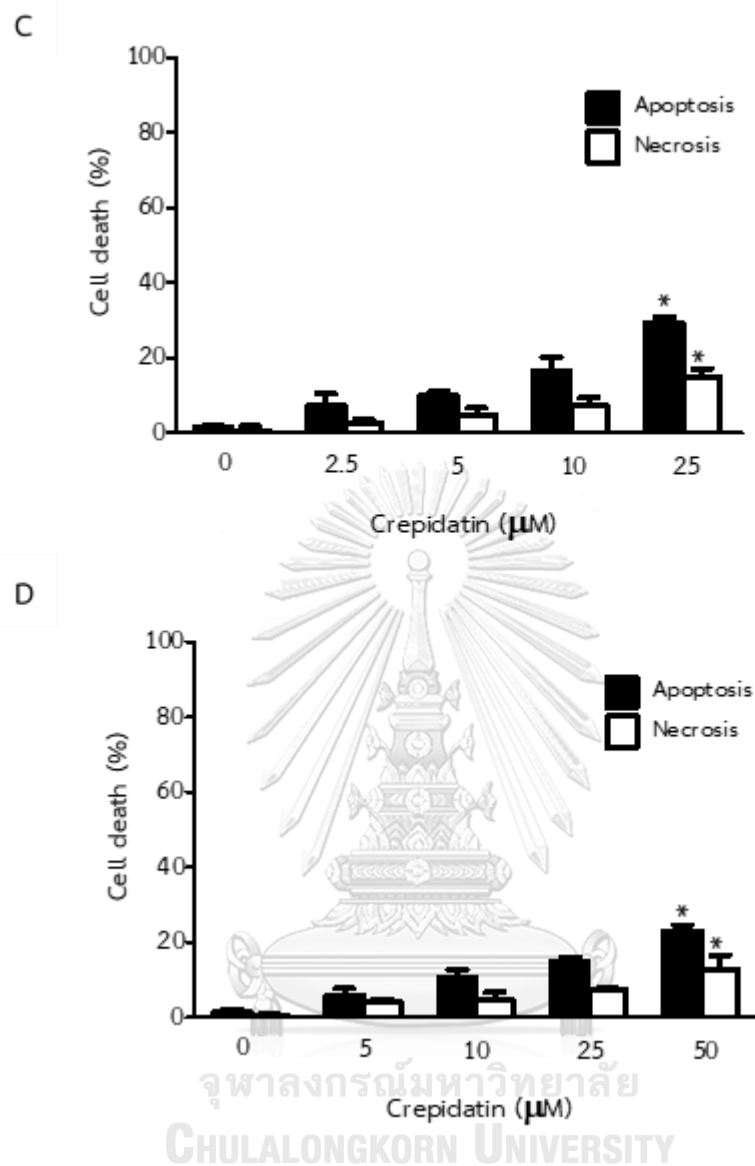


**Figure 14** Effect of crepidatin on apoptotic and necrotic cell death.

(A and C) H460 and (B and D) H23 were treated with various concentrations crepidatin for 48 h. The level of apoptotic and necrotic cell death was evaluated at the same time using Hoechst 33342/PI costaining and is shown relative to that of the untreated control cells. All plots show the mean  $\pm$  SD (n = 3). \*  $P < 0.05$  vs. untreated cells.

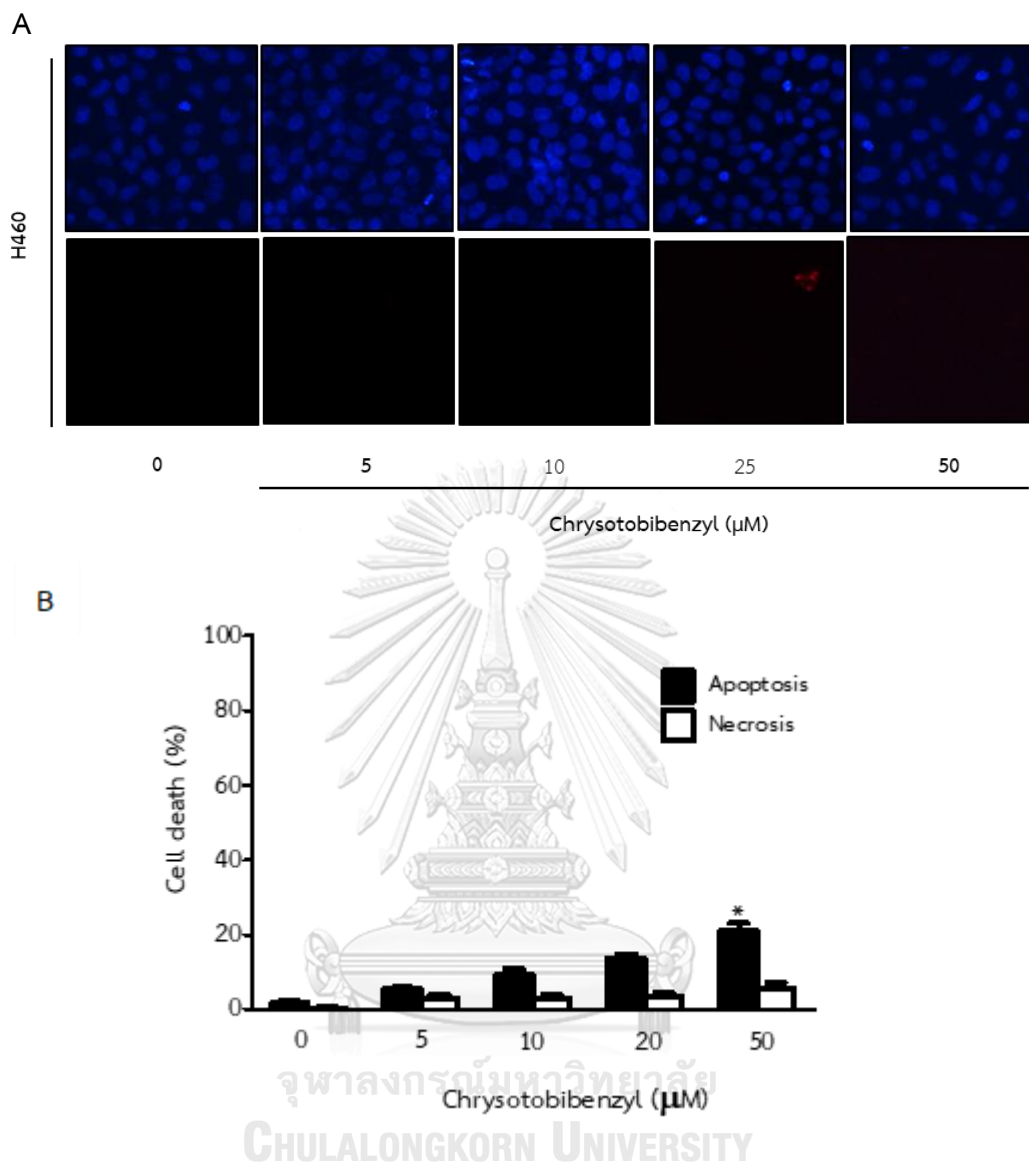
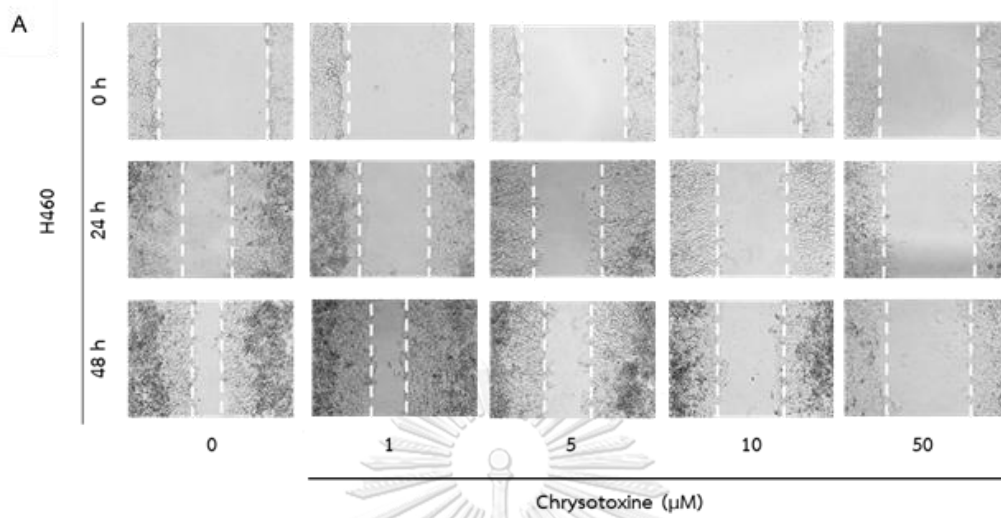


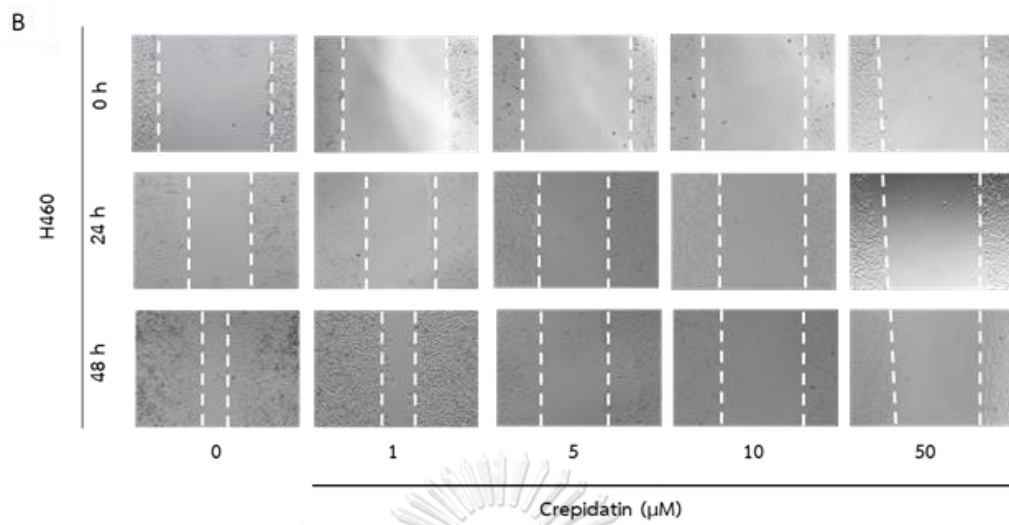
**Figure 15** Effect of chrysotobibenzyl on apoptotic and necrotic cell death.

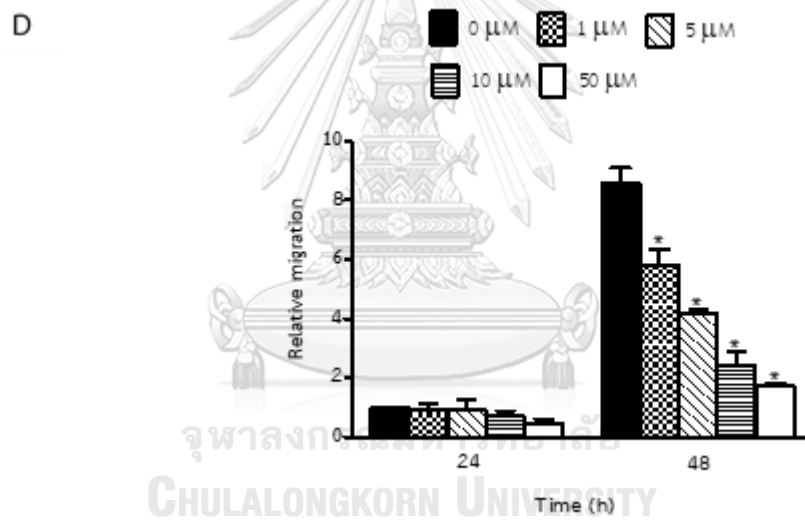
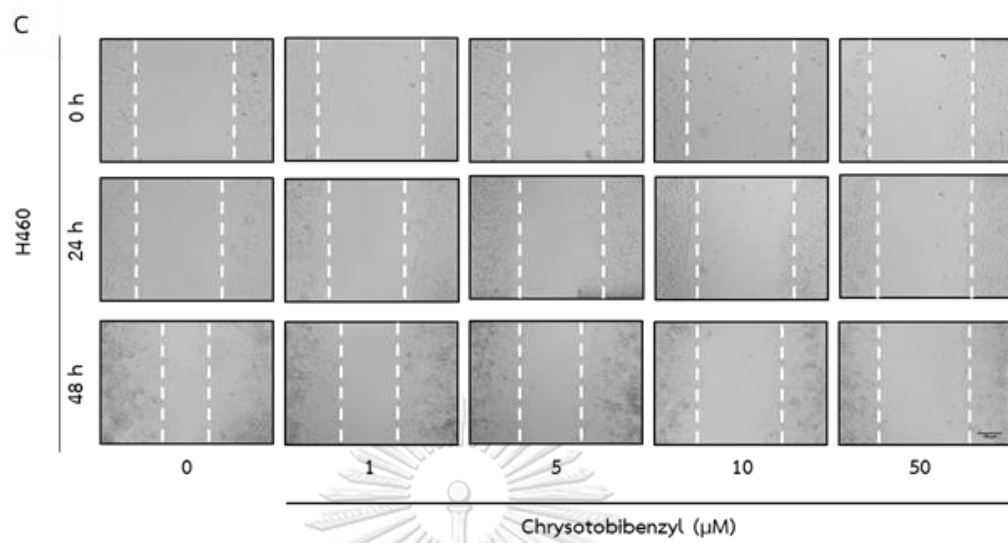
H460 were treated with various concentrations chrysotobibenzyl for 48 h. The level of apoptotic and necrotic cell death was evaluated at the same time using Hoechst 33342/PI costaining and is shown relative to that of the untreated control cells. All plots show the mean  $\pm$  SD (n = 3). \* P < 0.05 vs. untreated cells.

To study the effect of chrysotoxine, crepidatin and chrysotobibenzyl, cell migration assay was used to evaluate one of the important characteristics on metastatic properties. H460 and H23 cells were investigated in terms of cell migration using a scratch assay. Figures 16 showed that chrysotoxine, crepidatin, and chrysotobibenzyl significantly inhibited H460 cell migration at 1–50  $\mu\text{M}$  at 48 h, compared with the non-treated control. Taken together, these results suggested that chrysotoxine, crepidatin, and chrysotobibenzyl had an effective inhibition on cell migration, which may impair cellular protrusions at the edge of motile cells and decrease the potential of cell motility in lung cancer cells. However, both chrysotoxine and crepidatin showed significantly higher inhibition to cell migratory behavior in H460, when compared to chrysotobibenzyl. Therefore, we used two these compounds to further study for the effect on stemness of lung cancer cells.









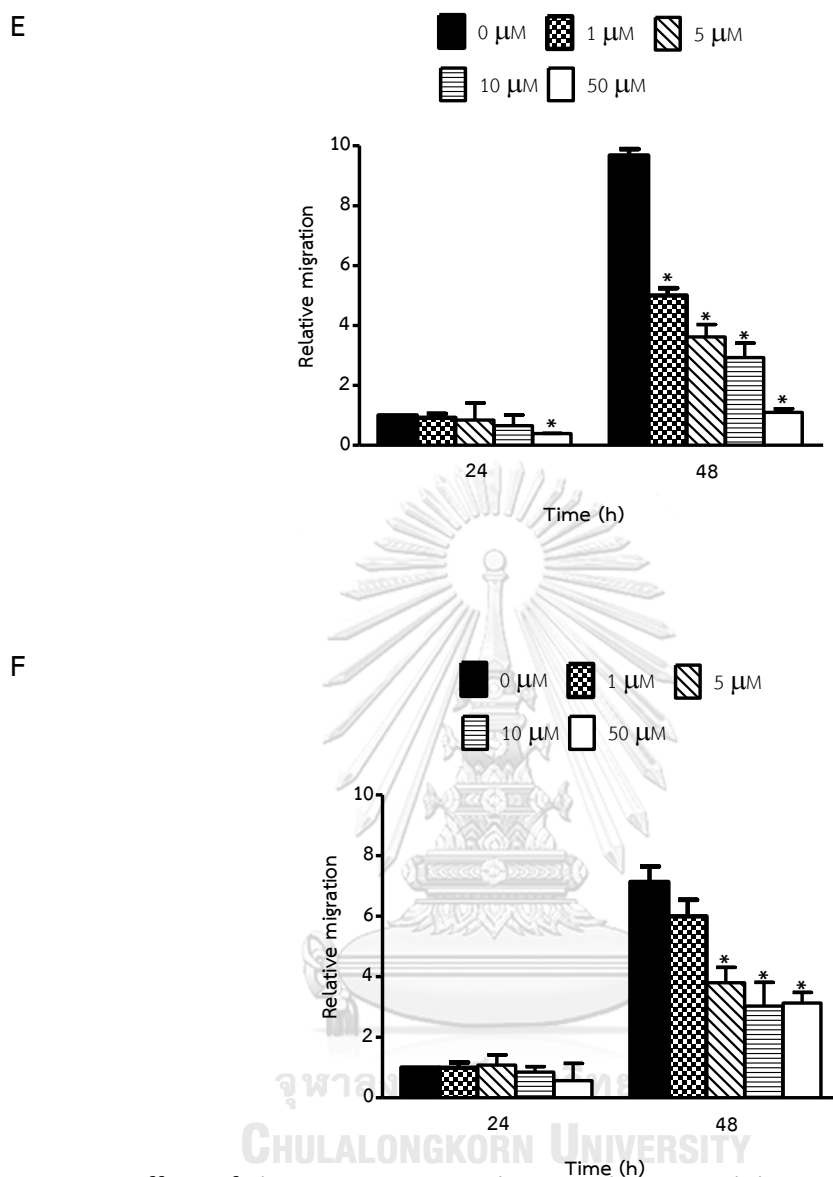


**Figure 16** Effect of chrysotoxine, crepidatin, and chrysotobibenzyl on lung cancer cell migration.

H460 cells were treated with 1–50  $\mu\text{M}$  of (A) and (D) chrysotoxine, (B) and (E) crepidatin, and (C) and (F) chrysotobibenzyl for 48 h. Cells were subjected to wound-healing assay for detecting wound space, with representing the relative migration levels. Data represent the mean  $\pm$  SD ( $n = 3$ ). \*  $p < 0.05$  versus non-treated control.

## Part 2. Evaluation the cytotoxicity of chrysotoxine on stemness of lung cancer cells.

### 2. The effects of chrysotoxine on the stem cell-like characteristics of lung cancer cells.

The key properties of CSCs include their ability for self-renewal and generation of differentiated progeny. CSCs and the self-renewal properties may be assessed by tumor sphere formation assay, which highlights the ability of tumor cells to form spheroids under accelerated conditions. Accordingly, the ability of chrysotoxine to suppress this activity was determined. A 3D-CSC-rich population was used as a primary baseline to examine the effect of the compound on CSCs, where the assay was exercised as previously described. Cells were passaged from first-generation tumor spheres to preserve the ability to form secondary spheroid generation. Following 14 days of culture, the secondary spheroids were selected into single 3D spheroids of a similar morphology and size, of which each spheroid was then treated with the various concentrations of chrysotoxine and subsequently monitored after 3 and 7 days of treatment. Representative images of the CSC spheroids in the control and chrysotoxine-treated cells at day 0, 3 and 7 are shown in Figure 17A. Treatment of the CSC spheres with chrysotoxine at 5–20  $\mu\text{M}$  significantly reduced the CSC populations in both H460 and H23 cells, with a significant decrease in the size of the H460 CSC spheres by approximately 40%, 53%, and 67% at day 3 after treatment with 5, 10, and 20  $\mu\text{M}$  of chrysotoxine, respectively, compared with the control (Figure 17B). In

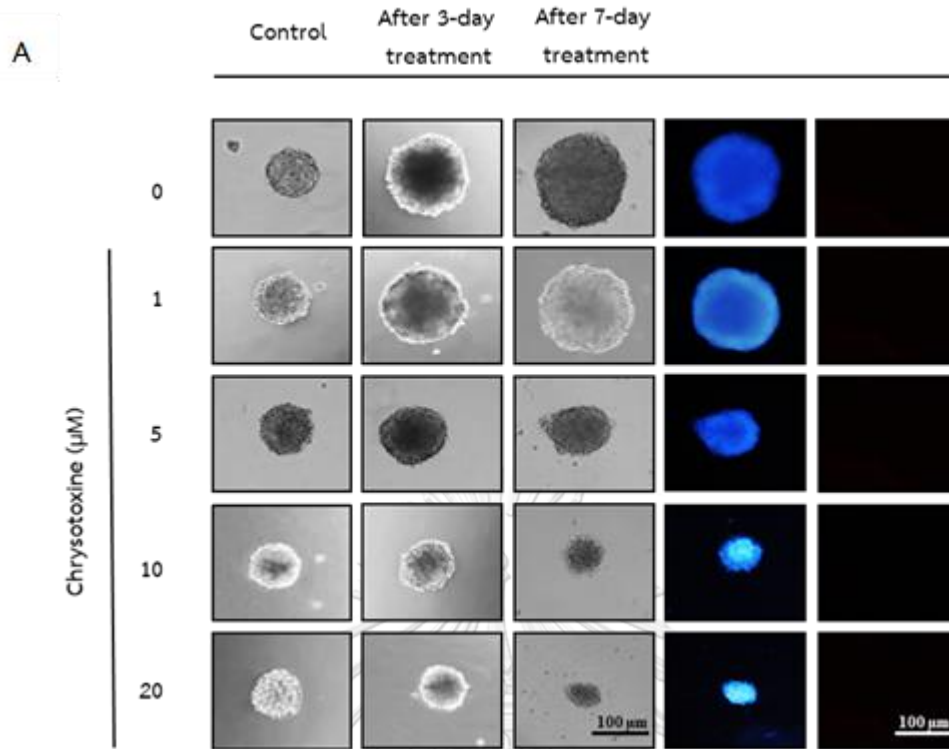
addition, a further decrease in the H460 CSC spheroid size by approximately 30%, 60%, 90%, and 95% relative to the control was seen in cells treated with 1, 5, 10, and 20  $\mu\text{M}$  of chrysotoxine, respectively, at day 7 (Figure 17B). Similar results were found for the H23 cells, in which treatment of H23 CSC spheres with chrysotoxine resulted in the dramatic shrinkage of spheroids in a dose-dependent manner (Figure 18A). Significant suppression was first detected in response to 5  $\mu\text{M}$  of chrysotoxine at day 3, with an approximately 30% size reduction of the CSC spheres; this decreased in size by approximately 40%, 60%, 80%, and 92% relative to the control after treatment with 1, 5, 10, and 20  $\mu\text{M}$  chrysotoxine, respectively, at day 7 (Figure 18B).

To assure the effect of chrysotoxine on the viability of CSC, CSC-rich populations of H460 and H23 cells were also treated with chrysotoxine for 48 h prior to determining the cell viability by the WST assay. Chrysotoxine at 5–50  $\mu\text{M}$  significantly decreased the CSC viability in both H460 and H23 cells (Figure 19 A and B), whereas chrysotoxine at 20 and 50  $\mu\text{M}$  induced a high level of apoptosis in both H460 and H23 CSCs after 48 h.

Moreover, an extreme limiting dilution assay was performed to examine the effect of chrysotoxine. Cells were treated for 48 h with compounds and then cells were re-plated again in 96 well plate with ultralow attach plate from 200 cells to 1 cell for 14 days. After 14 days, cells were counted to determine the capability to generate spheroids. Results indicated that while the non-treated control cells exhibited

ability to form tumor sphere, H460 and H23 cells treated with chrysotoxine failed to generate the spheres (Figure 20 A and B).





**B**

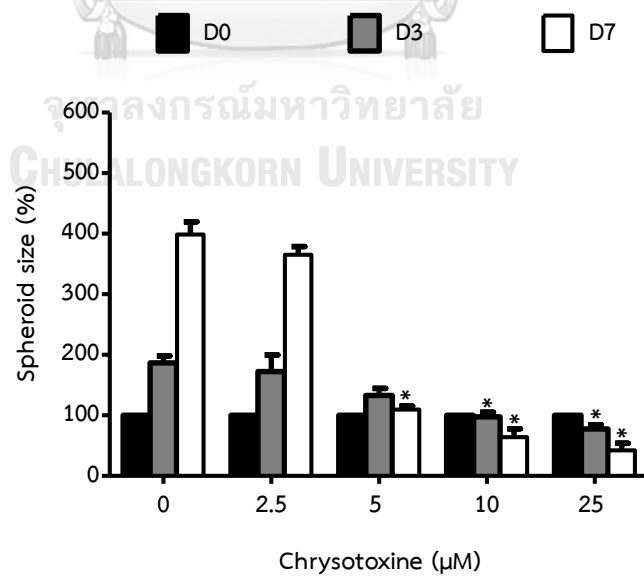




**Figure 17** The effect of chrysotoxine suppresses CSC-like phenotypes in CSC-rich population.

(A) H460 cells secondary spheroids were dissociated into single spheroids of the same size and treated with a non-cytotoxic concentration of chrysotoxine for 3 and 7 days. Phase-contrast images (4x) of secondary spheroids at day 0, 3 and 7 for the treated and untreated cells, and (B) the spheroid size relative to that of the untreated group.

All plots show the mean  $\pm$  SD (n = 3). \* P < 0.05 vs. untreated cells.



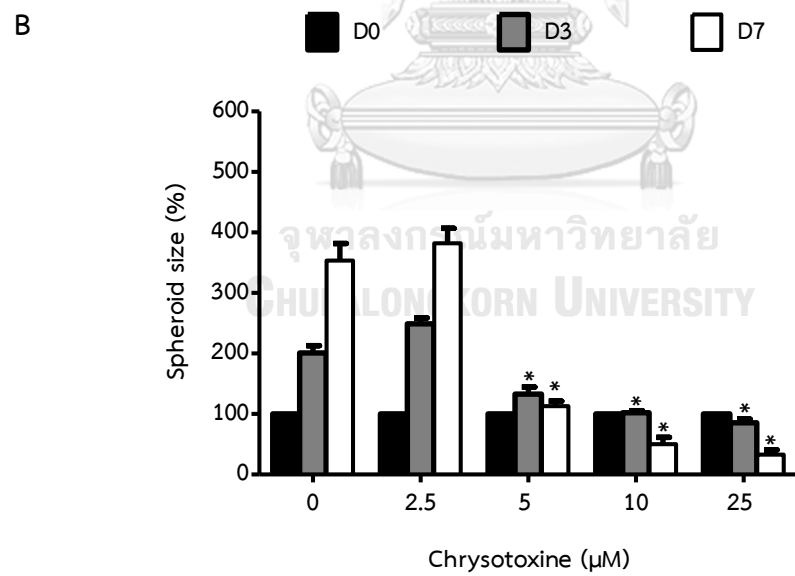
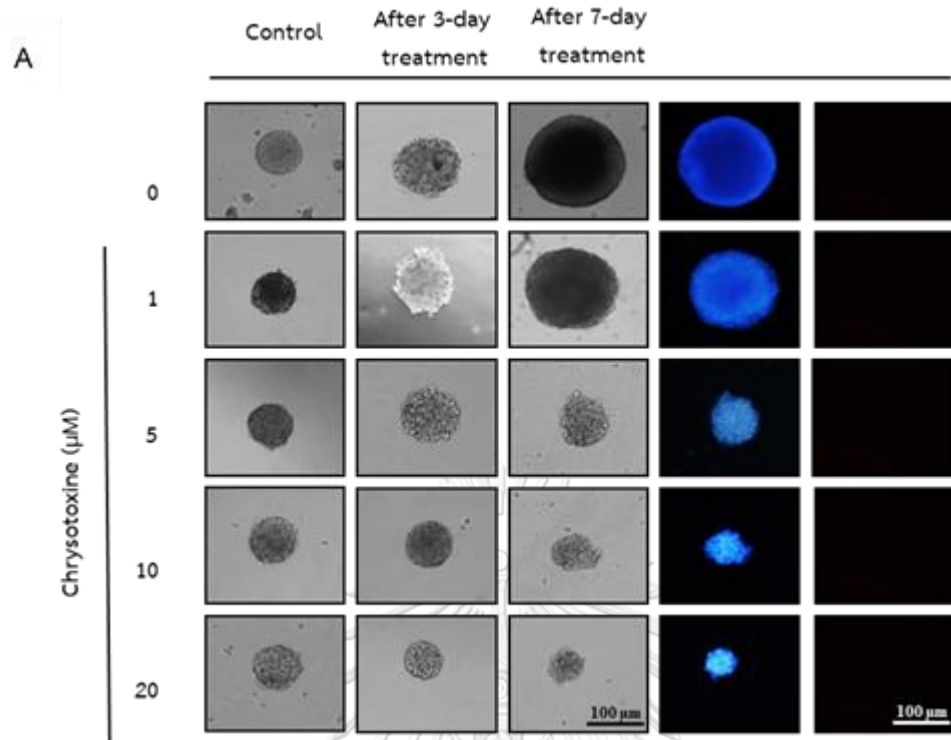


**Figure 18** The effect of chrysotoxine suppresses CSC-like phenotypes in CSC-rich population.

(A) H23 cells secondary spheroids were dissociated into single spheroids of the same size and treated with a non-cytotoxic concentration of chrysotoxine for 3 and 7 days. Phase-contrast images (4x) of secondary spheroids at day 0, 3 and 7 for the treated and untreated cells, and (B) the spheroid size relative to that of the untreated group.

All plots show the mean  $\pm$  SD (n = 3). \* P < 0.05 vs. untreated cells.



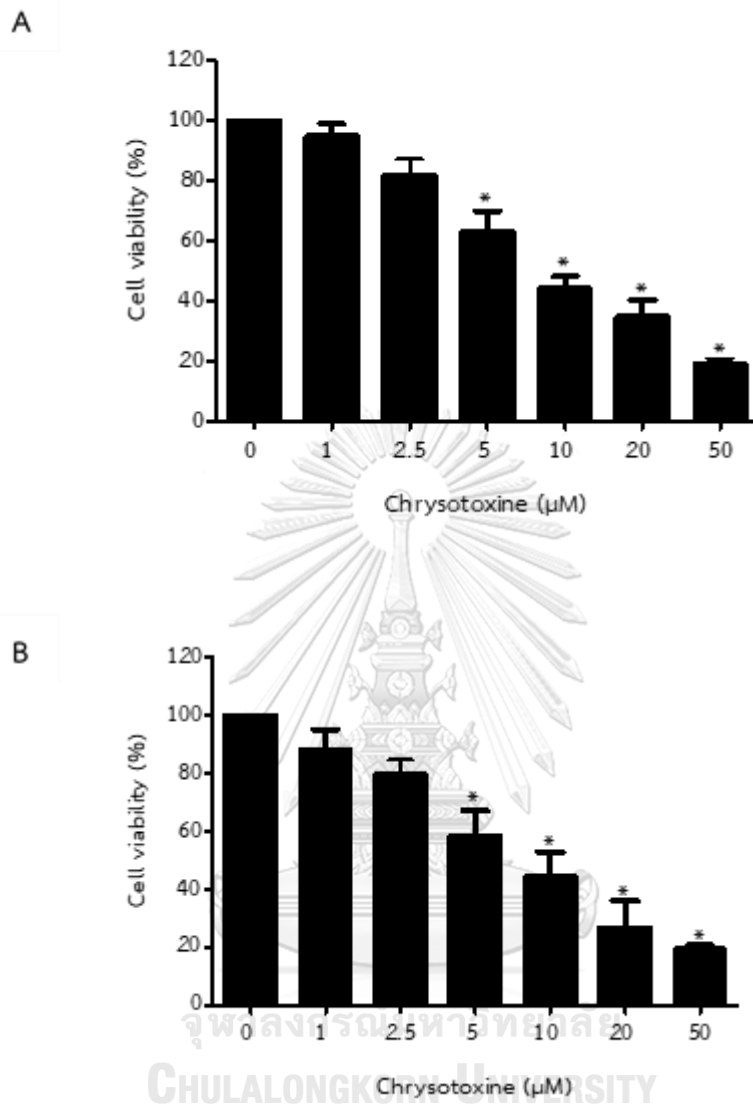


**Figure 19** The effect of chrysotoxine suppresses viability in CSC-rich population.

The cell viability of (A) H460 and (B) H23 cells in a detached condition were determined in the CSC-rich populations after treatment with or without a various concentration of chrysotoxine for 48 h and analyzed for cell viability using the WST assay. All plots show the mean  $\pm$  SD (n = 3). \* P < 0.05 vs. untreated cells.

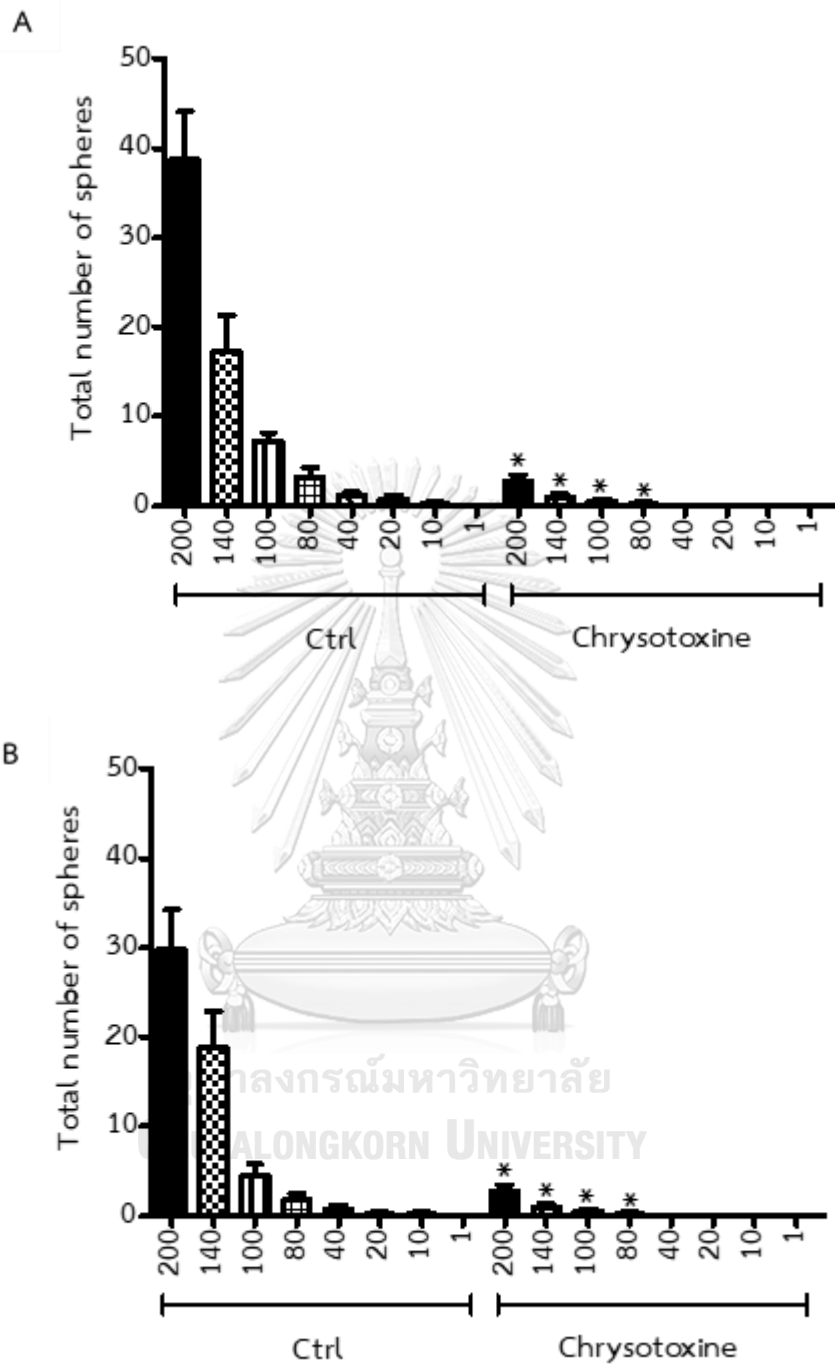


**Figure 20** The effect of chrysotoxine on the capability for generating spheroids.

(A) H460 and (B) H23 cells were plated in decreasing numbers from 200 cells/well to 1 cell/well in 200  $\mu$ l RPMI and cultured for 14 days whereupon the number of wells containing spheres for each cell was calculated. Bars are the mean  $\pm$  SD (n = 3). \* P < 0.05 vs. untreated cells.

### 3. The effects of chrysotoxine on the stem cell markers of lung cancer cells.

Given that chrysotoxine caused an apparent decline in CSCs in terms of the spheroid size and cell viability, the effect of chrysotoxine on the CSC biomarkers CD133, CD44, and ABCG2 was determined to further confirm the CSC-suppressing effect of compounds. H460 and H23 cells were treated with chrysotoxine (0–20  $\mu$ M) for 48 h. The expression levels of CD133, CD44, and ABCG2 were evaluated by Western blot analysis. Chrysotoxine significantly decreased the cellular levels of CD133, CD44, and ABCG2 in both H460 and H23 cells in dose-dependent manner (Figure 20). Taken together, a clear CSC-suppressive effect of chrysotoxine in these lung cancer cells was established.

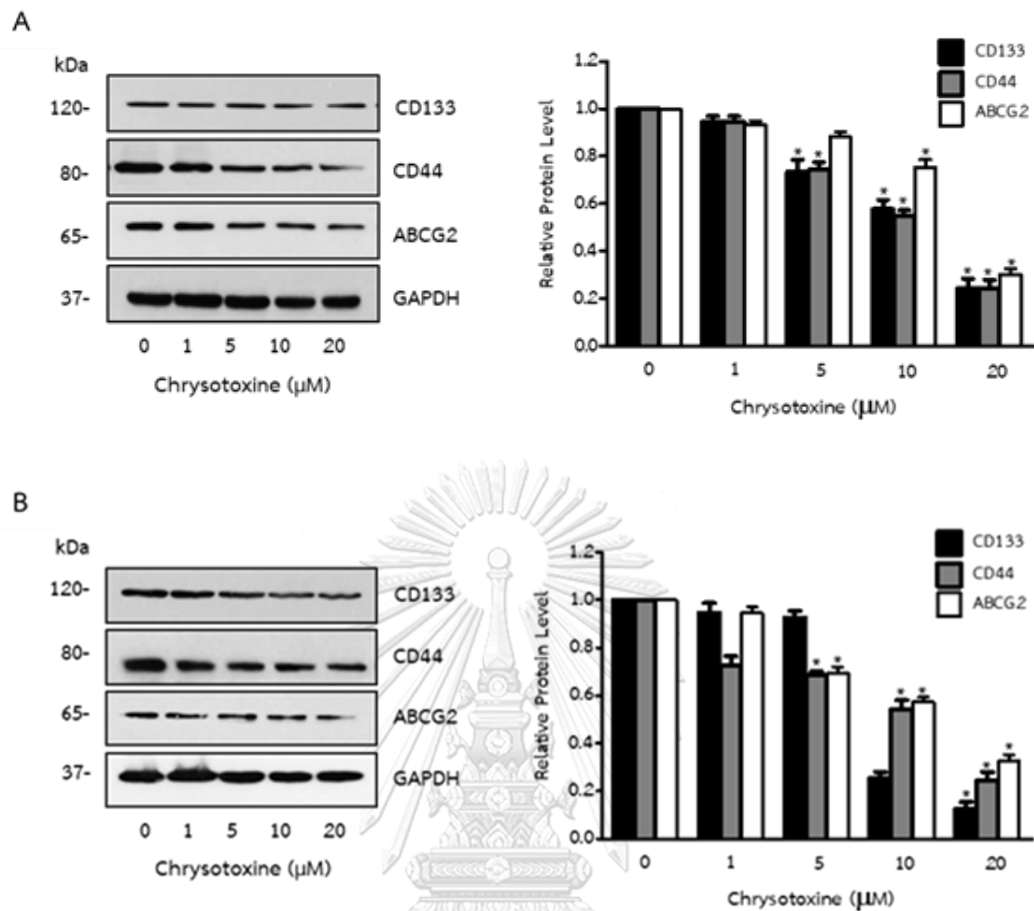


**Figure 21** Effect of chrysothoxine on CSC markers in H460 and H23 cells.

(A) H460 cells and (B) H23 were treated in the presence or absence of chrysothoxine (0 - 20  $\mu\text{M}$ ) for 48 h. The cell lysate was then collected and evaluated for the level of the lung CSC biomarkers as lysate levels of CD133, CD44, and ABCG2 using Western blotting, reprobing the blots with GAPDH to confirm equal loading of samples. Bars show the mean  $\pm$  SD (n = 3). \* P < 0.05 vs. untreated cells.

#### 4. The effects of chrysotoxine on Sox2 via Src-Akt signaling cascade in lung cancer cells.

As previously documented that stem cells possess the ability to retain the capacity for renewing themselves, we next investigated whether chrysotoxine could affect the self-renewal-related proteins. The major transcription factors involved in the maintenance of pluripotency and self-renewal in human lung cancer stem cells include Sox2, Oct4 and Nanog. Among all, Sox2 was shown to be involved in the maintenance of CSC characteristics in lung cancer. Recent studies have shown that proto-oncogene tyrosine-protein kinase Src is the upstream regulator of Sox2 (Weina & Utikal, 2014). Src is a critical component in many signaling pathways that regulate survival, metastasis, and stemness characteristics. Importantly, Src increases the cellular expression level of Sox2, the self-renewal pluripotency transcription factor in non-small cell lung cancer cells (S. Singh et al., 2012). The activation of Src via phosphorylation at Y416 was shown to activate Akt (phosphorylation at Ser473), which is an important mediator for cell survival, proliferation, and Sox2-regulated stemness. Taken together, the cellular signals mentioned are potential molecular targets for suppressing CSC-like phenotypes. In order to determine the underlying mechanism of chrysotoxine-mediated suppression of CSCs, human lung cancer cells were treated with chrysotoxine for 48 h and the expression levels of p-Src, Src, p-Akt, Akt and Sox2 were determined by western blot analysis. Compared to the control cells, chrysotoxine caused a significant decrease in the level of p-Src and p-Akt in a dose-dependent



manner (Figure 21 A and B), whereas the level of total Src and Akt were not altered. Also, the down-stream stem cell transcription factor Sox2 was significantly reduced following the decline in the level of p-Src. These results suggested that chrysotoxine decreased the stem cell machinery in lung cancer cells, at least in part, by suppressing transcription factor Sox2 through a Src-Akt pathway.

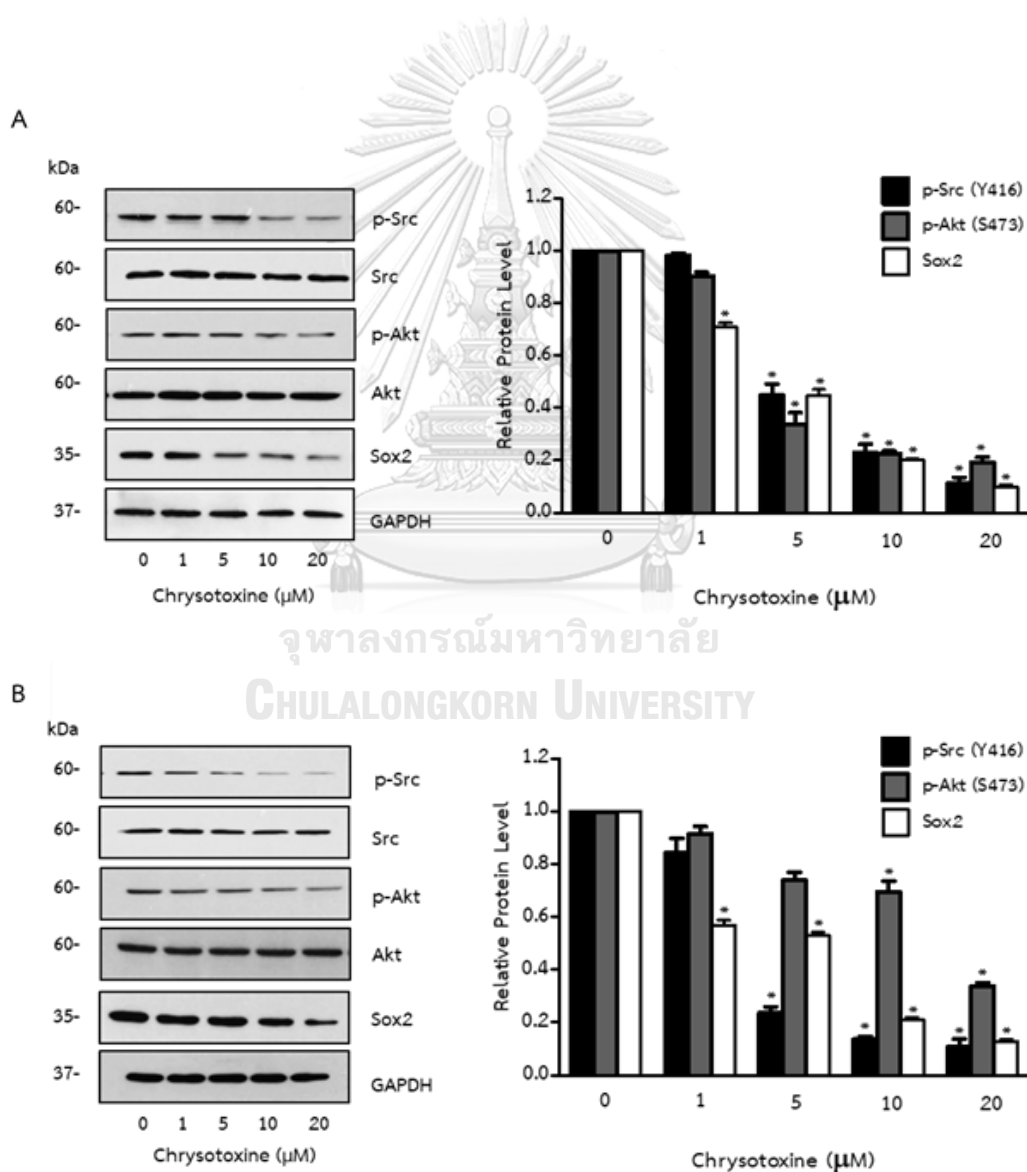


**Figure 22** Effect of chrysotoxine on Src/Akt/Sox2 mechanism in H460 and H23 cells.

(A) H460 and (B) H23 cells were treated in the presence or absence of chrysotoxine (0 - 20  $\mu$ M) for 48 h. The cell lysate was then collected and evaluated for the level of p-Src, Src, p-Akt, Akt and Sox2 using Western blotting, reprobing the blots with GAPDH to confirm equal loading of samples. Bars show the mean  $\pm$  SD (n = 3). \* P < 0.05 vs. untreated cells.

### 5. The effect of chrysotoxine on epithelial-mesenchymal transition (EMT) in lung cancer cells.

Recently, the process of the cell transition from epithelial to mesenchymal phenotypes (EMT) has gained increasing interest in cell biology, as it was reported to increase the stem cell-like phenotypes in various cells. Furthermore, previous reviews found that the up-regulated transcription factors during EMT process, such as slug, and snail were shown to maintain the cancer stem cell-like phenotypes in many cells. In order to investigate whether the treatment of lung cancer H460 cells with chrysotoxine have a part in the reduction of stem cell phenotypes through this pathway, the EMT activating transcription factors, which included Vimentin, Slug, and Snail and also with E-cadherin which is cell-cell adhesion molecule with pivotal roles in epithelial cells, were also detected by western blot analysis. Figure 23 illustrates that the significant down-regulation of cellular levels of Vimentin, Slug and Snail after incubation with chrysotoxine for 48 h. However, E-cadherin was found to be increased in response to chrysotoxine treatment. Taken together, these results illustrated that chrysotoxine

inhibit the cancer stem cell-like phenotypes in the human lung cancers H460 cells by the suppression of EMT.



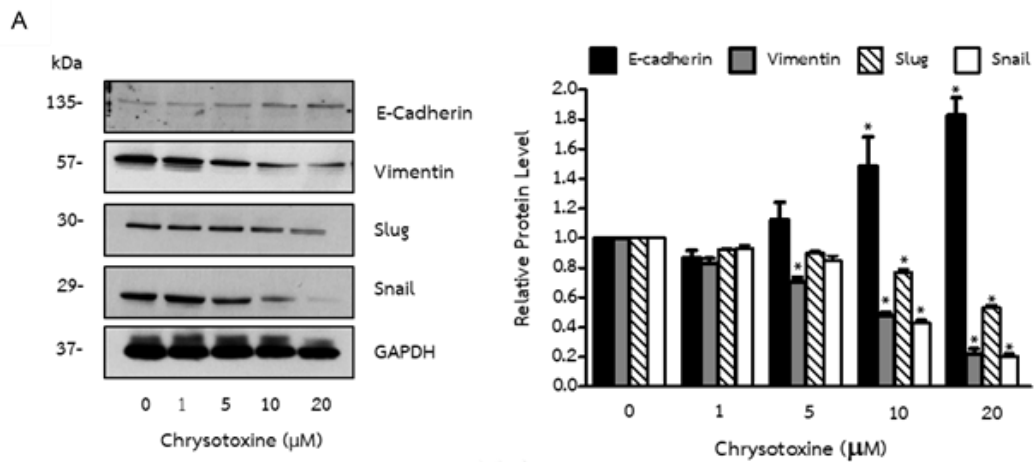


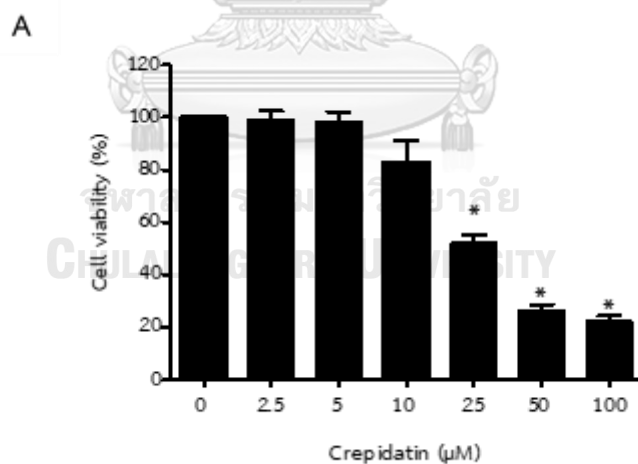
**Figure 23** Effect of chrysotoxine on EMT markers.

(A) H460 cells were treated in the presence or absence of chrysotoxine (0 - 20 μM) for 48 h. The cell lysate was then collected and evaluated for the level of E-cadherin, Vimentin, Slug and Snail using Western blotting, reprobing the blots with GAPDH to confirm equal loading of samples. Bars show the mean ± SD (n = 3). \* P < 0.05 vs. untreated cells.

### Part 3. Evaluation the cytotoxicity of crepidatin on stemness of lung cancer cells.

#### 6. Cytotoxic effect of crepidatin on human lung cancer cells.

Since crepidatin showed the highest potency to kill human lung cancer cells with the lowest  $IC_{50}$  values in H460 and H23 cells compared to chrysotoxine and chrysotobibenzyl. Crepidatin was used as a drug targeting model for lung cancer stem cells. Therefore, the effect of crepidatin were screened in various human lung cancer cell lines. It was found that crepidatin showed the highest cytotoxicity to decrease cell viability in H460 and A549 than others, thus, we next verified the effects of crepidatin on the stem cell-like phenotypes in H460 and A549 (Figure 24).



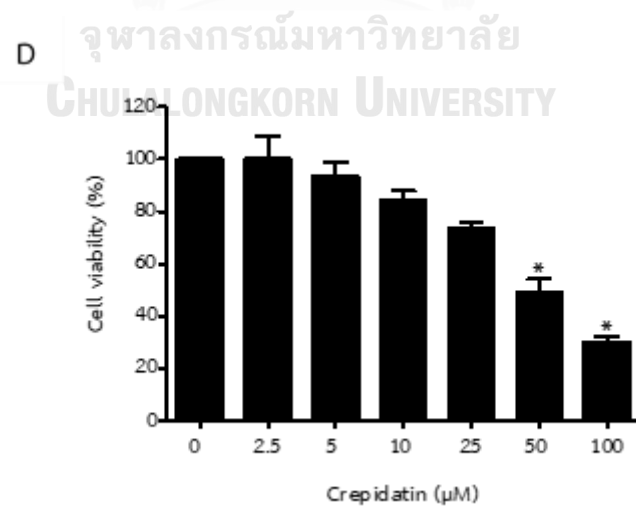
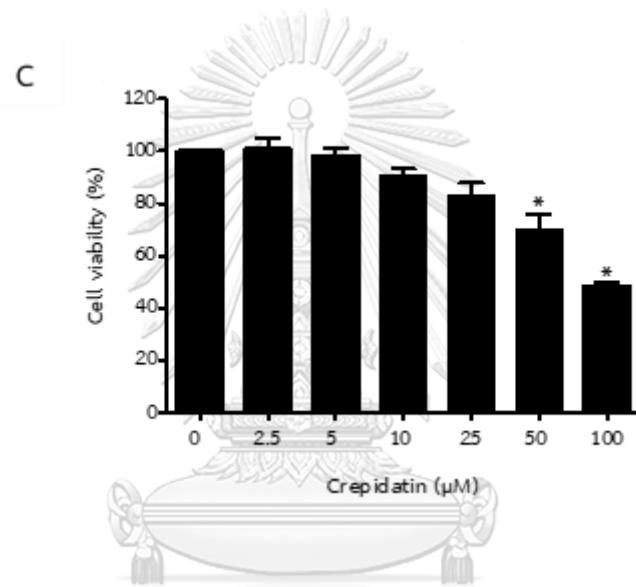
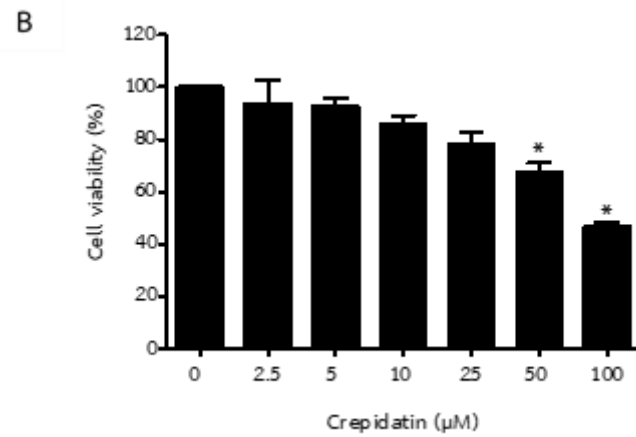


**Figure 24** Cytotoxic effect of crepidatin on various human lung cancer.

(A) H460, (B) H23, (C) H292 and (D) A549 cells were treated with various concentrations of crepidatin (0–100  $\mu\text{M}$ ) for 48 h and then the cell viability was determined by the MTT assay, relative to the viability of untreated cells set as 100%. The data is presented as mean  $\pm$  SD (n=3).

## 7. The effects of crepidatin on the stem cell-like characteristics of lung cancer cells.

A 3D-CSC rich model was also used to determine the effect of crepidatin on CSCs. After 14 days of culture, the secondary spheroids were selected into single 3D spheroids of a similar morphology and size. Each spheroid was then treated with the various concentrations of crepidatin and monitored after 3 and 7 days of treatment. Representative images of the CSC spheroids in the control and crepidatin-treated cells at days 0, 3, and 7 are shown in Figure 25 and Figure 26. Treatment of the CSC spheres with crepidatin at 5–25  $\mu\text{M}$  significantly reduced the CSC populations in both H460 and A549 cells, with a significant decrease in the size of the H460 CSC spheres by approximately 70%, and 80% at day 3 after treatment with 10 and 25  $\mu\text{M}$  crepidatin, respectively, compared with the control (Figure 25B). In addition, a further decrease in the H460 CSC spheroid size by approximately 80%, 90%, and 95% relative to the control was seen in cells treated with 5, 10, and 25  $\mu\text{M}$  of crepidatin, respectively, at day 7 (Figure 25B). Similar results were found for the A549 cells, in which treatment of

A549 CSC spheres with crepidatin resulted in the dramatic shrinkage of spheroids in a dose-dependent manner (Figure 26). Significant suppression was first detected in response to 5  $\mu\text{M}$  of crepidatin at day 3, with an approximately 30% size reduction of the CSC spheres; this decreased in size by approximately 20%, 70%, 80%, and 90% relative to the control after treatment with 2.5, 5, 10, and 25  $\mu\text{M}$  of crepidatin, respectively, at day 7 (Figure 26B). To support the effect of crepidatin on the viability of CSC, CSC-rich populations of H460 and A549 cells were also treated with crepidatin for 48 h before determining the cell viability by the WST assay. Crepidatin at 10–50  $\mu\text{M}$  significantly decreased the CSC viability in both H460 and A549 cells (Figure 27), whereas crepidatin at 25 and 50  $\mu\text{M}$  induced a high level of apoptosis in both H460 and A549 CSCs after 48 h (Figure 27).

Furthermore, a limiting dilution assay was conducted to verify the effect of crepidatin on CSC's phenotypes. Cells were also pre-treated for 48 h with crepidatin and subsequently re-plated again from 200 cells to 1 cell for 14 days. After 14 days, cells were counted for capable to generate spheroid. Results indicated that while the non-treated control cells exhibited ability to form tumor sphere, H460 and A549 cells treated with crepidatin failed to generate spheres as well as in chrysothoxine treatment compared to control cells (Figure 28).



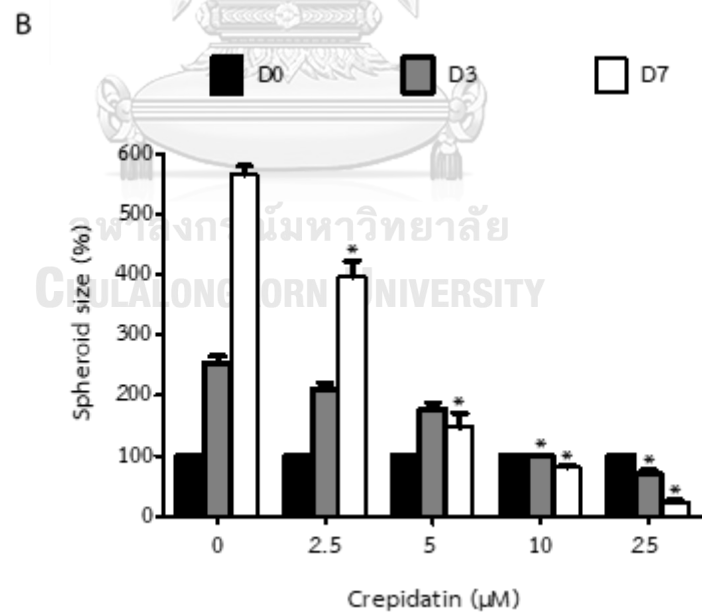
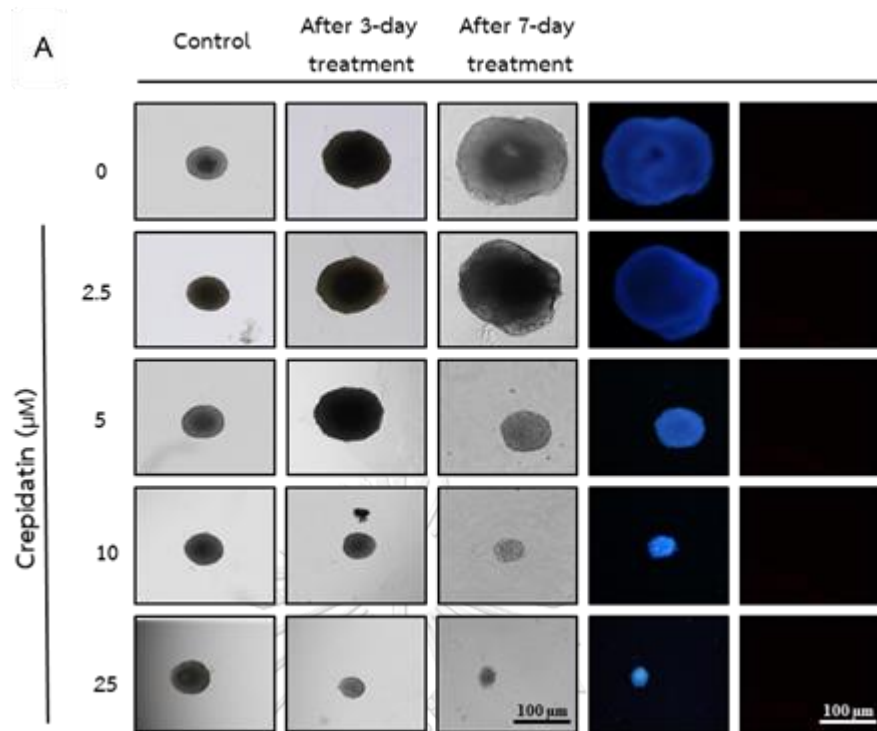
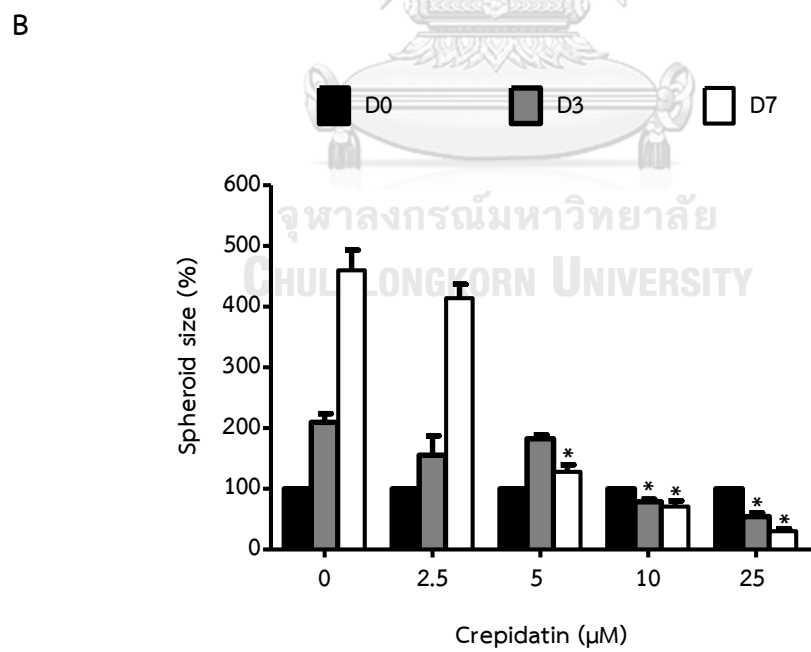
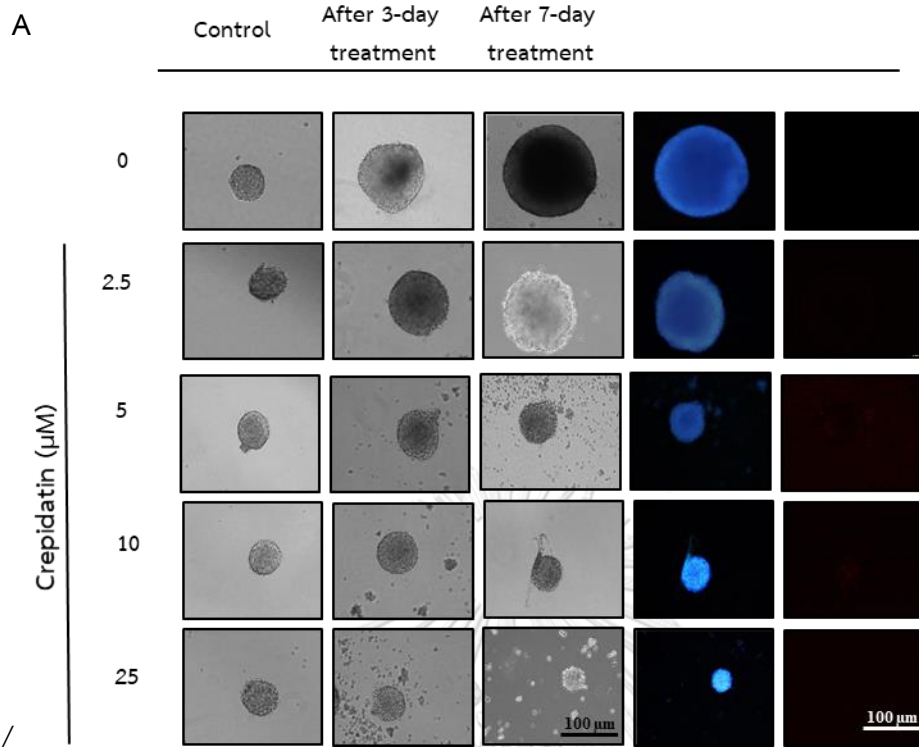


**Figure 25** The effect of crepidatin suppresses CSC-like phenotypes in CSC-rich population.

(A) H460 cells secondary spheroids were dissociated into single spheroids of the same size and treated with a non-cytotoxic concentration of chrysotoxine for 3 and 7 days. Phase-contrast images (4x) of secondary spheroids at day 0, 3 and 7 for the treated and untreated cells, and (B) the spheroid size relative to that of the untreated group.

All plots show the mean  $\pm$  SD (n = 3). \* P < 0.05 vs. untreated cells.

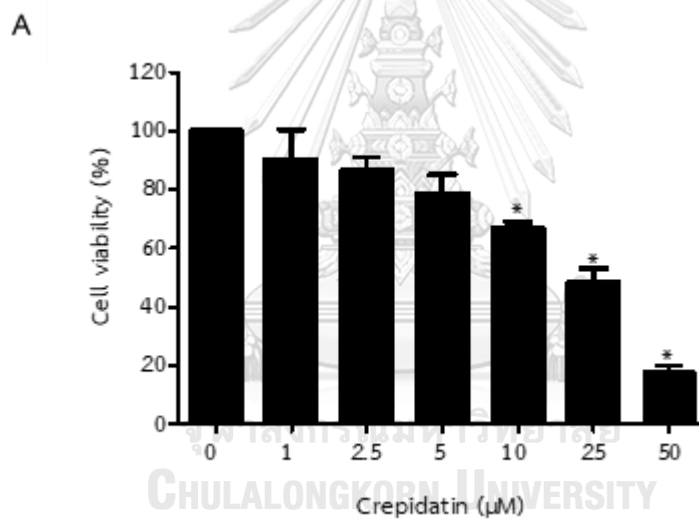




**Figure 26** The effect of crepidatin suppresses CSC-like phenotypes in CSC-rich population.

(A) A549 cells secondary spheroids were dissociated into single spheroids of the same size and treated with a non-cytotoxic concentration of chrysotoxine for 3 and 7 days. Phase-contrast images (4x) of secondary spheroids at day 0, 3 and 7 for the treated and untreated cells, and (B) the spheroid size relative to that of the untreated group.

All plots show the mean  $\pm$  SD (n = 3). \* P < 0.05 vs. untreated cells.



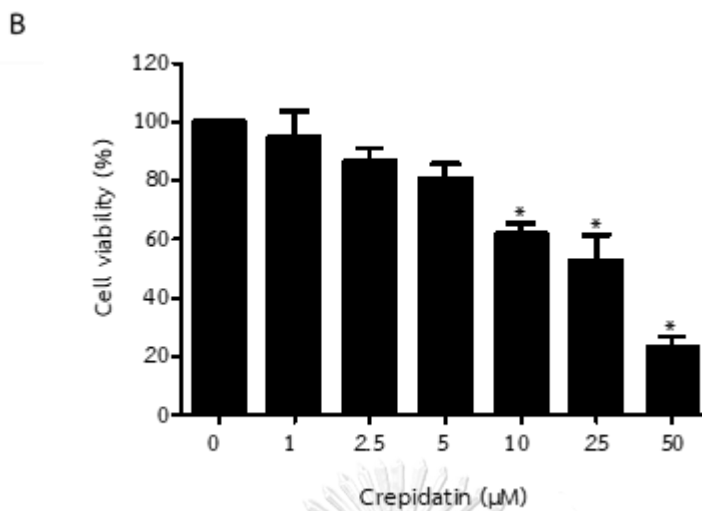


**Figure 27** The effect of crepidatin suppresses viability in CSC-rich population.

The cell viability of (A) H460 and (B) A549 cells in a detached condition were determined in the CSC-rich populations after treatment with or without a various concentration of crepidatin for 48 h and analyzed for cell viability using the WST assay.

All plots show the mean  $\pm$  SD (n = 3). \* P < 0.05 vs. untreated cells.

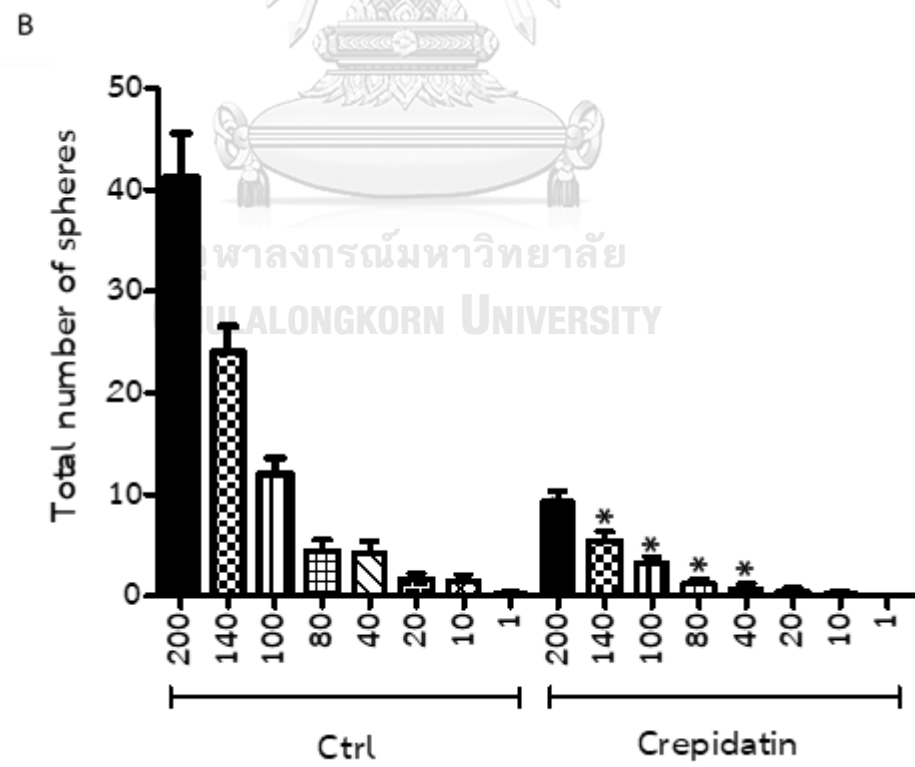
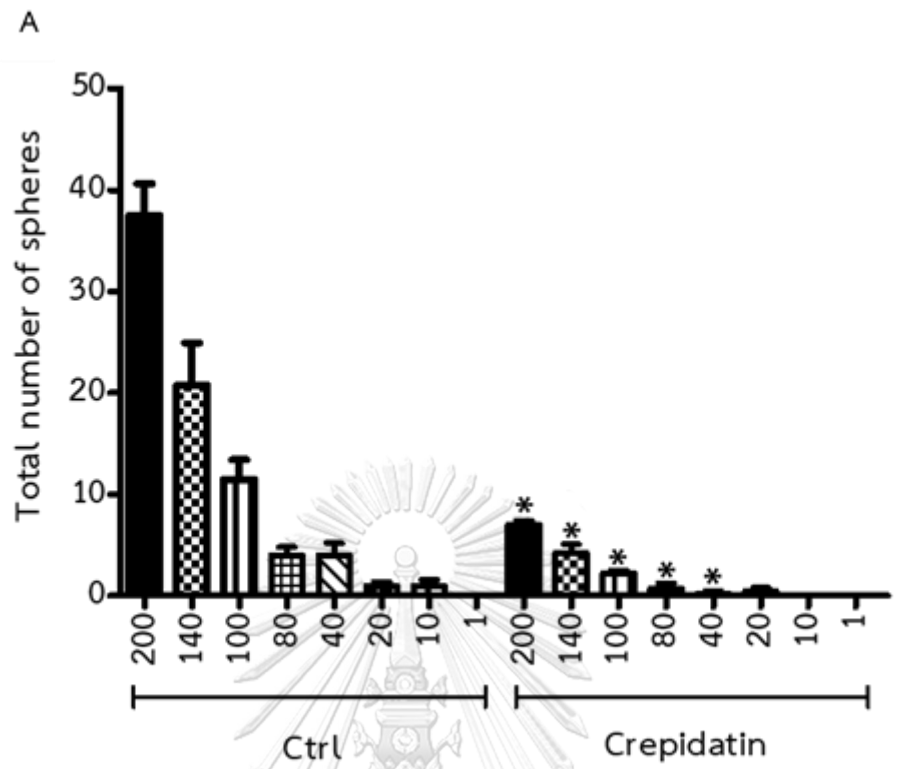


**Figure 28** The effect of crepidatin on the capability for generating spheroids.

(A) H460 and (B) A549 cells were plated in decreasing numbers from 200 cells/well to 1 cell/well in 200  $\mu$ l RPMI and cultured for 14 days whereupon the number of wells containing spheres for each cell was calculated. Bars are the mean  $\pm$  SD (n = 3). \* P < 0.05 vs. untreated cells.

### 8. The effects of crepidatin on the stem cell-like characteristics of lung cancer cells.



The results were similar to chrysotoxine treatment, as crepidatin also significantly decreased the expression level of CD133, CD44, and ABCG2 in H460 and A549 cells when compared to their control cells and significantly decreased by crepidatin in a dose-dependent manner more than an 70% reduced expression level in the both H460 at 25  $\mu$ M of crepidatin (Figure 29). Taken together, a clear CSC-suppressive effect of crepidatin in these lung cancer cells was established. Figure 30 also represents in H460 cells that there were the significant down-regulation of cellular levels of Vimentin, Slug and Snail after incubation with crepidatin for 48 h. On the other hand, increased E-cadherin expression was found in crepidatin treatment. Taken together, these results illustrated that crepidatin inhibited the cancer stem cell-like phenotypes in the human lung cancers H460 cells by the suppression of EMT.

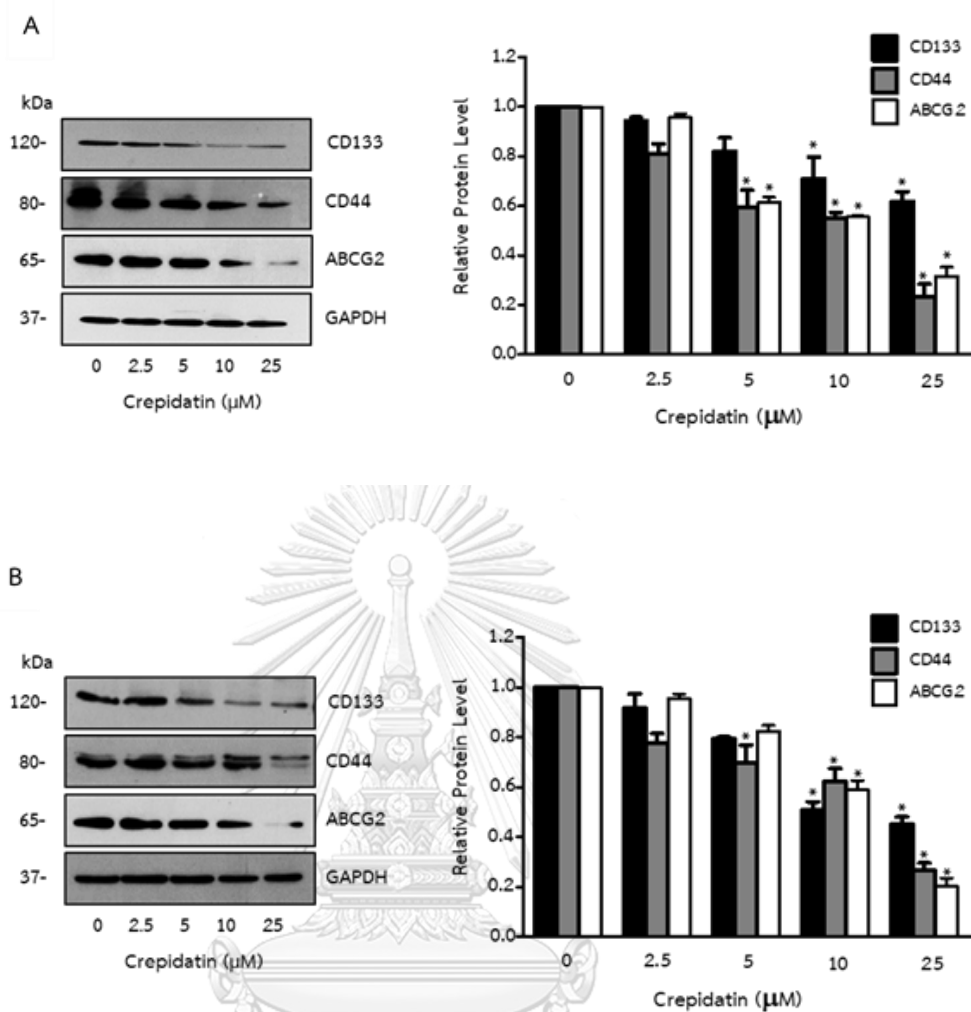


**Figure 29** Effect of crepidatin on CSC markers in H460 and A549 cells.

(A) H460 cells and (B) A549 were treated in the presence or absence of crepidatin (0 - 25  $\mu\text{M}$ ) for 48 h. The cell lysate was then collected and evaluated for the level of the lung CSC biomarkers as lysate levels of CD133, CD44, and ABCG2 using Western blotting, reprobing the blots with GAPDH to confirm equal loading of samples. Bars show the mean  $\pm$  SD (n = 3). \* P < 0.05 vs. untreated cells.



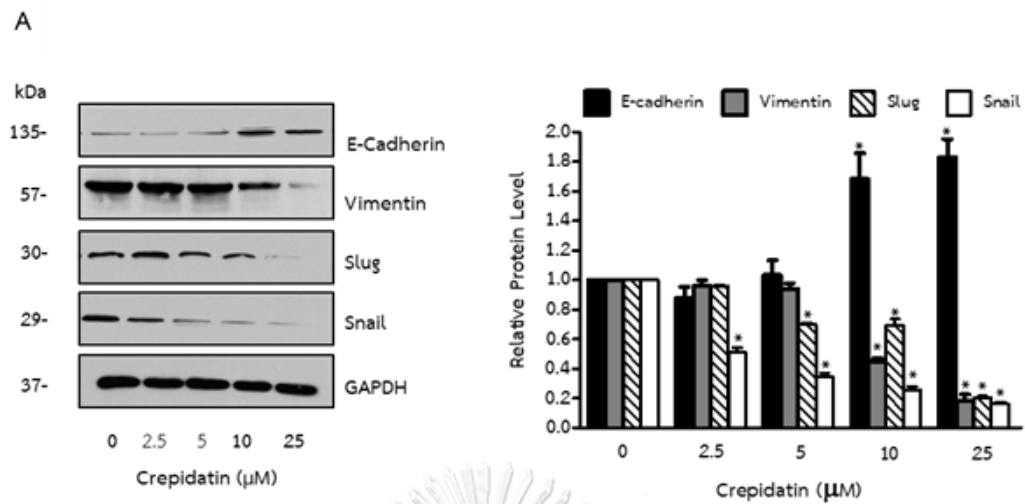


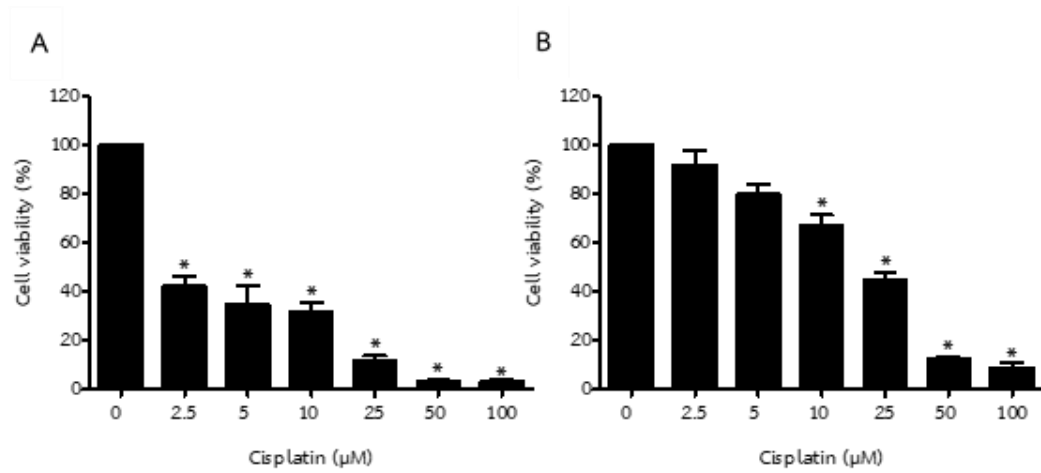
**Figure 30** Effect of crepidatin on EMT markers.

(A) H460 cells were treated in the presence or absence of crepidatin (0 - 25  $\mu\text{M}$ ) for 48 h. The cell lysate was then collected and evaluated for the level of EMT biomarkers as lysate levels of E-cadherin, Vimentin, Slug, and Snail using Western blotting, reprobing the blots with GAPDH to confirm equal loading of samples. Bars show the mean  $\pm$  SD (n = 3). \* P < 0.05 vs. untreated cells.

**Part 4. The effects of crepidatin developed as drug targeting of cancer stem cells treatment in lung cancer cells.**

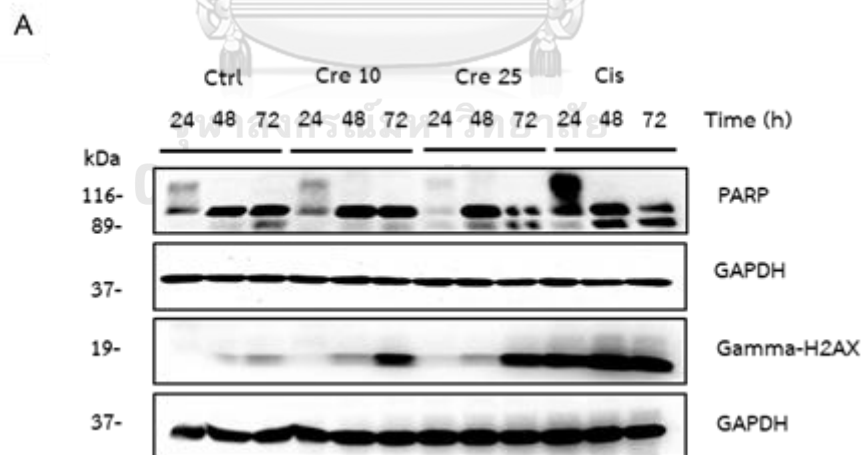
**9. The effect of crepidatin on apoptosis in lung cancer cells comparing to cisplatin.**

An important characteristic of lung CSCs is drug resistance; hence further tests were conducted to determine whether crepidatin could reverse drug resistance in lung cancer cells. In the treatment process of lung cancer, cisplatin is the most commonly prescribed drug for lung cancer therapy. In this study, cisplatin was used as a positive control (Figure 31). Western blotting results showed in Figure 32 demonstrated that crepidatin induced apoptotic marker cleaved PARP expression in lung cancer cells in time and dose-dependent manner in both H460 and A549 cells. The apoptosis induction is caused by mediated DNA damage. To detect DNA double strand breaks following crepidatin treatment, the levels of the DNA damage marker, p-H2AX, were determined by western blotting. An increased in p-H2AX levels was detected in both H460 and A549 cell lines in a time and dose dependent manner. Furthermore, cisplatin, which was used as positive control for treatment, also induced apoptosis by increasing cleaved PARP and p-H2AX markers in both cell lines. These results indicated that both crepidatin and cisplatin induced the pathway of apoptosis thus facilitating cell death in lung cancer cells.



**Figure 31** Cytotoxic effect of cisplatin on human lung cancer.

(A) H460 and (B) A549 cells were treated with various concentrations of cisplatin (0–100  $\mu\text{M}$ ) for 48 h and then the cell viability was determined by the MTT assay, relative to the viability of untreated cells set as 100%. The data is presented as mean  $\pm$  SD (n=3).



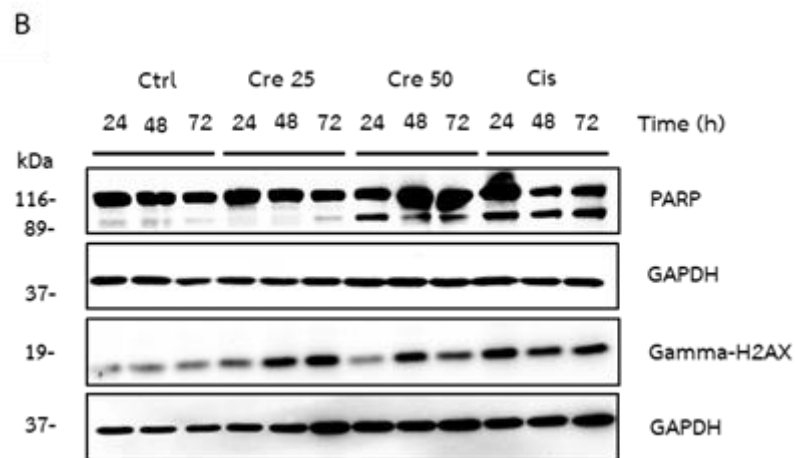


**Figure 32** Effect of crepidatin and cisplatin on apoptotic markers on human lung cancer H460 and A549 cells.

(A) H460 and (B) A549 cells lysate were then collected and evaluated for the level of apoptotic marker, including PARP, and DNA damage marker, p-H2AX using Western blotting. Blots were re-probed with GAPDH to confirm equal loading of samples. All plots are means  $\pm$  SD ( $n = 3$ ). \*  $P < 0.05$  vs. non-treated cells.

## 10. The effect of crepidatin and cisplatin on CSC-like phenotype on lung cancer cells.

As we conceived from previous results that crepidatin had ability to abrogate the growth of CSCs in sphere formation in lung cancer. To study long term survival of colony formation, according to determine the survival and proliferative capacity of the H460 and A549 cells following treatment with crepidatin and cisplatin, clonogenic assay was used for evaluation. In this assay, both cells were pretreated with crepidatin

and cisplatin in non-cytotoxic dose and  $IC_{50}$  concentrations for 48 h. After indicated time, cells then were counted and re-plated in a low number with 250 cells in 6-well plate. After 10 days of growth, cells were stained with crystal violet and colonies were counted. Representative stained colony plates are shown in Figure 33 and Figure 34. H460 cell colony numbers were significantly decreased in crepidatin treatment compared to untreated control groups with 35% reduction in 10  $\mu$ M of crepidatin and more than 60% reduction in 25  $\mu$ M of crepidatin (Figure 33). Figure 34 shows the colony numbers of A549 cells were significantly decreased in crepidatin treatment compared to untreated control groups with 40% reduction in 25  $\mu$ M of crepidatin and more than 80% reduction of  $IC_{50}$  of crepidatin. Interestingly, we discovered that it was found to be increased in colony number in response to cisplatin treatment in both cell lines. Likewise, limiting dilution assay was also performed to verify the effect of crepidatin and cisplatin. Cells were treated with both compounds at  $IC_{50}$  value for 48 h and then cells were re-plated from 200 cells to 1 cell for 14 days. After 14 days, cells were counted to assess the capability to generate spheroid. Results indicated that while the non-treated control cells exhibited ability to form tumor sphere, H460 and A549 cells treated with crepidatin failed to generate sphere. On the other hand, there were no effect on sphere generating in cisplatin treatment. (Figure 35).

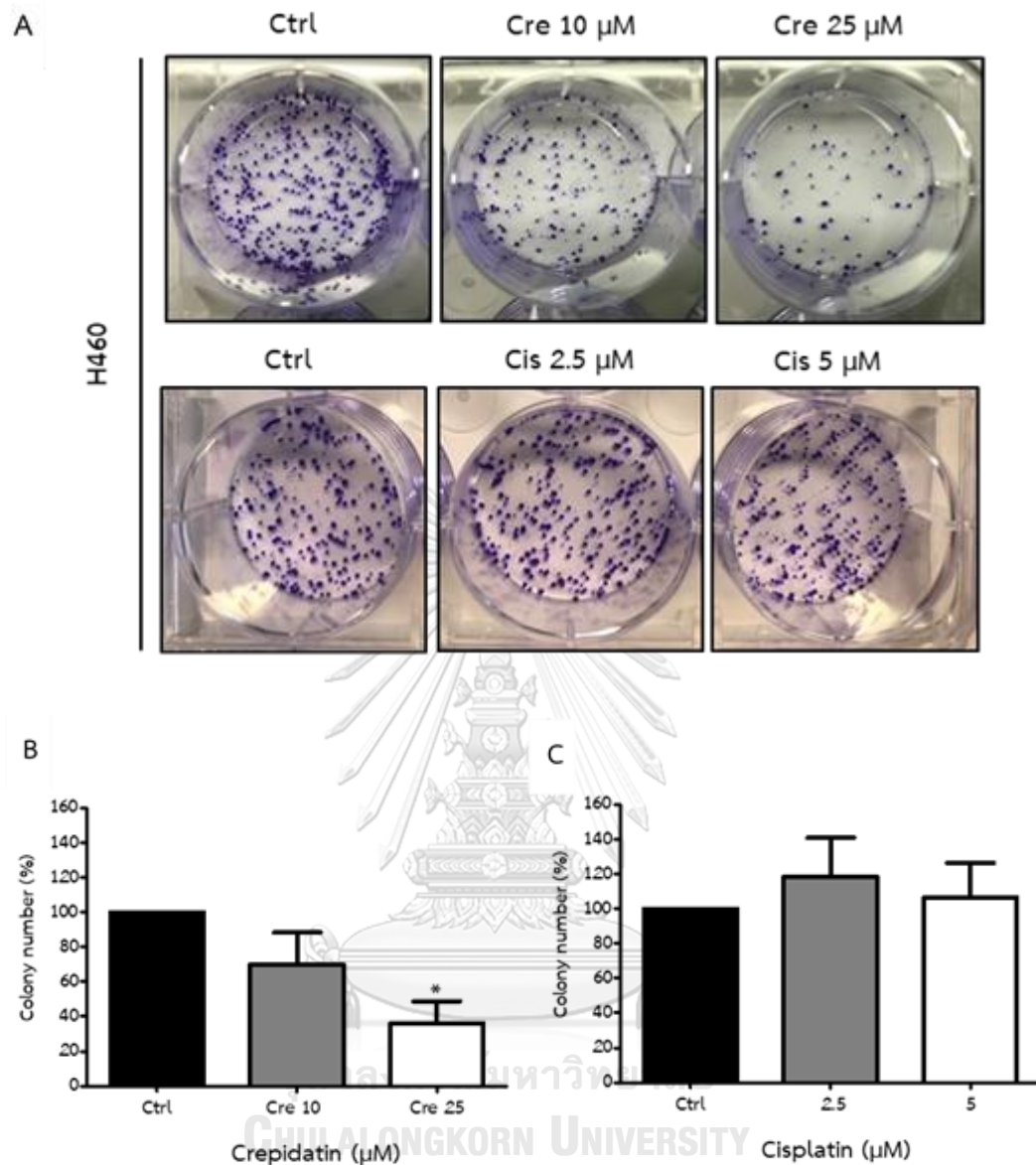


**Figure 33** Effect of crepidatin suppresses CSC-like phenotypes in H460 cells.

H460 cells were pretreated with crepidatin and cisplatin in non-cytotoxic dose and  $\text{IC}_{50}$  concentrations for 48 h. Then, cells were counted and re-plated in a low number with 250 cells for 10 days and then cells were stained with crystal violet and colonies were counted by Image Pro Plus program. All plots are means  $\pm$  SD (n = 3). \* P < 0.05 vs. non-treated cells.

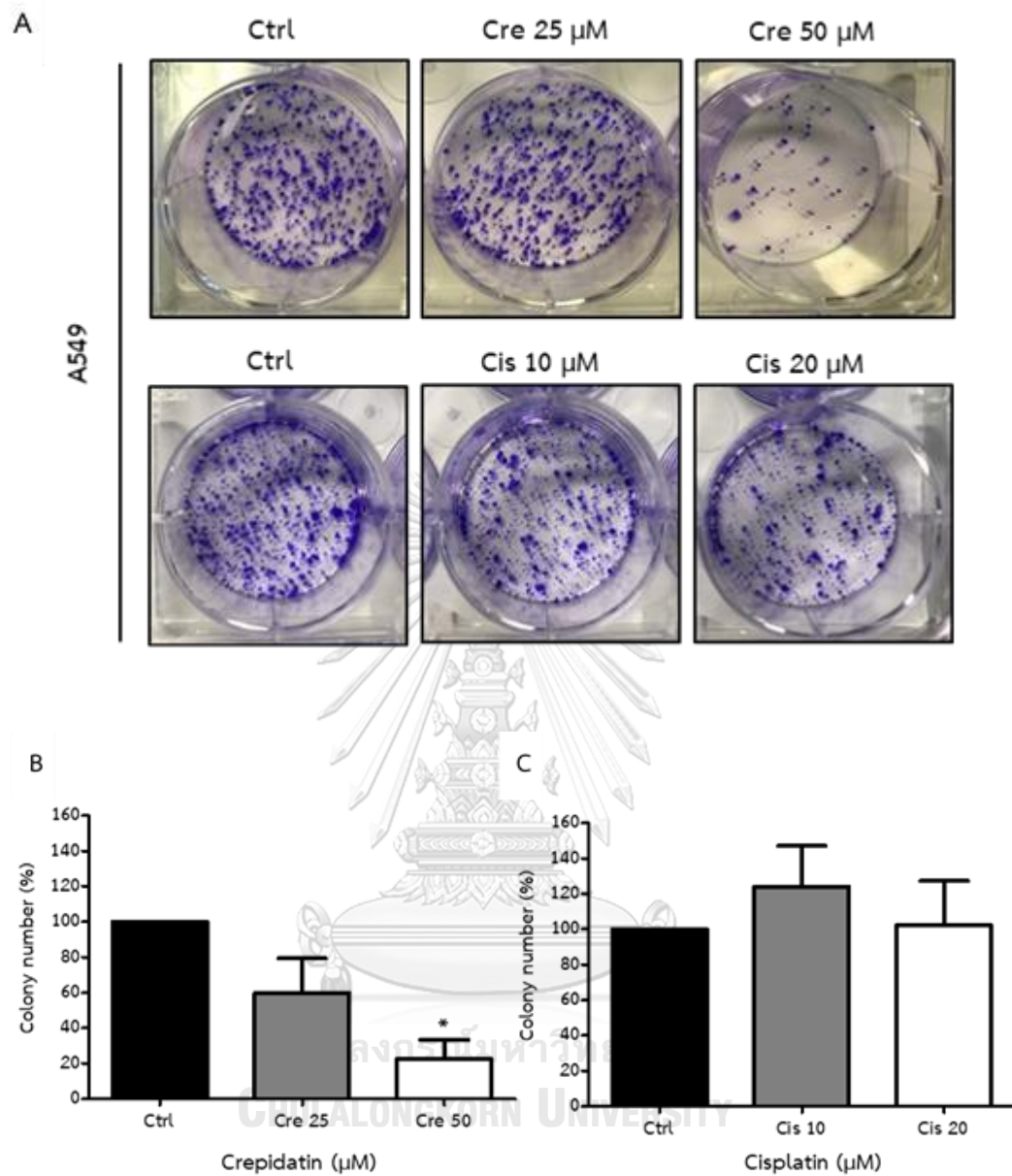


**Figure 34** Effect of crepidatin suppresses CSC-like phenotypes in A549 cells.

A549 cells were pretreated with crepidatin and cisplatin in non-cytotoxic dose and  $\text{IC}_{50}$  concentrations for 48 h. Then, cells were counted and re-plated in a low number with 250 cells for 10 days and then cells were stained with crystal violet and colonies were counted by Image Pro Plus program. All plots are means  $\pm$  SD (n = 3). \* P < 0.05 vs. non-treated cells.

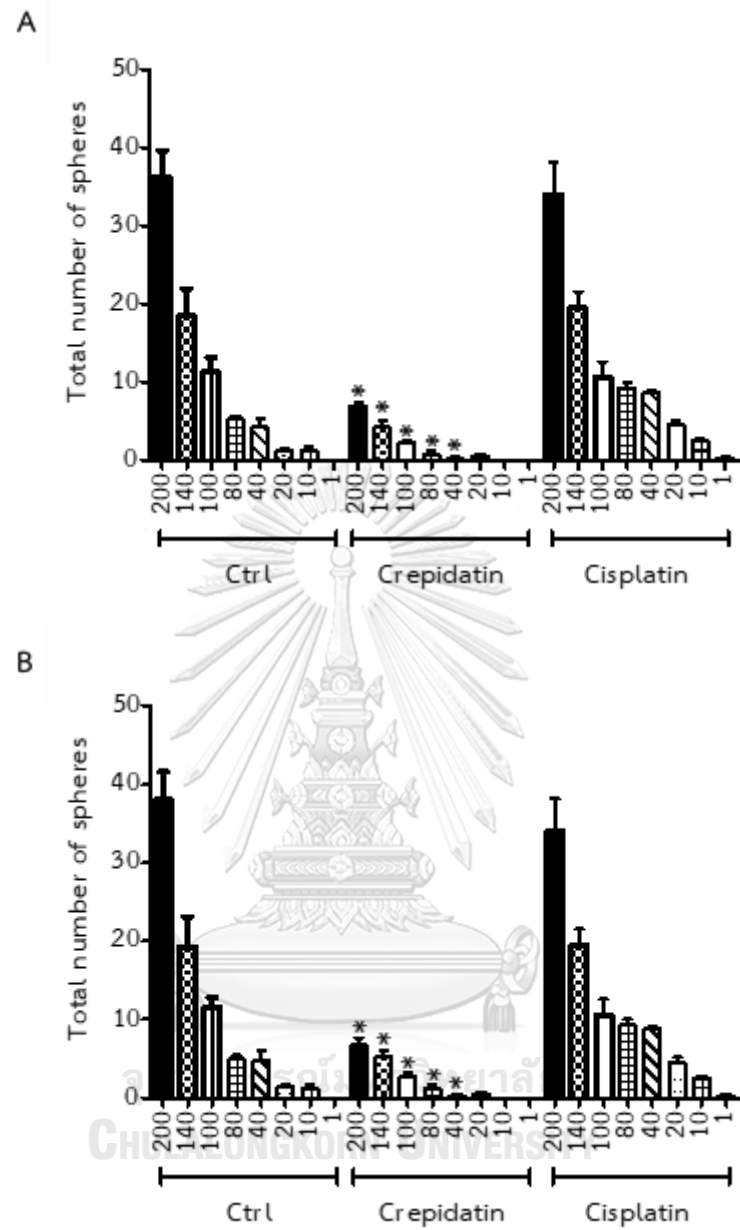


**Figure 35** The effect of crepidatin and cisplatin on the capability for generating spheroids.

(A) H460 and (B) A549 cells were pre-treated with compounds for 48 h and then replated in decreasing numbers from 200 cells/well to 1 cell/well in 200  $\mu$ l RPMI and



cultured for 14 days whereupon the number of wells containing spheres for each cell was calculated. Bars are the mean  $\pm$  SD (n = 3). \* P < 0.05 vs. untreated cells.

### **11. The effects of crepidatin and cisplatin on the stem cell markers of lung cancer cells.**

From the above results, we found that crepidatin decreased the CSC biomarkers CD133 and ABCG2. To assure the aforementioned effect, H460 and A549 cells were treated with crepidatin and cisplatin for 48 h. The expression of stem cell-like characteristics were investigated. Crepidatin significantly decreased the cellular levels of CD133 and ABCG2 in both H460 and A549 cells in time and dose-dependent manner, whereas cisplatin was found to induced cellular levels of CD133 and ABCG2 in time-dependent manner (Figure 36). Additionally, the EMT- factors Vimentin was found to be down-regulated and E-cadherin up-regulated in crepidatin-treated cells. However, similar results were shown for cisplatin treatment on EMT-activating markers compared to crepidatin treatment (Figure 37). Taken together, this data supported the earlier findings that crepidatin has ability to attenuate the stemness of lung cancer cells.

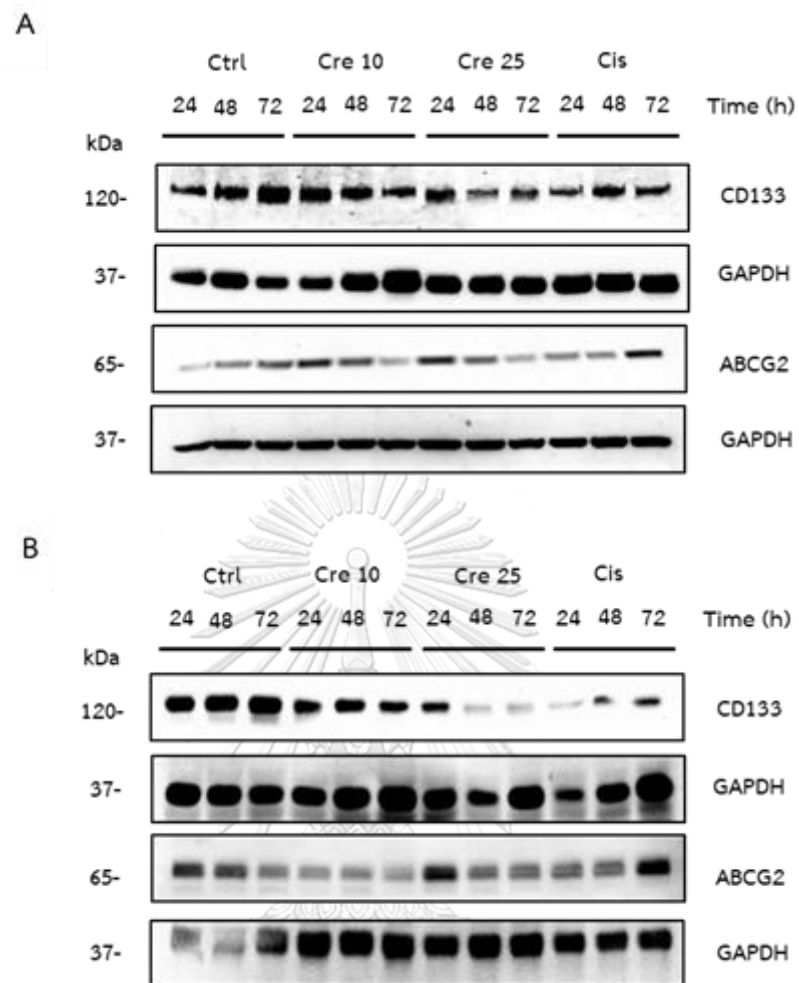


**Figure 36** Effect of crepidatin and cisplatin on CSC markers on human lung cancer H460 and A549 cells.

(A) H460 and (B) A549 cells lysate were then collected and evaluated for the level of CSC markers, including CD133 and ABCG2 using Western blotting. Blots were re-probed with GAPDH to confirm equal loading of samples. All plots are means  $\pm$  SD (n = 3). \* P < 0.05 vs. non-treated cells.

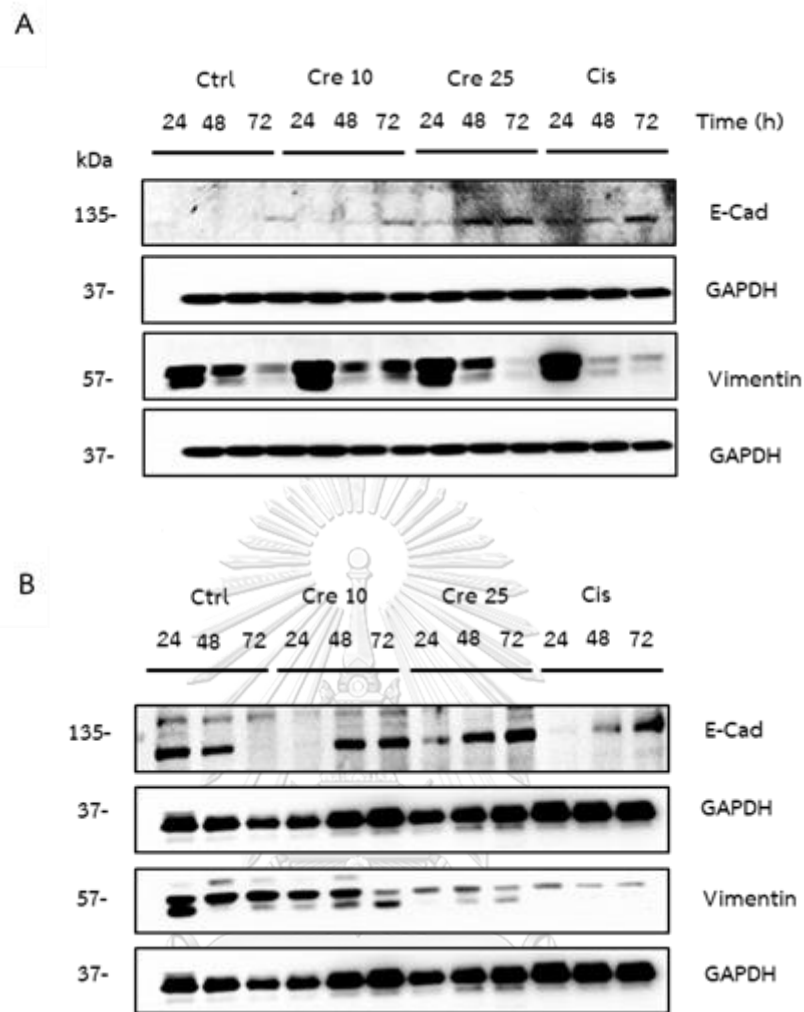


**Figure 37** Effect of crepidatin and cisplatin on EMT markers on human lung cancer H460 and A549 cells.

(A) H460 and (B) A549 cells lysate were then collected and evaluated for the level of EMT markers, including E-cadherin and Vimentin using Western blotting. Blots were re-probed with GAPDH to confirm equal loading of samples. All plots are means  $\pm$  SD (n = 3). \* P < 0.05 vs. non-treated cells.

## 12. The effects of crepidatin on the stem cell migratory behavior of lung cancer cells.

As previously mentioned, not only does CSC possess self-renewal ability, but it also has metastasis characteristic to invade secondary organ as well. Metastasis and migration are the key hallmarks for malignant tumor in cancer patients. In this study, the 3D tumor spheroid migration assay was used to evaluate the ability of cells to migrate out from tumor spheroid mass into extracellular matrix-like environment. The secondary spheroids were dissociated into a single spheroid which had the similar size and subsequently treated with the crepidatin in indicated concentrations for 7 days. Each spheroid was re-plated and evaluated every 24, 48, 72, and 96 h. After 96 h, each spheroid was stained with calcein AM to clarify cell viability and PI dye to determine apoptotic of cells. Figure 38 and Figure 39 represent crepidatin treatment, where both H460 and A549 spheroids were shown to exhibit strong signals of calcein AM dye, implying that these CSCs exhibited high level of proliferation in untreated control. In contrast, treatment of these CSCs with crepidatin at the concentrations of 10 and 25  $\mu\text{M}$  in H460 and 25 and 50  $\mu\text{M}$  in A549 resulted in a dramatic decrease in the cellular level of calcein dye with reduced spheroid size. Furthermore, results displayed consistency that crepidatin treatment also induced the apoptotic cell death with positive PI staining in CSC spheroids. Additionally, the relative migratory area of crepidatin treatment were shown to decrease in time-dependent manner, when compared to the control.

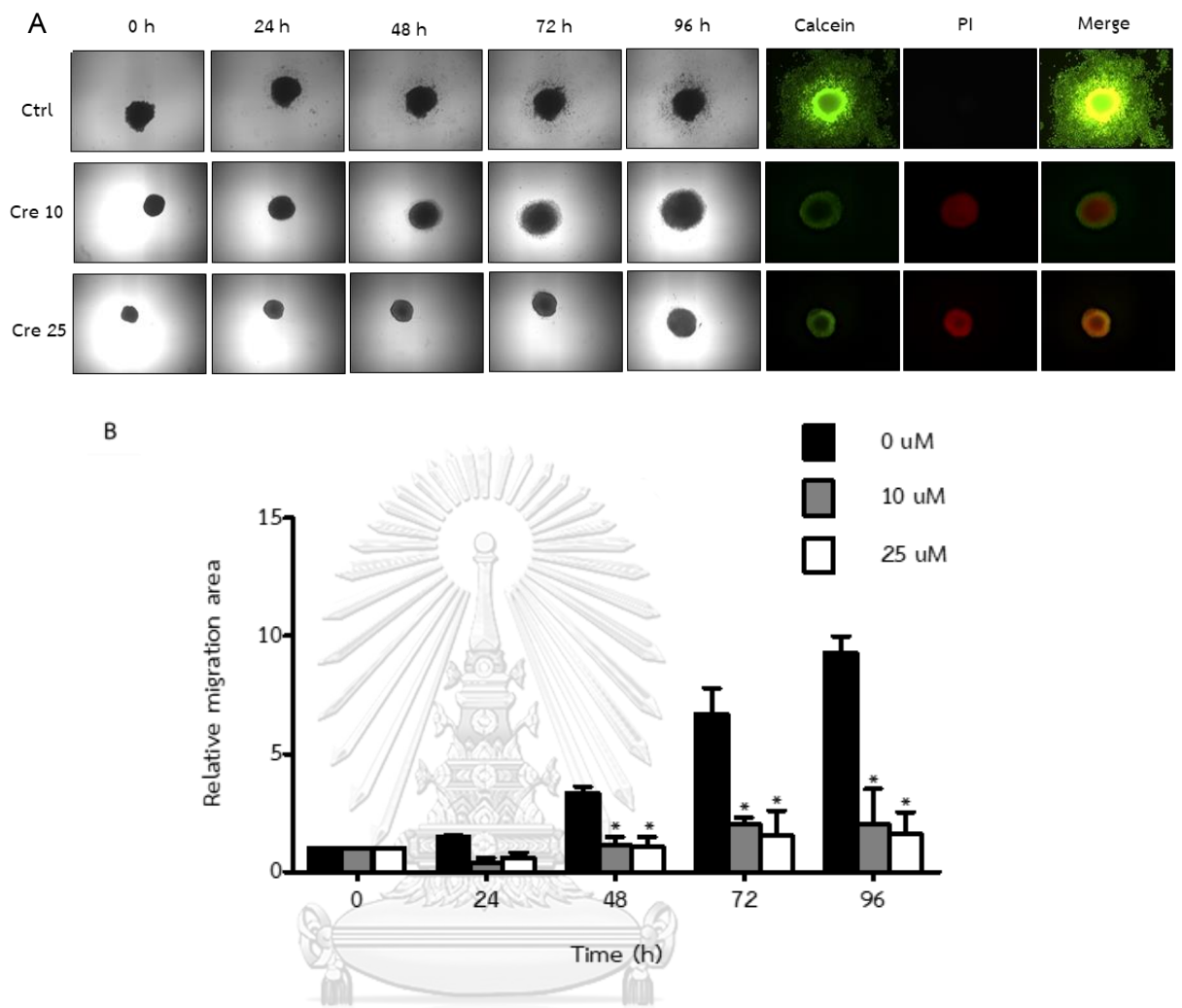


**Figure 38** Effects of crepidatin on the stem cell migratory behavior of lung cancer cells.

H460 secondary spheroids were dissociated into a single spheroid which had the similar size. Then each spheroid was treated with the crepidatin for 7 days and then each spheroid was re-plated and evaluated the invasion every 24, 48, 72, and 96 h. After 96 h, each spheroid was stained with calcein AM and PI dye. All plots are means  $\pm$  SD (n = 3). \* P < 0.05 vs. nontreated cells.

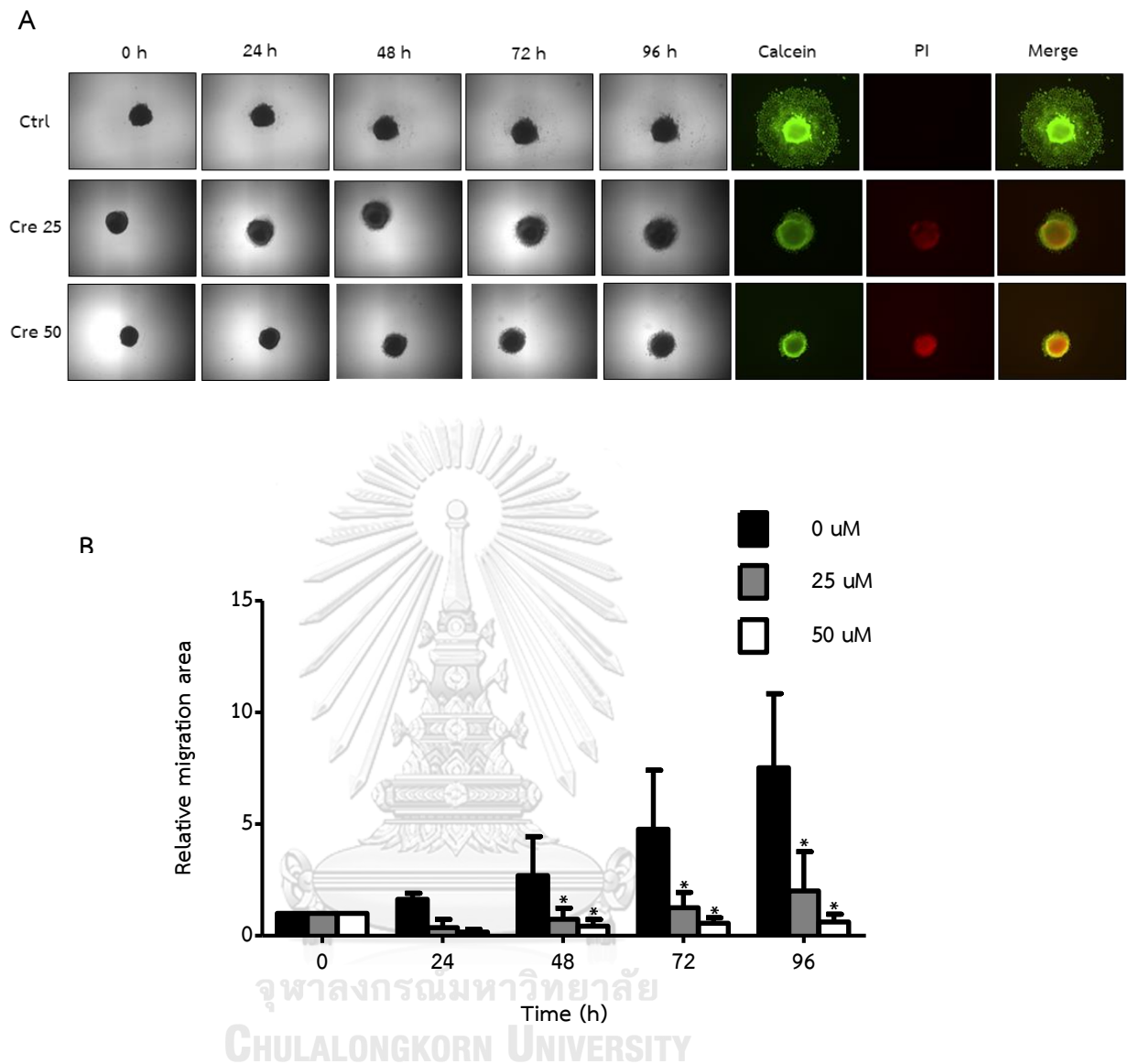


**Figure 39** Effects of crepidatin on the stem cell migratory behavior of lung cancer cells.

A549 secondary spheroids were dissociated into a single spheroid which had the similar size. Then each spheroid was treated with the crepidatin for 7 days and then each spheroid was re-plated and evaluated the invasion every 24, 48, 72, and 96 h. After 96

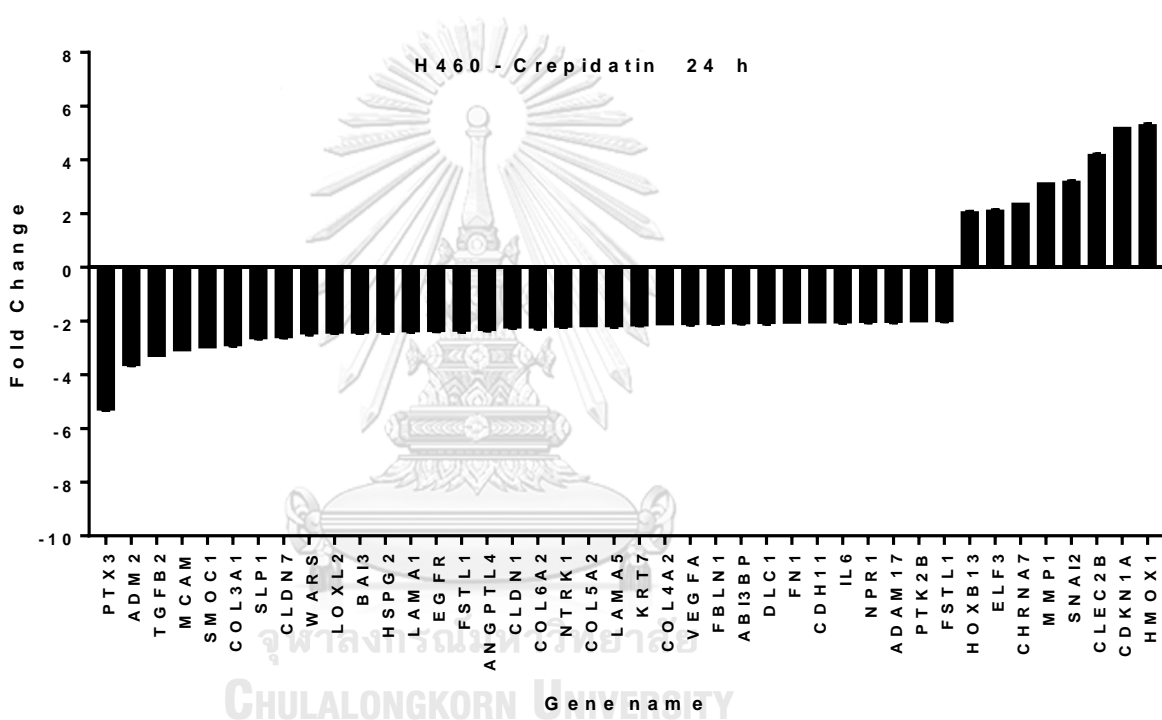
h, each spheroid was stained with calcein AM and PI dye. All plots are means  $\pm$  SD (n = 3). \* P < 0.05 vs. nontreated cells.

### 13. The effects of crepidatin on mRNA expression profile which targeted to CSC-like phenotypes in lung cancer cells.

Transcriptional analysis revealed different expression profiles in crepidatin and cisplatin treated in H460 cells. H460 cells were treated with IC<sub>50</sub> concentrations of crepidatin and cisplatin for 24 h and mRNA expression was analyzed by Nanostring in PanCancer Progression Panel. Barplots show relative expression of downregulated and upregulated genes in crepidatin treatment in 24 h. Various downregulated genes in crepidatin treatment displayed relation to angiogenesis, such as COLA4A2, FN1, and VEGFA, and genes that regulating cancer pathway such as TGF- $\beta$ 2, EGFR and IL6. The regulatory network using string function analysis showing that downregulated protein targeted network in crepidatin treatment. Red, green and blue colors represented the signaling pathway associated genes in angiogenesis, pathways in cancer and PI3K-Akt, respectively. Especially in COLA4A2, LAMA5, VEGFA, EGFR and IL6, thus, we further investigation for all those genes to verify the targeted of crepidatin treatment. We also used H460 cells treating with crepidatin (IC<sub>50</sub>) for 24 and 48 h vs cisplatin (IC<sub>50</sub>) for 24 h to study the target of crepidatin and cisplatin. Scatter plot represents the relative expression (log<sub>10</sub>) of differentially expressed mRNA treatment (Figure 40). We found that the target of crepidatin in 24 h treated cells showed the similar target

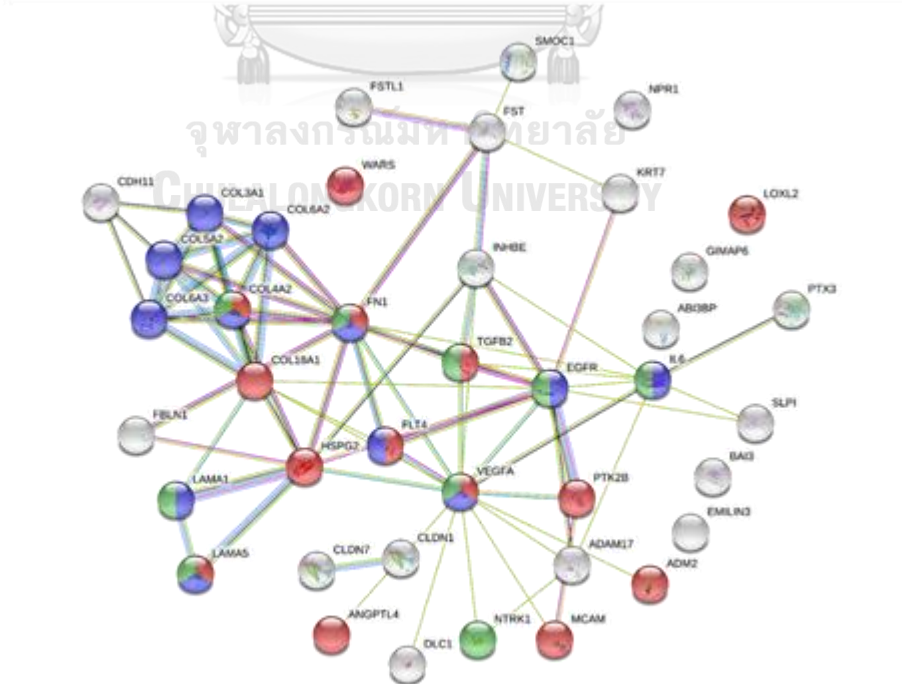
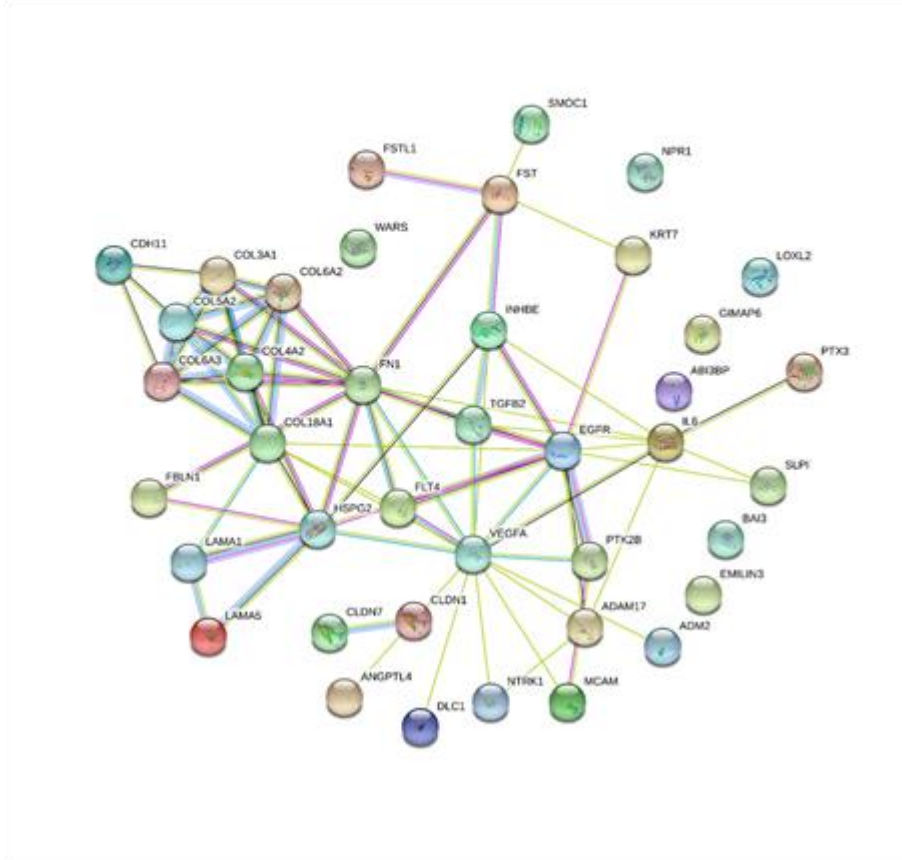
to cisplatin treatment. To verify the different target genes between crepidatin and cisplatin treatment, we used Venn diagrams to illustrate overlaps between the downregulation of crepidatin and cisplatin predicted targets. The results from nanostring analysis were further investigated for targeted pathway (Figure 40).

A





B



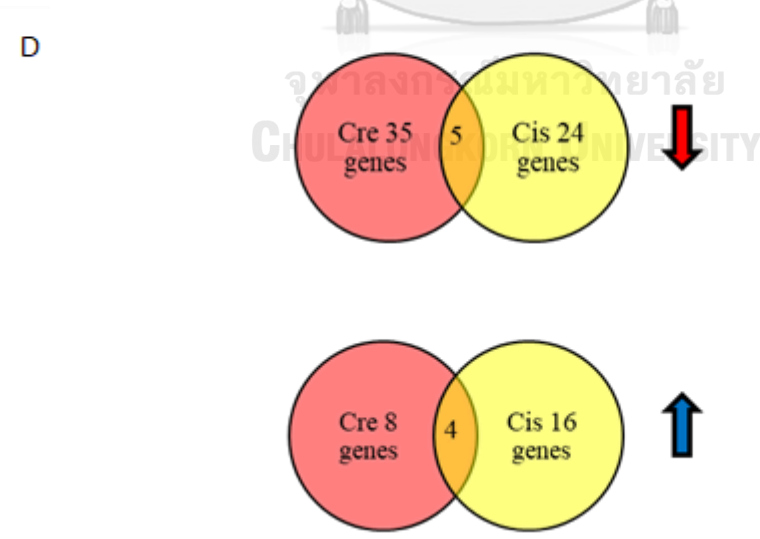
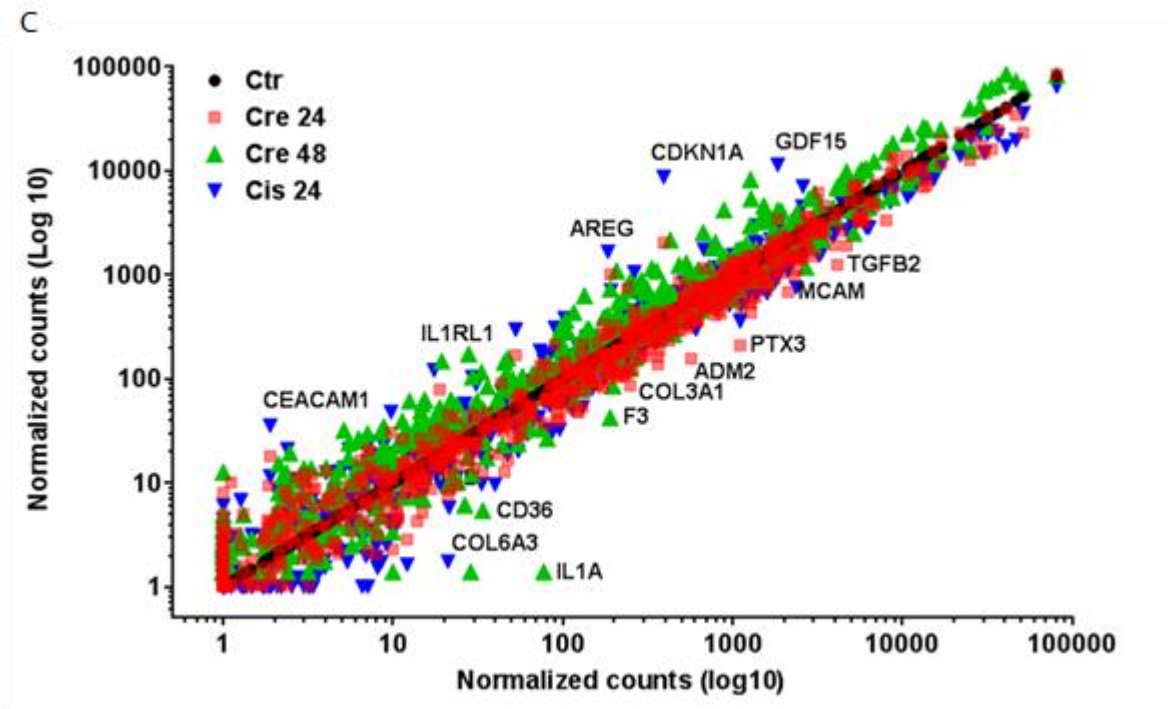


**Table 5** Dysregulated genes in H460 treated with crepidatin 24 h compared to control cells.

A: Downregulated genes					B: Upregulated genes				
Genes	Unigene No.	Ref. Seq. No.	Fold change	p-value	Genes	Unigene No.	Ref. Seq. No.	Fold change	p-value
ADM2 <sup>a</sup>	Hs.449099	NM_001253845.1	-3,7	0,009	CCL8 <sup>j</sup>	Hs.271387	NM_005623.2	4,9	0,024
COL3A1 <sup>b</sup>	Hs.443625	NM_000090.3	-2,9	0,024	CDKN1A <sup>k</sup>	Hs.370771	NM_000389.2	5,2	0,003
COL6A3 <sup>c</sup>	Hs.233240	NM_004369.3	-2,8	0,015	CHRNA7 <sup>l</sup>	Hs.511772	NR_046324.1	2,4	0,004
FLT4 <sup>d</sup>	Hs.646917	NM_002020.1	-2,9	0,008	CLEC2B <sup>m</sup>	Hs.85201	NM_005127.2	4,2	0,026
MCAM <sup>e</sup>	Hs.599039	NM_006500.2	-3,1	0,003	FLT1 <sup>n</sup>	Hs.594454	NM_002019.4	8,0	0,009
PTX3 <sup>f</sup>	Hs.591286	NM_002852.3	-5,3	0,015	HMOX1 <sup>o</sup>	Hs.517581	NM_002133.2	5,3	0,036
SLPI <sup>g</sup>	Hs.517070	NM_003064.2	-2,7	0,014	LOX <sup>p</sup>	Hs.102267	NM_002317.4	9,1	0,004
SMOC1 <sup>h</sup>	Hs.497349	NM_001034852.1	-3,0	0,007	MMP1 <sup>q</sup>	Hs.83169	NM_002421.2	3,1	0,000
TGFB2 <sup>i</sup>	Hs.133379	NM_003238.2	-3,3	0,001	SNAI2 <sup>r</sup>	Hs.360174	NM_003068.3	3,2	0,012

a: Adrenomedullin 2; b: Collagen, type III; alpha 1, c: Collagen, type VI, alpha 3; d: Fms-related tyrosine kinase 4; e: Melanoma cell adhesion molecule; f: Pentraxin 3; g: Secretory leukocyte peptidase inhibitor; h: SPARC related modular calcium binding 1; i: Transforming growth factor, beta 2; j: Chemokine (C-C motif) ligand 8; k: Cyclin-dependent kinase inhibitor 1A (p21, Cip1); l: Cholinergic receptor; m: C-type lectin domain family 2; n: Fms-related tyrosine kinase 1 (vascular endothelial growth factor/vascular permeability factor receptor); o: Heme oxygenase (decycling) 1; p: Lysyl oxidase; q: Matrix metalloproteinase 1 (interstitial collagenase); r: Snail homolog 2 (Drosophila)

**Figure 40** Transcriptional analysis revealed different expression profile in crepidatin and cisplatin treated in H460 cells.

H460 were treated with IC<sub>50</sub> concentrations of crepidatin and cisplatin for 24 h and mRNA expression was analyzed by Nanostring in PanCancer Progression Panel. (A) Barplots showing relative expression of downregulated and upregulated genes in crepidatin treatment. (B). String function analysis showed downregulated protein targeted network in crepidatin treatment. Green, red and blue represents, respectively, angiogenesis, pathways in cancer and PI3K-Akt signaling pathway. (C) H460 cells were

treated with crepidatin ( $IC_{50}$ ) for 24 and 48 h. vs cisplatin ( $IC_{50}$ ) for 24 h. Scatter plot showing relative expression ( $\log_{10}$ ) of differentially expressed mRNA treatment. (D) Venn diagrams show overlap between crepidatin and cisplatin downregulated predicted targets. Description of predicted targets downregulated and upregulated genes in crepidatin treatment after 24 h.

#### **14. The effect of crepidatin on tumor growth and angiogenesis in vivo using chick chorioallantoic membrane (CAM) assay.**

To confirm the effect of crepidatin on the aggressive stem-like and invasive phenotype in lung cancer cells, in this study, in vivo growth and aggressiveness of crepidatin and cisplatin treated cells were analyzed using the chorioallantoic membrane (CAM) assay. H460 and A549 cells were treated with crepidatin and cisplatin with  $IC_{50}$  dose, compared to nontreated control cells. The Ex ovo images of tumors harvested 5 days post-engraftment on the CAM of fertilized chicken eggs were measured and evaluated the tumor forming capacity. Ruler segments defined as a length of 1 mm. Tumor size of micro-tumors after 5 days of incubation were observed (Ctrl: n = 20; crepidatin treated cells: n = 17; cisplatin treated cells: n = 12). Figure represent that crepidatin significantly reduced tumor growth in both H460 and A549, compared to non-treated cells. On the contrary, the tumor sizes were significantly increased in cisplatin treatment. In addition, we also found that the vessel structure around the tumor on cam in crepidatin treated was completely destroyed. When

evaluating the H&E stined tumor sections, we found the control untreated tumors showed a classical characteristics of an adenocarcinoma with solid papillary growing tumor. In addition, a high proliferating tumor were also seen with a significantly enhanced proliferation, as determined by the showing a high number of mitotic rate in control and cisplatin treatment. Whereas in crepidatin treatment, the tumor masses were loosely packed with only small areas of vital cells with fibrosis and necrosis found and mitoses rate also showed significant decreased as well (Figure 41).

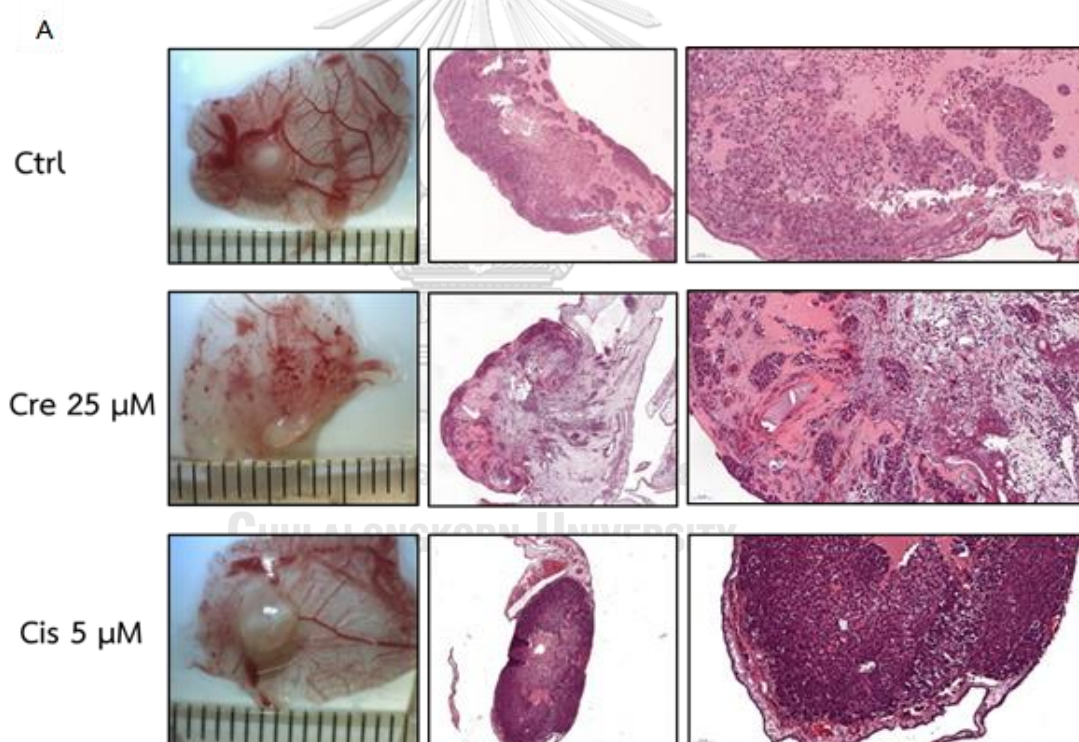




**Figure 41** In vivo growth and aggressiveness of crepidatin and cisplatin treated cells in H460 and A549 compared to control in the chorioallantoic membrane (CAM) xenograft assay.

(A) H460 and (B) A549 Ex ovo images of tumors harvested 5 days post-engraftment on the CAM of fertilized chicken eggs. Ruler segments defined as a length of 1 mm. (C) H460 and (D) A549 Barplots showing tumor size of micro-tumors after 5 days of incubation in crepidatin and cisplatin treatment compared to control cells (Ctrl: n = 20, crepidatin treated cells: n = 17, cisplatin treated cells: n = 12). (E) represents the graph of mitosis count is H460 cells with crepidatin and cisplatin treatment compared to control cells. \*  $P < 0.05$  vs. untreated cells.

### 15. The effect of crepidatin on primary human lung cancer cells.

To confirm, we elucidated the CSC suppressive effect of crepidatin in CSC-rich population derived from primary human lung cancer cells. Consistent with prior results, crepidatin also significantly reduced the ability of the primary human lung cancer cells to form spheroids (Figure 42).

## Primary lung cancer cells

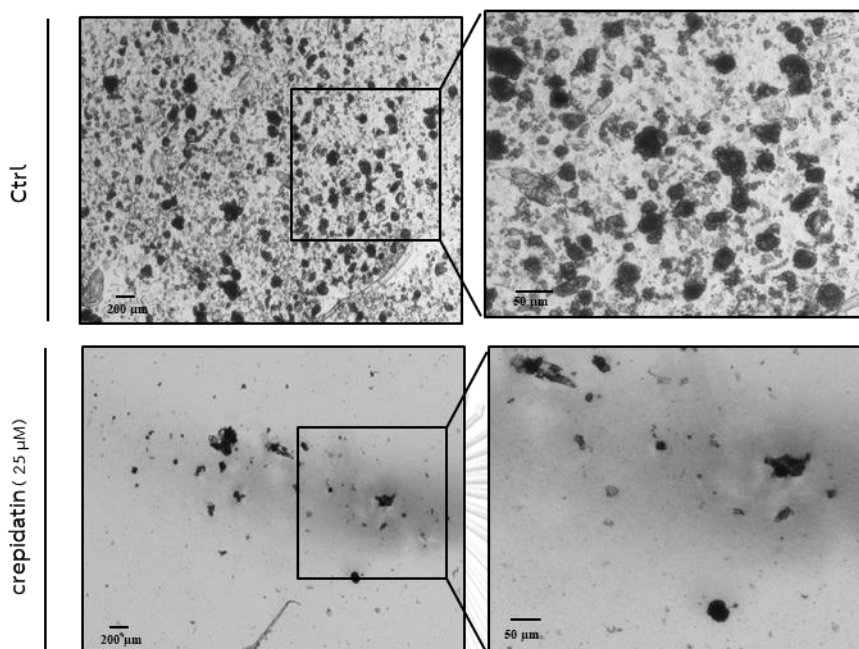


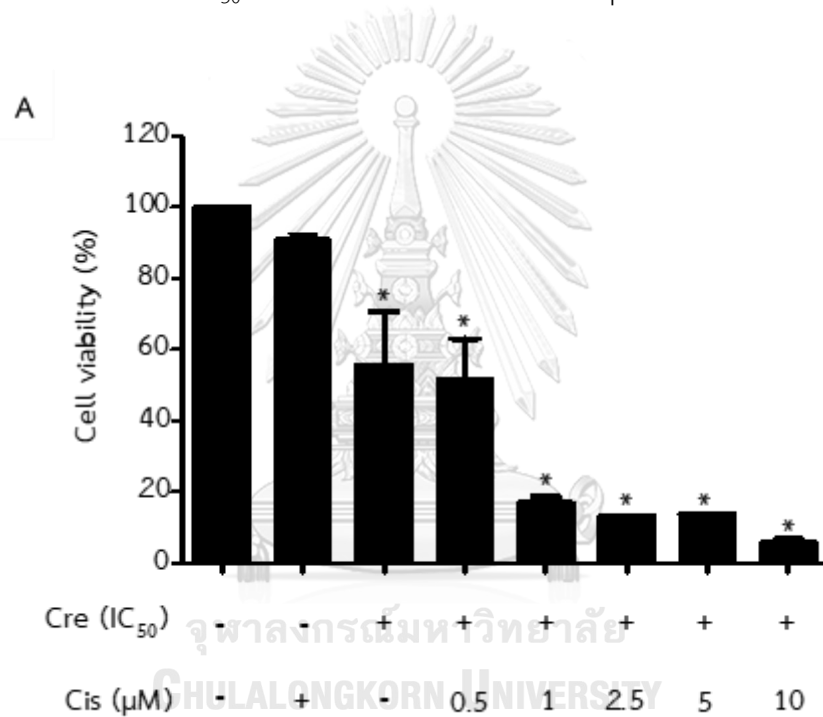
**Figure 42** The effect of crepidatin on enriched primary human lung CSC.

Enriched primary human lung CSC was treated with 25 μM crepidatin, spheroid size and spheroid number were visualized under phase contrast microscopy compared to control cells. Bars are the mean  $\pm$  SD (n = 4). \* P < 0.05 vs. untreated cells.



16. The effect of crepidatin on the induction of CSC-induced apoptosis and sensitization of chemotherapy-induced apoptosis in human lung cancer cells.

To confirm the effect of crepidatin in reduction of CSCs, we used crepidatin to sensitize chemotherapy-induced apoptosis in human lung cancer cells. In this study, crepidatin was used in  $IC_{50}$  dose and combined with cisplatin in various concentration.



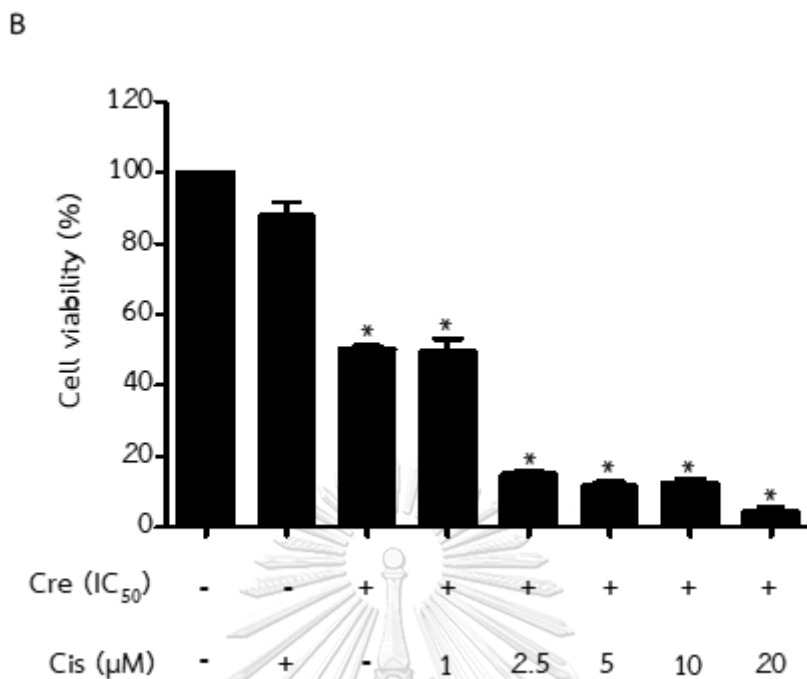


**Figure 43** Cytotoxic effect of crepidatin in combination treatment with cisplatin on human lung cancer H460 and A549 cells.

(A) H460, and (B) A549 cells were treated with various concentrations of cisplatin (0–20 µM) for 48 h in combined with crepidatin (IC<sub>50</sub>) and then the cell viability was determined by the MTT assay, relative to the viability of untreated cells set as 100%.

The data is presented as mean ± SD (n=3). \* P < 0.05 vs. untreated cells. The results found that crepidatin combination treatment with cisplatin decreased cell viability in dose-dependent manner.

## CHAPTER V

### DISCUSSION AND CONCLUSION

In the middle of human cancers, lung cancer is a major cause of death due to its high and rapid rate of metastasis, spreading the cancer cells to other parts of the whole body. The presence of CSCs is potentially the primary reason for the relapse and resistance of cancer after therapy. Therefore, CSCs have recently gained increasing awareness in cancer research (Buettner, Mesa, Vultur, Lee, & Jove, 2008; Peters et al., 2012; S. Singh et al., 2012).

Cancer stem cells (CSCs) or tumor-initiating cells are a small subpopulation of cancer cells inside a tumor, which have tumor disseminating (Bao et al., 2013; Vinogradov & Wei, 2012). The concept of cancer stem cells was first established by Bonnet & Dick in the year 1997. CSCs also have main characteristic which exhibiting the deregulated self-renewal and have ability to form tumors and can proliferate indefinitely (Chiou et al., 2010; Lobo et al., 2007). CSCs and normal stem cells are share a hallmark as they are both capable of self-renewal and can produce differentiated progeny. However, they are different to the high regulated differentiation and self-renewal process of normal stem cells.

It has been proposed that CSCs are the key driving force in tumorigenesis, cancer cell aggressiveness, drug resistance and metastasis (Dalerba et al., 2007; Medema, 2013). In addition, most of current anti-cancer chemotherapies found to only

target the bulk tumor cells not for CSCs and ultimately fail to achieve efficient clinical outcomes because CSCs show only a limited response to such treatments. Thereafter, attempts have been made to identify potential compounds that are effective against CSCs.

In addition, many evidences reported that EMT could play a major role in acquisition of CSC phenotypes (Shibue & Weinberg, 2017). EMT has been known to regulate many transcription factors such as snail, slug and ZEB1 which all known to control CSC phenotypes. Both Snail and Slug have been found to stabilize CSC transcription factors in lung cancer (W. Guo et al., 2012; Luanpitpong et al., 2015). However, some studies suggested that CSCs also exhibited some characteristics of EMT and induced EMT as well (Jayachandran, Dhungel, & Steel, 2016). Even though, it is still unclear about the theory, however, we found that both CSCs and EMT shared the special characteristics and behaviors which mediated the aggressiveness and metastasis of cancers. Thus, the concept that CSCs and EMT are critical factors which driving cancer cell aggressiveness and metastasis has led us to the

intensive investigations of the novel therapeutic that potential compounds which effective against CSCs and EMT.

Nowadays, the compounds isolated from the Thai orchids have been shown their cytotoxicity in various cancers including lung, liver, stomach and colon cancers.

This study demonstrated for the first time that chrysotoxine, a pure compound isolated from *Dendrobium pulchellum*, exhibited an in vitro CSCs suppressing activity in human NSCLC cells. Treatment with chrysotoxine resulted in decreased levels of CSC-rich populations of H460 and H23 cells in 3D culture (Figure 17 - 18), and significantly decreased the cellular levels of CD133, CD44, and ABCG2, which have been widely accepted as stem cell markers in lung cancer, and in CSC-rich populations in both H460 and H23 cells (Figure 21). Recently, the pluripotency transcription factor Sox2 was shown to be involved in the maintenance of stem cell characteristics (Lundberg et al., 2016), while Sox2 is regulated via Src-Akt activity (S. Singh et al., 2012; Tian et al., 2014). Src kinase is a family of non-receptor tyrosine kinases which interact with many cellular pathways and membrane proteins. Src has been divided as the vital member of a family of proteins in Src family kinases (SFKs) which is composing of nine members,

Src, Yes, Fyn, Lck, Hck, Lyn, Yrk, Fgr, and Blk (Thomas & Brugge, 1997). SFKs have been implicated in controlling many signal transductions downstream target in various of cell surfaces (Sen & Johnson, 2011). During the activation, Src is autophosphorylated at tyrosine residue 416. The phosphorylation of Src at tyrosine residues 416 is found in stimulating of migration, EMT and CSC markers. Several substrates have been discovered for the over expression may contribute to the progression of cellular transformation and oncogenic activity. On the other hand, the crucial for the regulation of Src is phosphorylation of tyrosine 527 (Irby & Yeatman, 2000; S. Singh et al., 2012). In normal situation, Src plays as mandatory roles in controlling of multiple integrin-dependent processes and regulating the actin cytoskeleton in numerous cell types (Tyrshkin et al., 2010). In addition, Src also has important role in regulating apoptotic pathway of cells. Previous studies revealed that apoptosis is coming from the loss of cell attachment to the extracellular matrix (ECM) which is well known as anoikis process (Frisch & Screaton, 2001). Normally, when cells begin to metastasize, the process has been required resistance to anoikis, in consequence, it is possibly that this resistance has been involved in aberrant integrin signaling independent of cell

adhesion (Seguin, Desgrosellier, Weis, & Cheresch, 2015). Many studies have demonstrated that various different integrins have a vital role in cell survival under Src activation (Seguin et al., 2015; Vachon, 2011). Even though Src is very important for cells in regulating many transcription factors for cell survival and proliferation, however, the activation of Src has been shown to play an important role in regulating the metastasis in many cancer cell models (S. Singh et al., 2012). Src is a classical non-receptor tyrosine kinase with the potential to cause cell transformation, including uncontrolled proliferation, and activates many downstream targets. Previous studies revealed that overexpression of Src significantly increased cancer stemness via inducing a self-renewal ability and stabilizing the expression of stemness genes (L. C. Kim, Song, & Haura, 2009; Picon-Ruiz et al., 2016; J. Zhang et al., 2007). An overview of signaling cascades demonstrates that Src regulates survival through phosphatidylinositol 3-kinase (PI3K)/Akt signaling pathway and interleukin 8 (IL-8). In addition, Src also controls angiogenesis by VEGF and modulates migration and invasion through pathways relating with focal adhesion kinase (FAK), paxillin, and JUN N-terminal kinase (JNK) (Mitra & Schlaepfer, 2006; S. Singh et al., 2012). Src has also been shown to play a role in

mitogen-activated protein kinase (MAPK) signaling. Previous reviews revealed that Src protein has been found to increase up to 15 times compared in normal level in cancer cells and autophosphorylation of Src at tyrosine residue 416 is also occurred. In addition, previous results suggested the mechanisms in the normal cells may block Wnt signaling, inhibit insulin-like growth factor activity, and promote host recognition of neighboring tumor cells (Alexander et al., 2004). In cancer cells, the growth receptors have been found to increase compared to normal cells.

As we known, Src has been mediated by many growth factor receptors such as EGFR which is related with tyrosine kinase receptor (S. Singh et al., 2012). Many cancers found to be upregulated EGFR with inducing various transcription factors. Excessive EGFR signaling is related to the development of a wide variety of types of solid tumor (Chen et al., 2018). EGFR family are found in all type of human cancers and their excessive signaling may be critical factors in the development (Sasaki, Hiroki, & Yamashita, 2013; Seshacharyulu et al., 2012; Yewale, Baradia, Vhora, Patil, & Misra, 2013). Therefore, EGFR was the first receptor to be proposed as a target for cancer therapy. Although Src can function independently, however, it also cooperates with other receptor tyrosine kinases signaling such as EGFR like a complex. Both EGFR and Src are found to be the primary upstream kinases which mediating signaling cascades



through their activation. The finding that many of the identified proteins have functions in cell adhesion, cell-cell junctions, and the actin cytoskeleton (Chen et al., 2018). The degradation of EGFR may also be affected by Src activity. Previous reports reviewed the abnormal activation of EGFR caused a decreasing in downstream signal mediators, including Src and Stat3, which occurring in human cancers and reflecting in overall signaling complexity that supports the cancer phenotypes (Turkson et al., 1998).

Moreover, VEGF is also a receptor that proposed to be mediate Src as well. VEGF is a signal protein produced by cells that stimulates the formation of blood vessels (Hoeben et al., 2004). Moreover, VEGF has been classified as sub-family of growth factors and the platelet-derived growth factors (Hoeben et al., 2004). VEGF is very crucial for many signaling proteins that involved in the process of vasculogenic and angiogenesis (Abu-Ghazaleh, Kabir, Jia, Lobo, & Zachary, 2001). The overexpression of VEGF can come up with severe of disease. In normal, solid cancers totally cannot grow within a limited size and without an adequate blood supply, consequently, cancers would increase the expression of VEGF for metastasizing and growing. VEGF are well-known gene which responsible for cell adhesion, migration, and proliferation, which are crucial for the complex processes including formation of the endothelial tube network during angiogenesis (Carmeliet, 2005). Angiogenesis is the process of new blood vessel formation from existing of vasculature, and plays major roles in tissue regeneration, tissue repairing in the pathogenesis of cancer. Angiogenesis is stimulated by angiogenic growth factors and their receptors in cooperating with

extracellular matrix (ECM) receptors such as integrin family (Carmeliet, 2005; Hoeben et al., 2004). During Integrin engagement, ECM triggers the activation of many intracellular signaling pathways that crucial for endothelial cell survival, proliferation and migration. Not only integrin and VEGF that regulate adhesion and cell growth, previous reports reviewed that  $\beta_3$  integrin tyrosine phosphorylation are directly mediated by c-Src (De et al., 2005). VEGF activated c-Src and  $\beta_3$  integrin tyrosine phosphorylation is crucial for interaction between VEGF receptor and  $\beta_3$  integrin. Furthermore, c-Src also mediates growth factor-induced  $\beta_3$  integrin activation, ligand binding,  $\beta_3$  integrin-dependent cell adhesion, directional migration of endothelial cells, and initiation of angiogenic programming in endothelial cells (De et al., 2005; Robinson, Reynolds, Wyder, Hicklin, & Hodivala-Dilke, 2004). Consequently, Src also has been implicated in controlling adhesion of epithelial cells to fibronectin for progression of cancer cells to metastatic cells (Jones et al., 2002). Pharmacological repressed of SFK impaired adhesion, whereas exogenous expression of activated Src promoted cell adhesion.

The activation of Src via phosphorylation at Y416 has been shown to activate Akt (phosphorylation at Ser473), which is an important mediator for cell survival, proliferation. Akt is one of the most significantly dysregulated pathways in all of cancers, with a mutation, gene alterations, aberrant epigenetic regulation and increased expression in cancers (Mundi, Sachdev, McCourt, & Kalinsky, 2016). Normally Akt has a

major role in maintenance of homeostatic balance of cell division, cell growth, inflammation and DNA damage (Mundi et al., 2016). Akt has been known to relevance with various downstream effectors involved in cell survival and proliferation, and the well-characterized direct interactions of AKT make it a highly attractive a target for cancer therapy (Narumol Bhummaphan & Chanvorachote, 2015; N. Bhummaphan, Pongrakhananon, Sritularak, & Chanvorachote, 2018). The overexpression of Akt has been observed in many cancers, including lung, ovarian, colon and pancreatic cancers, and is associated with increased cancer cell proliferation and survival (Haynes et al., 2003). Therefore, targeting AKT could provide an important approach for cancer prevention and therapy. In CSCs, Akt plays an important and specific role in CSC initiating growth, self-renewal, maintaining survival, and induction of EMT phenotype in glioma, lung, colon, liver, and breast cancer. In NSCLC, Akt signaling cascade was reported to connect to the self-renewal characteristic of stem-like cells. Phosphorylated Akt was displayed to phosphorylated Oct4 and Nanog which resulted in the increase of tumorigenic potential (Narumol Bhummaphan & Chanvorachote, 2015).

Previous studies revealed that in gastric and colorectal cancer, the phosphorylation of Src and Akt led to increase of Rho A and Cdc42 activity which mediated invasion (Guarino, 2010). Moreover, combination targeting of AKT and SRC resulted in a synergistic efficacy against human pancreatic cancer growth and metastasis. Indeed, Src-Akt was found to be linked with cancer stemness, and inhibition

of Src reduced p-Akt and decreased tumor sphere formation (N. Bhummaphan et al., 2018; S. Singh et al., 2012). Therefore, Src-Akt would be a new perspective target for designing new and more efficient therapeutic strategies to counteract cancer cell. In addition, Src also found to be interacted with CD133 and regulated migration and survival of cancer. Src has been found to support the TIC/CSC state and induces EMT by driving expression of EMT regulators and stem cell markers (C. Liu et al., 2016). Therefore, Src act as regulator of stem-like capacity in cancer cells and that these coactivators can serve as potential therapeutic targets to prevent the recurrence of cancer. Recently, the pluripotency transcription factor Sox2 was shown to be involved in the maintenance of stem cell characteristics. The elevated expression of stem cell associated markers like Oct4, Sox2 and Nanog as well as demonstrated intrinsic epithelial to mesenchymal transition features in CSCs. Especially in Sox2, they found that Sox2 significantly elevated in human NSCLC samples and inhibition of Dasatinib which is Src inhibitor also decreased CSCs in lung cancer. (Lundberg et al., 2016; S. Singh et al., 2012). Thus, Src would be the great target for CSCs treatment.

Chrysotoxine caused a decrease in CSCs in terms of the spheroid size and cell viability, the effect of chrysotoxine on the CSC biomarkers were significantly reduced the cellular levels of CD133, CD44, and ABCG2 in both H460 and H23 cells in dose-dependent manner (Figure 21). Taken together, a clear CSC-suppressive effect of chrysotoxine in these lung cancer cells was established. Correlated to the results on CSC-like phenotypes, chrysotoxine also inhibited the ability to form and generate

spheroids in H460 and H23 cells whereas the non-treated control cells exhibited ability to form tumor sphere.

In this study chrysotoxine treatment caused a significant reduction in the level of p-Src and p-Akt in a dose-dependent manner, whereas the total Src and Akt expression levels were not affected, supporting a post-translational (phosphorylation/dephosphorylation) control. In addition, the down-stream stem cell transcription factor Sox2 was significantly reduced following the decline in p-Src levels in both H460 and H23 cells. These results suggest that chrysotoxine treatment decreased the CSC machinery in lung cancer cells, at least in part, by suppressing the transcription factor Sox2 through the Src-Akt pathway (Figure 22). Taken together, these results demonstrated that the CSC in these lung cancer cells were mediated through a Src-Akt-Sox2-dependent mechanism and that Chrysotoxine decreased the stemness of lung cancer cells.

Furthermore, we also found that another one compound from *Dendrobium pulchellum*, crepidatin which also exhibited an in vitro CSCs suppressing activity in human NSCLC cells. Crepidatin treated H460 and A549 cells also failed to generate spheres compared to control cells whereas cisplatin which is well known as therapeutic drug for lung cancer had capable to generate spheres. Crepidatin induced the down-regulation of the CSC markers CD133 and ABCG2 as well as the ability to form and maintain 3D spheres. CD133 was found in various lung cancer cell lines and exhibited specific characteristics such as self-renewal and tumorigenic capacity

(Prabavathy, Swarnalatha, & Ramadoss, 2018; Zakaria et al., 2017). ABCG2 is an ABC transport membrane that is responsible for stem cell formation. Moreover, ABCG2 also contributes to chemotherapy drug resistance in NSCLC patients. However, cisplatin treatment seems to induce the upregulation of CSC markers. In addition, crepidatin also reduced the migratory behavior of lung 3D-CSC spheres after incubation for 7 days and decreased EMT markers which is related to metastasis and known as the key hallmarks for malignant tumor in cancer patients. In vivo studies, H460 and A549 cells were treated with crepidatin and cisplatin with  $IC_{50}$  dose compared to nontreated control cells. The Ex ovo images of tumors harvested 5 days post-engraftment on the CAM of fertilized chicken eggs were measured and evaluated the tumor forming capacity. Crepidatin significantly reduces tumor growth in both H460 and A549 compared to nontreated cells whereas the tumor sizes have been significantly increased in cisplatin treatment. In addition, we also found that the vessel structure around the tumor on cam in crepidatin treated was destroyed. Consistently with prior results, crepidatin also significantly minimized the ability of the primary human lung cancer cells to form spheroid. Finally, we also found that crepidatin could be an alternative for combine with chemotherapeutic drug. In this study found that only with cisplatin on H460 and A549 failed to kill lung cancer cells whereas combination treatment with cisplatin and crepidatin ( $IC_{50}$ ) diminished CSCs. Therefore, the findings from this study provide vital insights that possible and promote the further investigation and development of crepidatin for CSC-targeted approaches.

In this study, we used Cisplatin which is a chemotherapy medication often used for NSCLC patients. Although cisplatin can kill many cancer cells, but the majority of cancer patients will eventually relapse with cisplatin-resistant phenotypes. Many mechanisms of cisplatin resistance have been proposed including changes in cellular uptake and efflux of the drug, inhibition of apoptosis and increased DNA repair (Dasari & Tchounwou, 2014). Recently, Cisplatin found to be resisted to cancer treatment with increasing anoikis resistance and inducing CSC enrichment in various cancers (Kartalou & Essigmann, 2001). Previous studies showed Cisplatin also promoted transcriptional upregulation of PIK3CA, and cause of activating in PI3K/AKT signaling in resistant cells. In vivo results confirmed drug-resistant tumors revealed the highly expressions of CSC transcription factors in cisplatin treated cells (Thakur & Ray, 2017). In addition, inhibition of EMT would cause of relapse in drug resistance in many types of cancers. In lung cancer, Cisplatin has been denoted to be an effective drug for lung carcinoma therapy, however, it will develop drug-resistance later (Sarin et al., 2017). Cisplatin-resistance is still a main course for chemotherapy failure of lung cancer patients and exhibited increased metastatic ability. Therefore, a novel perspective in development of new drug for chemotherapy resistance and combination with cisplatin treatment may provide a promising approach for the treatment of patients with NSCLC (Shafee et al., 2008; Thakur & Ray, 2017; L. Wang et al., 2017).

Correlated to our results, Cisplatin has been found to induce apoptosis by increasing cleaved PARP and p-H2AX markers in both H460 and A549 cell lines.

However, we discovered Cisplatin was found to be increased in colony number in response to cisplatin treatment. Likewise, limiting dilution assay was also performed to verify the effect of cisplatin also induced the ability to form spheroids as in control group. We also reported that cisplatin was found to induced cellular levels of CD133 and ABCG2 in time-dependent manner whereas cisplatin treatment found to decrease on EMT-activating markers. The reason that cisplatin can kill EMT-like phenotypes cells would be related to previous study that Cisplatin induced apoptosis and kill non-CSCs cells, however, Cisplatin resistant cells which is non-EMT (CSCs) would recover from apoptosis reversal have higher tumorigenicity and metastatic potential to maintain in quiescence stage and caused of recurrence of cancer. Nevertheless, more recent studies have proposed the concept of CSC plasticity in which cells can transit from the non-CSC to the CSC states (Dalerba, Cho, & Clarke, 2007). Besides, previous study also reported that the increasing of CSCs after chemotherapeutic treatment may be involved by inhibiting DNA methylation or demethylation before apoptosis induction and epigenetic mechanisms (Xu, So, Lam, Fung, & Tsang, 2018).

In this study, we hopefully that findings from this research would provide the important insights that facilitate the further investigation and development of compound for CSC-targeted approaches and less or non-toxic to normal cells. Nowadays, there is no therapeutic drugs or compounds that specify or target to CSCs. Chrysotoxine and crepidatin are not only normal plant that used for this research, but they also have structure which like drugs or compounds which used and tested with



patients. Normally, new compounds need to be studied and tested to assure whether safe to use for medication. Clinical trials for new drugs should be approved by the U.S. FDA (Food and Drug Administration) to believe that a new test or treatment may improve the care of patients. Both chrysotoxine and crepidatin have the structures that like some compounds such as curcumin which well-known accepted to use in patients. Curcumin was used as drug to reduce the growth of prostate and breast cancer with the randomize phase II trials (Kwon, 2014). Chrysotoxine and crepidatin also have similar structure to resveratrol which using for clinical trial for colon cancer therapy phase II (C. K. Singh, George, & Ahmad, 2013). Moreover, chrysotoxine and crepidatin also have structures which similar to Genistein which used as drug combination for chemotherapy in bladder, prostate and lung cancer (S. Zhang et al., 2013). Therefore, both chrysotoxine and crepidatin having the effect to kill CSCs led us to develop these compounds as novel therapeutic as well as drugs targeting the CSCs. Furthermore, both compounds also used as alternative medicine to sensitize or combine with chemotherapy drug such as cisplatin and decrease the growth of tumor. We hopefully that these compounds could be developed as a drug aimed for CSCs treatment. These compounds could be an option that will benefit for cancer treatment and increase the survival rate of lung cancer patients.

In conclusion, we sought here to provide proof of the CSC-suppressing activity of chrysotoxine and crepidatin, a pure compound obtained from the *Dendrobium pulchellum* in orchid plant, in human lung cancer cell lines and primary lung cancer

cells. The mechanism of how the compound suppresses CSC phenotypes is via the inhibition of Src-Akt-Sox2, which controls the stemness of the cells. Crepidatin also decreased CSCs markers and suppressed CSC and EMT phenotypes. Moreover, crepidatin also decreased the tumor growth and angiogenesis in vivo using chick chorioallantoic membrane (CAM) assay. In showing the role of chrysotoxine and crepidatin in the regulation of lung cancer CSCs, we issue a novel mechanism of CSC suppression, which may be benefited in cancer therapy.



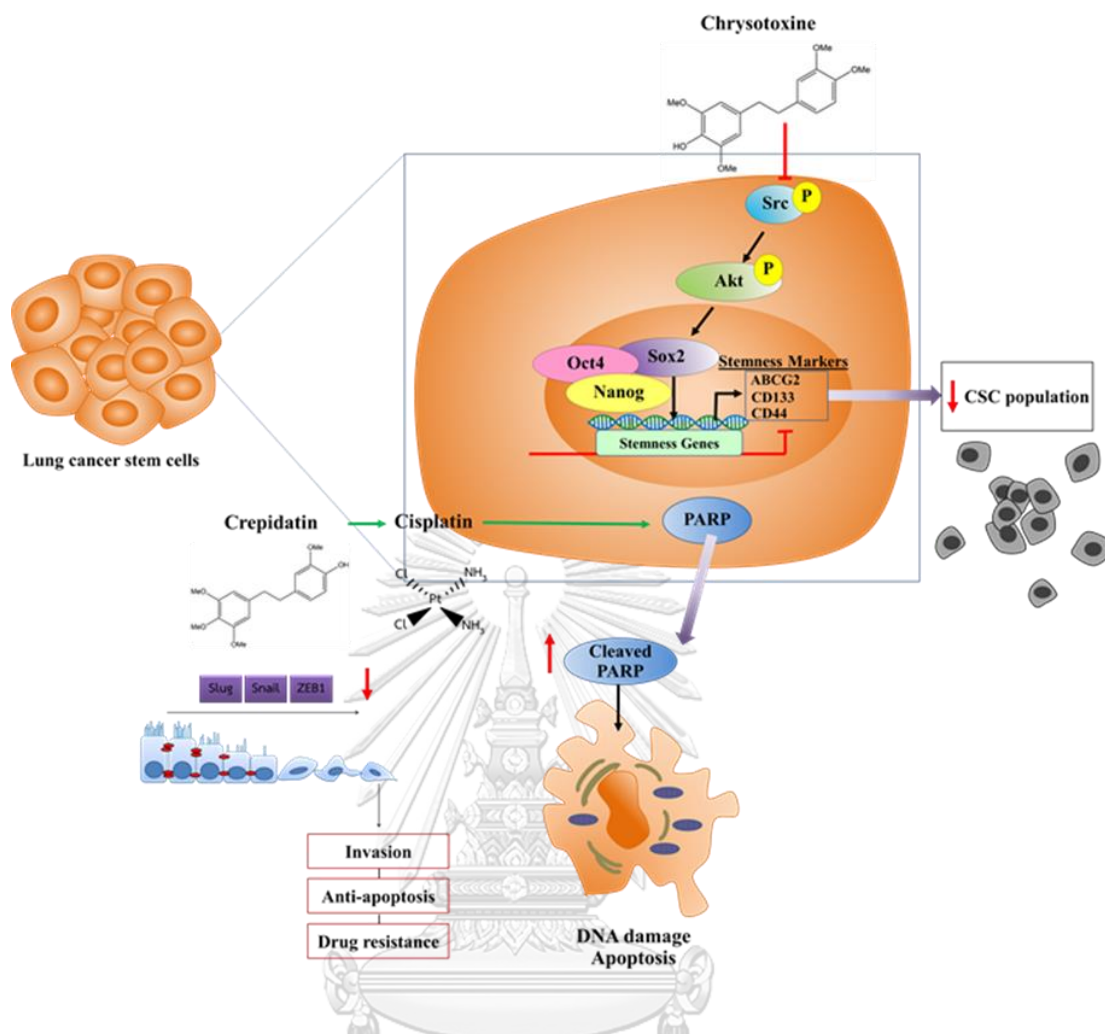


**Figure 44** Schematic diagram illustrates the effect of chrysotoxine and crepidatin in negatively regulating CSC-like phenotypes in inhibiting EMT and sensitizing resistant cancer cells to apoptosis.

## APPENDIX

## TABLE OF EXPERIMENTAL RESULTS

**Table 6** Cytotoxicity of chrysotoxine on H460 cells

chrysotoxine ( $\mu\text{M}$ )	Cell viability (%)
0	100 $\pm$ 0.00
1	90.40 $\pm$ 4.62
5	87.27 $\pm$ 2.31
10	79.78 $\pm$ 1.29
20	74.15 $\pm$ 0.58
50	64.85 $\pm$ 0.24*
100	38.79 $\pm$ 0.44*

The data is presented as mean  $\pm$  SD (n = 3). \* P < 0.05 vs. untreated cells.

**Table 7** Cytotoxicity of chrysotoxine on H23 cells

chrysotoxine ( $\mu\text{M}$ )	Cell viability (%)
0	100 $\pm$ 0.00
1	93.88 $\pm$ 5.45
5	92.62 $\pm$ 3.10
10	85.60 $\pm$ 1.52
20	78.04 $\pm$ 1.17
50	67.87 $\pm$ 0.79*
100	42.56 $\pm$ 0.81*

The data is presented as mean  $\pm$  SD (n = 3). \* P < 0.05 vs. untreated cells.

**Table 8** Cytotoxicity of chrysotoxine on HaCaT cells

chrysotoxine ( $\mu\text{M}$ )	Cell viability (%)
0	100 $\pm$ 0.00
1	101.16 $\pm$ 0.21
5	98.37 $\pm$ 0.19
10	95.15 $\pm$ 0.03
20	90.97 $\pm$ 0.17
50	86.89 $\pm$ 0.12
100	82.00 $\pm$ 0.08

The data is presented as mean  $\pm$  SD (n = 3). \* P < 0.05 vs. untreated cells.

**Table 9** Cytotoxicity of crepidatin on H460 cells

crepidatin ( $\mu\text{M}$ )	Cell viability (%)
0	100 $\pm$ 0.00
1	98.97 $\pm$ 3.21
5	98.14 $\pm$ 2.14
10	83.15 $\pm$ 4.29
20	56.20 $\pm$ 1.58*
50	26.04 $\pm$ 1.24*
100	22.01 $\pm$ 1.18*

The data is presented as mean  $\pm$  SD (n = 3). \* P < 0.05 vs. untreated cells.

**Table 10** Cytotoxicity of crepidatin on H23 cells

crepidatin ( $\mu\text{M}$ )	Cell viability (%)
0	100 $\pm$ 0.00
1	93.88 $\pm$ 7.25
5	92.82 $\pm$ 2.15
10	85.60 $\pm$ 2.03
20	80.04 $\pm$ 3.17
50	68.67 $\pm$ 2.61*
100	46.93 $\pm$ 0.25*

The data is presented as mean  $\pm$  SD (n = 3). \* P < 0.05 vs. untreated cells.

**Table 11** Cytotoxicity of crepidatin on HaCaT cells

crepidatin ( $\mu\text{M}$ )	Cell viability (%)
0	100 $\pm$ 0.00
1	98.39 $\pm$ 2.21
5	99.16 $\pm$ 2.08
10	96.44 $\pm$ 1.87
20	92.38 $\pm$ 0.92
50	87.23 $\pm$ 0.24
100	84.49 $\pm$ 0.03

The data is presented as mean  $\pm$  SD (n = 3). \* P < 0.05 vs. untreated cells.

**Table 12** Cytotoxicity of chrysotobibenzyl on H460 cells

chrysotobibenzyl ( $\mu\text{M}$ )	Cell viability (%)
0	100 $\pm$ 0.00
1	96.84 $\pm$ 3.86
5	86.65 $\pm$ 4.14
10	91.03 $\pm$ 2.50
20	90.65 $\pm$ 0.50
50	91.28 $\pm$ 0.88
100	78.05 $\pm$ 2.11*

The data is presented as mean  $\pm$  SD (n = 3). \* P < 0.05 vs. untreated cells.

**Table 13** Cytotoxicity of chrysotobibenzyl on H23 cells

chrysotobibenzyl ( $\mu\text{M}$ )	Cell viability (%)
0	100 $\pm$ 0.00
1	95.64 $\pm$ 4.11
5	92.26 $\pm$ 3.15
10	90.65 $\pm$ 0.50
20	89.89 $\pm$ 4.04
50	87.95 $\pm$ 4.06
100	87.97 $\pm$ 7.09

The data is presented as mean  $\pm$  SD (n = 3). \* P < 0.05 vs. untreated cells.

**Table 14** Cytotoxicity of chrysotobibenzyl on HaCaT cells

chrysotobibenzyl ( $\mu\text{M}$ )	Cell viability (%)
0	100 $\pm$ 0.00
1	103.17 $\pm$ 9.21
5	98.36 $\pm$ 9.34
10	94.84 $\pm$ 5.80
20	93.91 $\pm$ 4.80
50	92.13 $\pm$ 7.09
100	93.31 $\pm$ 9.68

The data is presented as mean  $\pm$  SD (n = 3). \* P < 0.05 vs. untreated cells.

**Table 15** The effect of chrysotoxine exposure on H460 cell migration

Time	chrysotoxine ( $\mu\text{M}$ )	Relative cell migration
24 h	0	1.00 $\pm$ 0.00
	1	0.95 $\pm$ 0.18
	5	0.89 $\pm$ 0.37
	10	0.72 $\pm$ 0.16
	50	0.48 $\pm$ 0.12
48 h	0	8.58 $\pm$ 0.51
	1	5.80 $\pm$ 0.55*
	5	4.20 $\pm$ 0.11*
	10	2.43 $\pm$ 0.48*
	50	1.70 $\pm$ 0.12*

The data is presented as mean  $\pm$  SD (n = 3). \* P < 0.05 vs. untreated cells.



**Table 16** The effect of crepidatin exposure on H460 cell migration

Time	crepidatin ( $\mu\text{M}$ )	Relative cell migration
24 h	0	1.00 $\pm$ 0.00
	1	0.92 $\pm$ 0.13
	5	0.84 $\pm$ 0.57
	10	0.65 $\pm$ 0.36
	50	0.39 $\pm$ 0.10*
48 h	0	9.68 $\pm$ 0.21
	1	5.00 $\pm$ 0.25*
	5	3.62 $\pm$ 0.41*
	10	2.93 $\pm$ 0.48*
	50	1.10 $\pm$ 1.02*

The data is presented as mean  $\pm$  SD (n = 3). \* P < 0.05 vs. untreated cells.

**Table 17** The effect of chrysotobibenzyl exposure on H460 cell migration

Time	chrysotobibenzyl ( $\mu\text{M}$ )	Relative cell migration
24 h	0	1.00 $\pm$ 0.00
	1	0.99 $\pm$ 0.18
	5	1.08 $\pm$ 0.34
	10	0.85 $\pm$ 0.18
	50	0.57 $\pm$ 0.37
48 h	0	7.13 $\pm$ 0.51
	1	5.99 $\pm$ 0.55
	5	3.80 $\pm$ 0.51*
	10	3.03 $\pm$ 0.78*
	50	3.13 $\pm$ 0.15*

The data is presented as mean  $\pm$  SD (n = 3). \* P < 0.05 vs. untreated cells.

**Table 18** The effect of chrysotoxine suppresses on H460 CSC-rich population

Time	chrysotoxine ( $\mu\text{M}$ )	Spheroid size (%)
Day 0	0	100 $\pm$ 0.00
	1	100 $\pm$ 0.01
	5	100 $\pm$ 0.02
	10	100 $\pm$ 0.03
	20	100 $\pm$ 0.04
	Day 3	0
1		172.33 $\pm$ 2.11
5		133.00 $\pm$ 1.02
10		97.67 $\pm$ 0.05*
20		77.67 $\pm$ 0.21*
Day 7		0
	1	365.33 $\pm$ 1.52
	5	109.67 $\pm$ 0.47*
	10	64.00 $\pm$ 1.24*
	20	42.33 $\pm$ 0.81*

The data is presented as mean  $\pm$  SD (n = 3). \* P < 0.05 vs. untreated cells.

**Table 19** The effect of chrysotoxine suppresses on H23 CSC-rich population

Time	chrysotoxine ( $\mu\text{M}$ )	Spheroid size (%)
Day 0	0	100 $\pm$ 0.00
	1	100 $\pm$ 0.01
	5	100 $\pm$ 0.02
	10	100 $\pm$ 0.03
	20	100 $\pm$ 0.04
Day 3	0	201.08 $\pm$ 1.22
	1	249.00 $\pm$ 0.92
	5	134.20 $\pm$ 0.87*
	10	102.00 $\pm$ 0.05*
	20	85.25 $\pm$ 0.20*
Day 7	0	353.67 $\pm$ 4.33
	1	382.00 $\pm$ 5.09
	5	113.00 $\pm$ 2.17*
	10	50.03 $\pm$ 1.23*
	20	33.33 $\pm$ 0.87*

The data is presented as mean  $\pm$  SD (n = 3). \* P < 0.05 vs. untreated cells.

**Table 20** Cytotoxicity of chrysotoxine on H460 CSC-rich population

chrysotoxine ( $\mu\text{M}$ )	Cell viability (%)
0	100 $\pm$ 0.00
1	95.11 $\pm$ 3.45
2.5	81.97 $\pm$ 4.23
5	63.34 $\pm$ 3.89*
10	44.25 $\pm$ 1.87*
20	34.85 $\pm$ 3.84*
50	19.31 $\pm$ 0.52*

The data is presented as mean  $\pm$  SD (n = 3). \* P < 0.05 vs. untreated cells.

**Table 21** Cytotoxicity of chrysotoxine on H23 CSC-rich population

chrysotoxine ( $\mu\text{M}$ )	Cell viability (%)
0	100 $\pm$ 0.00
1	87.99 $\pm$ 3.32
2.5	79.79 $\pm$ 2.89
5	52.29 $\pm$ 4.51*
10	44.37 $\pm$ 4.3*
20	26.78 $\pm$ 5.25*
50	19.71 $\pm$ 0.79*

The data is presented as mean  $\pm$  SD (n = 3). \* P < 0.05 vs. untreated cells.

**Table 22** The effect of chrysotoxine on CSC markers in H460 cells

chrysotoxine ( $\mu\text{M}$ )	CD133	CD44	ABCG2
0	1.00 $\pm$ 0.00	1.00 $\pm$ 0.00	1.00 $\pm$ 0.00
1	0.95 $\pm$ 0.06	0.95 $\pm$ 0.07	0.93 $\pm$ 0.12
5	0.74 $\pm$ 0.22*	0.75 $\pm$ 0.19*	0.88 $\pm$ 0.22
10	0.58 $\pm$ 0.30*	0.55 $\pm$ 0.12*	0.76 $\pm$ 0.21*
20	0.25 $\pm$ 0.24*	0.24 $\pm$ 0.17*	0.30 $\pm$ 0.13*

The data is presented as mean  $\pm$  SD (n = 3). \* P < 0.05 vs. untreated cells.

**Table 23** The effect of chrysotoxine on CSC markers in H23 cells

chrysotoxine ( $\mu\text{M}$ )	CD133	CD44	ABCG2
0	1.00 $\pm$ 0.00	1.00 $\pm$ 0.00	1.00 $\pm$ 0.00
1	0.94 $\pm$ 0.26	0.73 $\pm$ 0.27	0.95 $\pm$ 0.13
5	0.92 $\pm$ 0.09	0.68 $\pm$ 0.02*	0.70 $\pm$ 0.08
10	0.26 $\pm$ 0.08*	0.54 $\pm$ 0.13*	0.57 $\pm$ 0.09*
20	0.12 $\pm$ 0.17*	0.24 $\pm$ 0.21*	0.33 $\pm$ 0.12*

The data is presented as mean  $\pm$  SD (n = 3). \* P < 0.05 vs. untreated cells.

**Table 24** The effect of chrysotoxine on Src/Akt/Sox2 regulating mechanism in H460 cells

chrysotoxine ( $\mu\text{M}$ )	p-Src (Y416)	p-Akt (S473)	Sox2
0	1.00 $\pm$ 0.00	1.00 $\pm$ 0.00	1.00 $\pm$ 0.00
1	0.98 $\pm$ 0.01	0.90 $\pm$ 0.02	0.71 $\pm$ 0.11*
5	0.45 $\pm$ 0.23*	0.34 $\pm$ 0.27*	0.45 $\pm$ 0.09*
10	0.23 $\pm$ 0.16*	0.23 $\pm$ 0.04*	0.20 $\pm$ 0.01*
20	0.11 $\pm$ 0.13*	0.19 $\pm$ 0.05*	0.10 $\pm$ 0.03*

The data is presented as mean  $\pm$  SD (n = 3). \* P < 0.05 vs. untreated cells.

**Table 25** The effect of chrysotoxine on Src/Akt/Sox2 regulating mechanism in H23 cells

chrysotoxine ( $\mu\text{M}$ )	p-Src (Y416)	p-Akt (S473)	Sox2
0	1.00 $\pm$ 0.00	1.00 $\pm$ 0.00	1.00 $\pm$ 0.00
1	0.84 $\pm$ 0.21	0.91 $\pm$ 0.11	0.57 $\pm$ 0.08*
5	0.24 $\pm$ 0.07*	0.74 $\pm$ 0.12	0.53 $\pm$ 0.02
10	0.14 $\pm$ 0.04*	0.70 $\pm$ 0.15*	0.21 $\pm$ 0.03*
20	0.11 $\pm$ 0.08*	0.34 $\pm$ 0.02*	0.13 $\pm$ 0.01*

The data is presented as mean  $\pm$  SD (n = 3). \* P < 0.05 vs. untreated cells.

**Table 26** The effect of chrysotoxine on EMT markers in H460 cells

chrysotoxine ( $\mu\text{M}$ )	E-cadherin	Vimentin	Slug	Snail
0	1.00 $\pm$ 0.00	1.00 $\pm$ 0.00	1.00 $\pm$ 0.00	1.00 $\pm$ 0.00
1	0.87 $\pm$ 0.05	0.83 $\pm$ 0.03	0.92 $\pm$ 0.01	0.93 $\pm$ 0.03
5	1.12 $\pm$ 0.10	0.71 $\pm$ 0.03*	0.90 $\pm$ 0.02	0.85 $\pm$ 0.05
10	1.48 $\pm$ 0.18*	0.48 $\pm$ 0.02*	0.77 $\pm$ 0.03*	0.43 $\pm$ 0.03*
20	1.83 $\pm$ 0.10*	0.22 $\pm$ 0.03*	0.53 $\pm$ 0.03*	0.20 $\pm$ 0.03*

The data is presented as mean  $\pm$  SD (n = 3). \* P < 0.05 vs. untreated cells.

**Table 27** Cytotoxicity of crepidatin on H460 cells

crepidatin ( $\mu\text{M}$ )	Cell viability (%)
0	100 $\pm$ 0.00
2.5	98.97 $\pm$ 3.14
5	98.14 $\pm$ 3.56
10	83.15 $\pm$ 7.38
25	51.87 $\pm$ 3.27*
50	26.05 $\pm$ 2.39*
100	22.01 $\pm$ 3.86*

The data is presented as mean  $\pm$  SD (n = 3). \* P < 0.05 vs. untreated cells.



**Table 28** Cytotoxicity of crepidatin on H23 cells

crepidatin ( $\mu\text{M}$ )	Cell viability (%)
0	100 $\pm$ 0.00
2.5	93.88 $\pm$ 8.07
5	92.62 $\pm$ 2.95
10	85.60 $\pm$ 3.07
25	78.04 $\pm$ 4.34
50	67.87 $\pm$ 2.95*
100	46.93 $\pm$ 2.33*

The data is presented as mean  $\pm$  SD (n = 3). \* P < 0.05 vs. untreated cells.

**Table 29** Cytotoxicity of crepidatin on H292 cells

crepidatin ( $\mu\text{M}$ )	Cell viability (%)
0	100 $\pm$ 0.00
2.5	100.97 $\pm$ 3.41
5	98.47 $\pm$ 2.24
10	90.15 $\pm$ 2.82
25	82.87 $\pm$ 4.39
50	69.71 $\pm$ 5.45*
100	48.68 $\pm$ 1.4*

The data is presented as mean  $\pm$  SD (n = 3). \* P < 0.05 vs. untreated cells.

**Table 30** Cytotoxicity of crepidatin on A549 cells

crepidatin ( $\mu\text{M}$ )	Cell viability (%)
0	100 $\pm$ 0.00
2.5	100.33 $\pm$ 7.43
5	93.60 $\pm$ 4.94
10	84.42 $\pm$ 3.13
25	73.44 $\pm$ 2.17
50	49.44 $\pm$ 4.20*
100	30.27 $\pm$ 3.24*

The data is presented as mean  $\pm$  SD (n = 3). \* P < 0.05 vs. untreated cells.

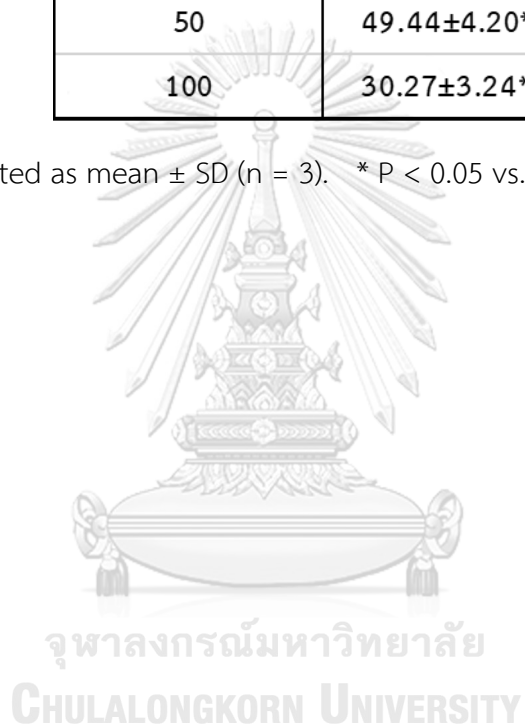


**Table 31** The effect of crepidatin suppresses on H460 CSC-rich population

Time	crepidatin ( $\mu\text{M}$ )	Spheroid size (%)
Day 0	0	100 $\pm$ 0.00
	2.5	100 $\pm$ 0.01
	5	100 $\pm$ 0.02
	10	100 $\pm$ 0.03
	25	100 $\pm$ 0.04
Day 3	0	252.80 $\pm$ 1.71
	2.5	208.89 $\pm$ 3.22
	5	176.33 $\pm$ 0.12
	10	98.64 $\pm$ 0.15*
	25	70.67 $\pm$ 0.21*
Day 7	0	566.74 $\pm$ 0.15
	2.5	397.31 $\pm$ 0.12*
	5	147.99 $\pm$ 0.28*
	10	80.81 $\pm$ 0.03*
	25	23.07 $\pm$ 0.01*

The data is presented as mean  $\pm$  SD (n = 3). \* P < 0.05 vs. untreated cells.

**Table 32** The effect of crepidatin suppresses on A549 CSC-rich population

Time	crepidatin ( $\mu\text{M}$ )	Spheroid size (%)
Day 0	0	100 $\pm$ 0.00
	2.5	100 $\pm$ 0.01
	5	100 $\pm$ 0.02
	10	100 $\pm$ 0.03
	25	100 $\pm$ 0.04
Day 3	0	209.46 $\pm$ 0.18
	2.5	155.56 $\pm$ 0.32
	5	182.67 $\pm$ 0.07
	10	78.64 $\pm$ 0.02*
	25	54.47 $\pm$ 0.01*
Day 7	0	460.07 $\pm$ 4.13
	2.5	413.98 $\pm$ 3.09
	5	127.99 $\pm$ 1.67*
	10	70.81 $\pm$ 0.09*
	25	30.49 $\pm$ 0.03*

The data is presented as mean  $\pm$  SD (n = 3). \* P < 0.05 vs. untreated cells.

**Table 33** Cytotoxicity of crepidatin on H460 CSC-rich population

crepidatin ( $\mu\text{M}$ )	Cell viability (%)
0	100 $\pm$ 0.00
1	90.35 $\pm$ 4.63
2.5	86.50 $\pm$ 2.62
5	78.67 $\pm$ 3.52
10	66.60 $\pm$ 1.05*
20	48.23 $\pm$ 1.84*
50	17.70 $\pm$ 0.54*

The data is presented as mean  $\pm$  SD (n = 3). \* P < 0.05 vs. untreated cells.

**Table 34** Cytotoxicity of crepidatin on A549 CSC-rich population

crepidatin ( $\mu\text{M}$ )	Cell viability (%)
0	100 $\pm$ 0.00
1	94.94 $\pm$ 7.21
2.5	86.50 $\pm$ 2.42
5	80.66 $\pm$ 3.22
10	61.80 $\pm$ 1.30*
20	52.83 $\pm$ 7.24*
50	23.71 $\pm$ 2.10*

The data is presented as mean  $\pm$  SD (n = 3). \* P < 0.05 vs. untreated cells.

**Table 35** The effect of crepidatin on CSC markers in H460 cells

crepidatin ( $\mu\text{M}$ )	CD133	CD44	ABCG2
0	1.00 $\pm$ 0.00	1.00 $\pm$ 0.00	1.00 $\pm$ 0.00
2.5	0.94 $\pm$ 5.24	0.81 $\pm$ 2.31	0.96 $\pm$ 0.12
5	0.82 $\pm$ 0.27	0.60 $\pm$ 4.80*	0.61 $\pm$ 0.13*
10	0.71 $\pm$ 6.69*	0.55 $\pm$ 2.12*	0.56 $\pm$ 0.07*
25	0.62 $\pm$ 4.44*	0.24 $\pm$ 4.60*	0.32 $\pm$ 0.19*

The data is presented as mean  $\pm$  SD (n = 3). \* P < 0.05 vs. untreated cells.

**Table 36** The effect of crepidatin on CSC markers in A549 cells

crepidatin ( $\mu\text{M}$ )	CD133	CD44	ABCG2
0	1.00 $\pm$ 0.00	1.00 $\pm$ 0.00	1.00 $\pm$ 0.00
2.5	0.92 $\pm$ 6.26	0.78 $\pm$ 3.27	0.95 $\pm$ 0.03
5	0.79 $\pm$ 2.09	0.70 $\pm$ 5.02*	0.72 $\pm$ 2.08
10	0.51 $\pm$ 1.08*	0.62 $\pm$ 2.13*	0.59 $\pm$ 1.09*
25	0.45 $\pm$ 2.17*	0.27 $\pm$ 1.81*	0.20 $\pm$ 2.12*

The data is presented as mean  $\pm$  SD (n = 3). \* P < 0.05 vs. untreated cells.

**Table 37** The effect of crepidatin on EMT markers in H460 cells

crepidatin ( $\mu\text{M}$ )	E-cadherin	Vimentin	Slug	Snail
0	1.00 $\pm$ 0.00	1.00 $\pm$ 0.00	1.00 $\pm$ 0.00	1.00 $\pm$ 0.00
2.5	0.88 $\pm$ 0.06	0.96 $\pm$ 0.03	0.96 $\pm$ 0.02	0.51 $\pm$ 0.05*
5	1.03 $\pm$ 0.09	0.94 $\pm$ 0.03	0.70 $\pm$ 0.02*	0.34 $\pm$ 0.04*
10	1.68 $\pm$ 0.16*	0.45 $\pm$ 0.02*	0.70 $\pm$ 0.06*	0.26 $\pm$ 0.04*
25	1.83 $\pm$ 0.11*	0.18 $\pm$ 0.04*	0.20 $\pm$ 0.02*	0.16 $\pm$ 0.02*

The data is presented as mean  $\pm$  SD (n = 3). \* P < 0.05 vs. untreated cells.

**Table 38** Cytotoxicity of cisplatin on H460 cells

cisplatin ( $\mu\text{M}$ )	Cell viability (%)
0	100 $\pm$ 0.00
2.5	98.97 $\pm$ 3.14*
5	98.14 $\pm$ 3.56*
10	83.15 $\pm$ 7.38*
25	51.87 $\pm$ 3.27*
50	26.05 $\pm$ 2.39*
100	22.01 $\pm$ 3.86*

The data is presented as mean  $\pm$  SD (n = 3). \* P < 0.05 vs. untreated cells.

**Table 39** Cytotoxicity of cisplatin on A549 cells

cisplatin ( $\mu\text{M}$ )	Cell viability (%)
0	100 $\pm$ 0.00
2.5	91.94 $\pm$ 4.96
5	79.91 $\pm$ 3.31
10	66.88 $\pm$ 3.79*
25	44.56 $\pm$ 2.81*
50	12.79 $\pm$ 0.52*
100	9.05 $\pm$ 2.13*

The data is presented as mean  $\pm$  SD (n = 3). \* P < 0.05 vs. untreated cells.

**Table 40** Effect of crepidatin suppression colony formation in H460 by clonogenic assay

crepidatin ( $\mu\text{M}$ )	Colony number (%)
0	100 $\pm$ 0.00
10	69.78 $\pm$ 17.46
25	35.99 $\pm$ 12.09*

The data is presented as mean  $\pm$  SD (n = 3). \* P < 0.05 vs. untreated cells.

**Table 41** Effect of cisplatin suppression colony formation in H460 by clonogenic assay

cisplatin ( $\mu\text{M}$ )	Colony number (%)
0	100 $\pm$ 0.00
2.5	118.41 $\pm$ 21.36
5	106.53 $\pm$ 18.85

The data is presented as mean  $\pm$  SD (n = 3). \* P < 0.05 vs. untreated cells.



**Table 42** Effect of crepidatin suppression colony formation in A549 by clonogenic assay

crepidatin ( $\mu\text{M}$ )	Colony number (%)
0	100 $\pm$ 0.00
25	59.72 $\pm$ 18.53
50	22.50 $\pm$ 10.32*

The data is presented as mean  $\pm$  SD (n = 3). \* P < 0.05 vs. untreated cells.

**Table 43** Effect of cisplatin suppression colony formation in A549 by clonogenic assay

cisplatin ( $\mu\text{M}$ )	Colony number (%)
0	100 $\pm$ 0.00
10	124.07 $\pm$ 21.4
20	102.25 $\pm$ 23.19

The data is presented as mean  $\pm$  SD (n = 3). \* P < 0.05 vs. untreated cells.

**Table 44** Effect of crepidatin on stem cell 3D-migration in H460 cells

Time	crepidatin ( $\mu\text{M}$ )	Spheroid size (%)
0 h	0	1.00 $\pm$ 0.00
	10	1.00 $\pm$ 0.00
	25	1.00 $\pm$ 0.00
24 h	0	1.51 $\pm$ 0.03
	10	0.391 $\pm$ 0.17
	25	0.58 $\pm$ 0.20
48 h	0	3.34 $\pm$ 0.23
	10	1.14 $\pm$ 0.27*
	25	1.08 $\pm$ 0.33*
72 h	0	6.88 $\pm$ 0.91
	10	2.02 $\pm$ 0.23*
	25	1.55 $\pm$ 0.86*
96 h	0	9.29 $\pm$ 0.57
	10	2.00 $\pm$ 1.24*
	25	1.60 $\pm$ 0.77*

The data is presented as mean  $\pm$  SD (n = 3). \* P < 0.05 vs. untreated cells.

**Table 45** Effect of crepidatin on stem cell 3D-migration in A549 cells

Time	crepidatin ( $\mu\text{M}$ )	Spheroid size (%)
0 h	0	1.00 $\pm$ 0.00
	25	1.00 $\pm$ 0.00
	50	1.00 $\pm$ 0.00
24 h	0	1.63 $\pm$ 0.22
	25	0.36 $\pm$ 0.29
	50	0.16 $\pm$ 0.10
48 h	0	2.70 $\pm$ 1.42
	25	0.74 $\pm$ 0.41*
	50	0.43 $\pm$ 0.25*
72 h	0	4.77 $\pm$ 2.16
	25	1.26 $\pm$ 0.56*
	50	0.56 $\pm$ 0.20*
96 h	0	7.52 $\pm$ 2.71
	25	2.10 $\pm$ 1.44*
	50	0.62 $\pm$ 0.28*

The data is presented as mean  $\pm$  SD (n = 3). \* P < 0.05 vs. untreated cells.

**Table 46** Cytotoxicity in combination treatment in H460 cells

crepidatin ( $\mu\text{M}$ )	cisplatin ( $\mu\text{M}$ )	Cell viability (%)
0	0	100 $\pm$ 0.00
0	0.5	88.05 $\pm$ 0.58
25	0	50.29 $\pm$ 0.24*
25	0.5	49.35 $\pm$ 0.53*
25	1	14.92 $\pm$ 0.95*
25	2.5	11.58 $\pm$ 0.68*
25	5	12.61 $\pm$ 0.92*
25	10	4.60 $\pm$ 0.13*

The data is presented as mean  $\pm$  SD (n = 3). \* P < 0.05 vs. untreated cells.

**Table 47** Cytotoxicity in combination treatment in A549 cells

crepidatin ( $\mu\text{M}$ )	cisplatin ( $\mu\text{M}$ )	Cell viability (%)
0	0	100 $\pm$ 0.00
0	1	91.05 $\pm$ 12.26
50	0	55.71 $\pm$ 09.21*
50	1	51.77 $\pm$ 1.56*
50	2.5	16.96 $\pm$ 0.08*
50	5	13.38 $\pm$ 0.07*
50	10	13.85 $\pm$ 2.79*
50	20	6.23 $\pm$ 0.14*

The data is presented as mean  $\pm$  SD (n = 3). \* P < 0.05 vs. untreated cells.

## REFERENCES

- Abu-Ghazaleh, R., Kabir, J., Jia, H., Lobo, M., & Zachary, I. (2001). Src mediates stimulation by vascular endothelial growth factor of the phosphorylation of focal adhesion kinase at tyrosine 861, and migration and anti-apoptosis in endothelial cells. *Biochem J*, 360(Pt 1), 255-264. doi:10.1042/0264-6021:3600255
- Alamgeer, M., Peacock, C. D., Matsui, W., Ganju, V., & Watkins, D. N. (2013). Cancer stem cells in lung cancer: Evidence and controversies. *Respirology (Carlton, Vic.)*, 18(5), 757-764. doi:10.1111/resp.12094
- Alexander, D. B., Ichikawa, H., Bechberger, J. F., Valiunas, V., Ohki, M., Naus, C. C., . . . Goldberg, G. S. (2004). Normal cells control the growth of neighboring transformed cells independent of gap junctional communication and SRC activity. *Cancer Res*, 64(4), 1347-1358.
- An, Y., & Ongkeko, W. M. (2009). ABCG2: the key to chemoresistance in cancer stem cells? *Expert Opin Drug Metab Toxicol*, 5(12), 1529-1542. doi:10.1517/17425250903228834
- Angadi, P., & Kale, A. (2015). Epithelial-mesenchymal transition - A fundamental mechanism in cancer progression: An overview. 8(2), 77-84. doi:10.4103/2349-5006.174233
- Baccelli, I., & Trumpp, A. (2012). The evolving concept of cancer and metastasis stem cells. 198(3), 281-293. doi:10.1083/jcb.201202014 %J The Journal of Cell Biology

- Bao, B., Ahmad, A., Azmi, A. S., Ali, S., & Sarkar, F. H. (2013). Cancer Stem Cells (CSCs) and Mechanisms of Their Regulation: Implications for Cancer Therapy. *Current protocols in pharmacology / editorial board, S.J. Enna (editor-in-chief) ... [et al.]*, 0 14, Unit-14.25. doi:10.1002/0471141755.ph1425s61
- Bhummaphan, N., & Chanvorachote, P. (2015). Gigantol Suppresses Cancer Stem Cell-Like Phenotypes in Lung Cancer Cells %J Evidence-Based Complementary and Alternative Medicine. 2015, 10. doi:10.1155/2015/836564
- Bhummaphan, N., Pongrakhananon, V., Sritularak, B., & Chanvorachote, P. (2018). Cancer Stem Cell-Suppressing Activity of Chrysotoxine, a Bibenzyl from *Dendrobium pulchellum*. *J Pharmacol Exp Ther*, 364(2), 332-346. doi:10.1124/jpet.117.244467
- Bonnet, D., & Dick, J. E. (1997). Human acute myeloid leukemia is organized as a hierarchy that originates from a primitive hematopoietic cell. *Nat Med*, 3(7), 730-737.
- Buettner, R., Mesa, T., Vultur, A., Lee, F., & Jove, R. (2008). Inhibition of Src family kinases with dasatinib blocks migration and invasion of human melanoma cells. *Mol Cancer Res*, 6(11), 1766-1774. doi:10.1158/1541-7786.Mcr-08-0169
- Carmeliet, P. (2005). VEGF as a key mediator of angiogenesis in cancer. *Oncology*, 69 Suppl 3, 4-10. doi:10.1159/000088478
- Chaffer, C. L., & Weinberg, R. A. (2011). A Perspective on Cancer Cell Metastasis. *Science*, 331(6024), 1559. doi:10.1126/science.1203543

- Chanvorachote, P., Kowitdamrong, A., Ruanghirun, T., Sritularak, B., Mungmee, C., & Likhitwitayawuid, K. (2013). Anti-metastatic activities of bibenzyls from *Dendrobium pulchellum*. *Nat Prod Commun*, 8(1), 115-118.
- Chen, Z., Oh, D., Dubey, A. K., Yao, M., Yang, B., Groves, J. T., & Sheetz, M. (2018). EGFR family and Src family kinase interactions: mechanics matters? *Current opinion in cell biology*, 51, 97-102. doi:<https://doi.org/10.1016/j.ceb.2017.12.003>
- Chiou, S. H., Wang, M. L., Chou, Y. T., Chen, C. J., Hong, C. F., Hsieh, W. J., . . . Wu, C. W. (2010). Coexpression of Oct4 and Nanog enhances malignancy in lung adenocarcinoma by inducing cancer stem cell-like properties and epithelial-mesenchymal transdifferentiation. *Cancer Res*, 70(24), 10433-10444. doi:10.1158/0008-5472.can-10-2638
- Crocker, A. K., & Allan, A. L. (2008). Cancer stem cells: implications for the progression and treatment of metastatic disease. *J Cell Mol Med*, 12(2), 374-390. doi:10.1111/j.1582-4934.2007.00211.x
- Dalerba, P., Cho, R. W., & Clarke, M. F. (2007). Cancer stem cells: models and concepts. *Annu Rev Med*, 58, 267-284. doi:10.1146/annurev.med.58.062105.204854
- Dasari, S., & Tchounwou, P. B. (2014). Cisplatin in cancer therapy: molecular mechanisms of action. *European journal of pharmacology*, 740, 364-378. doi:10.1016/j.ejphar.2014.07.025

- De, S., Razorenova, O., McCabe, N. P., O'Toole, T., Qin, J., & Byzova, T. V. (2005). VEGF-integrin interplay controls tumor growth and vascularization. *Proceedings of the National Academy of Sciences of the United States of America*, *102*(21), 7589-7594. doi:10.1073/pnas.0502935102
- Du, Y., Ma, C., Wang, Z., Liu, Z., Liu, H., & Wang, T. (2013). Nanog, a novel prognostic marker for lung cancer. *Surg Oncol*, *22*(4), 224-229. doi:10.1016/j.suronc.2013.08.001
- Du, Z., & Lovly, C. M. (2018). Mechanisms of receptor tyrosine kinase activation in cancer. *Mol Cancer*, *17*(1), 58. doi:10.1186/s12943-018-0782-4
- Eramo, A., Haas, T. L., & De Maria, R. (2010). Lung cancer stem cells: tools and targets to fight lung cancer. *Oncogene*, *29*(33), 4625-4635.
- Fatima, S., Zhou, S., & Sorrentino, B. P. (2012). Abcg2 expression marks tissue-specific stem cells in multiple organs in a mouse progeny tracking model. *Stem Cells*, *30*(2), 210-221. doi:10.1002/stem.1002
- Frisch, S. M., & Screaton, R. A. (2001). Anoikis mechanisms. *Curr Opin Cell Biol*, *13*(5), 555-562.
- Gil, J., Stembalska, A., Pesz, K. A., & Sasiadek, M. M. (2008). Cancer stem cells: the theory and perspectives in cancer therapy. *J Appl Genet*, *49*(2), 193-199. doi:10.1007/bf03195612



- Goel, H. L., & Mercurio, A. M. (2013). VEGF targets the tumour cell. *Nature reviews. Cancer*, 13(12), 871-882. doi:10.1038/nrc3627
- Guarino, M. (2010). Src signaling in cancer invasion. *J Cell Physiol*, 223(1), 14-26. doi:10.1002/jcp.22011
- Guo, W., Keckesova, Z., Donaher, J. L., Shibue, T., Tischler, V., Reinhardt, F., . . . Weinberg, R. A. (2012). Slug and Sox9 cooperatively determine the mammary stem cell state. *Cell*, 148(5), 1015-1028. doi:10.1016/j.cell.2012.02.008
- Guo, W., Keckesova, Z., Donaher, Joana L., Shibue, T., Tischler, V., Reinhardt, F., . . . Weinberg, Robert A. Slug and Sox9 Cooperatively Determine the Mammary Stem Cell State. *Cell*, 148(5), 1015-1028. doi:10.1016/j.cell.2012.02.008
- Hanahan, D., & Weinberg, R. A. (2011). Hallmarks of cancer: the next generation. *Cell*, 144(5), 646-674. doi:10.1016/j.cell.2011.02.013
- Haynes, M. P., Li, L., Sinha, D., Russell, K. S., Hisamoto, K., Baron, R., . . . Bender, J. R. (2003). Src kinase mediates phosphatidylinositol 3-kinase/Akt-dependent rapid endothelial nitric-oxide synthase activation by estrogen. *J Biol Chem*, 278(4), 2118-2123. doi:10.1074/jbc.M210828200
- Herreros-Villanueva, M., Zhang, J. S., Koenig, A., Abel, E. V., Smyrk, T. C., Bamlet, W. R., . . . Billadeau, D. D. (2013). SOX2 promotes dedifferentiation and imparts stem cell-like features to pancreatic cancer cells. *Oncogenesis*, 2(8), e61. doi:10.1038/oncsis.2013.23

- Hoeben, A., Landuyt, B., Highley, M. S., Wildiers, H., Van Oosterom, A. T., & De Bruijn, E. A. (2004). Vascular endothelial growth factor and angiogenesis. *Pharmacol Rev*, *56*(4), 549-580. doi:10.1124/pr.56.4.3
- Hollestelle, A., Peeters, J. K., Smid, M., Timmermans, M., Verhoog, L. C., Westenend, P. J., . . . Martens, J. W. (2013). Loss of E-cadherin is not a necessity for epithelial to mesenchymal transition in human breast cancer. *Breast Cancer Res Treat*, *138*(1), 47-57. doi:10.1007/s10549-013-2415-3
- Hubbard, S. R., & Miller, W. T. (2007). Receptor tyrosine kinases: mechanisms of activation and signaling. *Current opinion in cell biology*, *19*(2), 117-123. doi:10.1016/j.ceb.2007.02.010
- Irby, R. B., & Yeatman, T. J. (2000). Role of Src expression and activation in human cancer. *Oncogene*, *19*(49), 5636-5642. doi:10.1038/sj.onc.1203912
- Ishiwata, T. (2016). Cancer stem cells and epithelial-mesenchymal transition: Novel therapeutic targets for cancer. *Pathol Int*, *66*(11), 601-608. doi:10.1111/pin.12447
- Jayachandran, A., Dhungel, B., & Steel, J. C. (2016). Epithelial-to-mesenchymal plasticity of cancer stem cells: therapeutic targets in hepatocellular carcinoma. *Journal of hematology & oncology*, *9*(1), 74-74. doi:10.1186/s13045-016-0307-9
- Jeter, C. R., Liu, B., Liu, X., Chen, X., Liu, C., Calhoun-Davis, T., . . . Tang, D. G. (2011). NANOG promotes cancer stem cell characteristics and prostate cancer resistance to androgen deprivation. *Oncogene*, *30*(36), 3833-3845. doi:10.1038/onc.2011.114

- Jing, F., Kim, H. J., Kim, C. H., Kim, Y. J., Lee, J. H., & Kim, H. R. (2015). Colon cancer stem cell markers CD44 and CD133 in patients with colorectal cancer and synchronous hepatic metastases. *Int J Oncol*, *46*(4), 1582-1588. doi:10.3892/ijo.2015.2844
- Jones, R. J., Avizienyte, E., Wyke, A. W., Owens, D. W., Brunton, V. G., & Frame, M. C. (2002). Elevated c-Src is linked to altered cell-matrix adhesion rather than proliferation in KM12C human colorectal cancer cells. *British journal of cancer*, *87*(10), 1128-1135. doi:10.1038/sj.bjc.6600594
- Kalluri, R., & Weinberg, R. A. (2009). The basics of epithelial-mesenchymal transition. *The Journal of Clinical Investigation*, *119*(6), 1420-1428. doi:10.1172/JCI39104
- Kartalou, M., & Essigmann, J. M. (2001). Mechanisms of resistance to cisplatin. *Mutat Res*, *478*(1-2), 23-43.
- Kashyap, V., Rezende, N. C., Scotland, K. B., Shaffer, S. M., Persson, J. L., Gudas, L. J., & Mongan, N. P. (2009). Regulation of stem cell pluripotency and differentiation involves a mutual regulatory circuit of the NANOG, OCT4, and SOX2 pluripotency transcription factors with polycomb repressive complexes and stem cell microRNAs. *Stem Cells Dev*, *18*. doi:10.1089/scd.2009.0113
- Kim, E. S. (2016). Chemotherapy Resistance in Lung Cancer. *Adv Exp Med Biol*, *893*, 189-209. doi:10.1007/978-3-319-24223-1\_10
- Kim, L. C., Song, L., & Haura, E. B. (2009). Src kinases as therapeutic targets for cancer. *Nature reviews. Clinical oncology*, *6*(10), 587-595. doi:10.1038/nrclinonc.2009.129

- Kokkinos, M. I., Wafai, R., Wong, M. K., Newgreen, D. F., Thompson, E. W., & Waltham, M. (2007). Vimentin and epithelial-mesenchymal transition in human breast cancer-observations in vitro and in vivo. *Cells Tissues Organs*, *185*(1-3), 191-203. doi:10.1159/000101320
- Kwon, Y. (2014). Curcumin as a cancer chemotherapy sensitizing agent. *Journal of the Korean Society for Applied Biological Chemistry*, *57*(2), 273-280. doi:10.1007/s13765-014-4077-1
- Lamouille, S., Xu, J., & Derynck, R. (2014). Molecular mechanisms of epithelial-mesenchymal transition. *Nature reviews. Molecular cell biology*, *15*(3), 178-196. doi:10.1038/nrm3758
- Leon, G., MacDonagh, L., Finn, S. P., Cuffe, S., & Barr, M. P. (2016). Cancer stem cells in drug resistant lung cancer: Targeting cell surface markers and signaling pathways. *Pharmacology & Therapeutics*, *158*, 71-90. doi:<http://dx.doi.org/10.1016/j.pharmthera.2015.12.001>
- Leung, E. L.-H., Fiscus, R. R., Tung, J. W., Tin, V. P.-C., Cheng, L. C., Sihoe, A. D.-L., . . . Wong, M. P. (2010). Non-Small Cell Lung Cancer Cells Expressing CD44 Are Enriched for Stem Cell-Like Properties. *PLoS One*, *5*(11), e14062. doi:10.1371/journal.pone.0014062
- Li, Z. (2013). CD133: a stem cell biomarker and beyond. *Experimental Hematology & Oncology*, *2*, 17-17. doi:10.1186/2162-3619-2-17

Liu, C., Li, Y., Xing, Y., Cao, B., Yang, F., Yang, T., . . . Jiang, J. (2016). The Interaction between Cancer Stem Cell Marker CD133 and Src Protein Promotes Focal Adhesion Kinase (FAK) Phosphorylation and Cell Migration. *J Biol Chem*, *291*(30), 15540-15550. doi:10.1074/jbc.M115.712976

Liu, X., & Fan, D. (2015). The epithelial-mesenchymal transition and cancer stem cells: functional and mechanistic links. *Curr Pharm Des*, *21*(10), 1279-1291.

Lobo, N. A., Shimono, Y., Qian, D., & Clarke, M. F. (2007). The biology of cancer stem cells. *Annu Rev Cell Dev Biol*, *23*, 675-699. doi:10.1146/annurev.cellbio.22.010305.104154

Luanpitpong, S., Li, J., Manke, A., Brundage, K., Ellis, E., McLaughlin, S. L., . . . Rojanasakul, Y. (2015). SLUG is required for SOX9 stabilization and functions to promote cancer stem cells and metastasis in human lung carcinoma. *Oncogene*, *35*, 2824. doi:10.1038/onc.2015.351

<https://www.nature.com/articles/onc2015351#supplementary-information>

Luanpitpong, S., Li, J., Manke, A., Brundage, K., Ellis, E., McLaughlin, S. L., . . . Rojanasakul, Y. (2016). SLUG is required for SOX9 stabilization and functions to promote cancer stem cells and metastasis in human lung carcinoma. *Oncogene*, *35*(22), 2824-2833. doi:10.1038/onc.2015.351

- Lundberg, I. V., Edin, S., Eklöf, V., Öberg, Å., Palmqvist, R., & Wikberg, M. L. (2016). SOX2 expression is associated with a cancer stem cell state and down-regulation of CDX2 in colorectal cancer. *BMC Cancer*, *16*, 471. doi:10.1186/s12885-016-2509-5
- Majumder, P. L., & Chatterjee, S. (1989). Crepidatin, a bibenzyl derivative from the orchid *Dendrobium crepidatum*. *Phytochemistry*, *28*(7), 1986-1988. doi:[https://doi.org/10.1016/S0031-9422\(00\)97904-4](https://doi.org/10.1016/S0031-9422(00)97904-4)
- Medici, D., Hay, E. D., & Olsen, B. R. (2008). Snail and Slug Promote Epithelial-Mesenchymal Transition through  $\beta$ -Catenin-T-Cell Factor-4-dependent Expression of Transforming Growth Factor- $\beta$ 3. *Molecular Biology of the Cell*, *19*(11), 4875-4887. doi:10.1091/mbc.E08-05-0506
- Mitra, S. K., & Schlaepfer, D. D. (2006). Integrin-regulated FAK-Src signaling in normal and cancer cells. *Curr Opin Cell Biol*, *18*(5), 516-523. doi:10.1016/j.ceb.2006.08.011
- Mundi, P. S., Sachdev, J., McCourt, C., & Kalinsky, K. (2016). AKT in cancer: new molecular insights and advances in drug development. *Br J Clin Pharmacol*, *82*(4), 943-956. doi:10.1111/bcp.13021
- NAGATA, T., SAKAKURA, C., KOMIYAMA, S., MIYASHITA, A., NISHIO, M., MURAYAMA, Y., . . . OTSUJI, E. (2011). Expression of Cancer Stem Cell Markers CD133 and CD44 in Locoregional Recurrence of Rectal Cancer. *Anticancer Res*, *31*(2), 495-500.
- Pan, G. J., Chang, Z. Y., Scholer, H. R., & Pei, D. (2002). Stem cell pluripotency and transcription factor Oct4. *Cell Res*, *12*(5-6), 321-329. doi:10.1038/sj.cr.7290134

- Paul, M. K., & Mukhopadhyay, A. K. (2004). Tyrosine kinase - Role and significance in Cancer. *International journal of medical sciences*, 1(2), 101-115.
- Peters, S., Adjei, A. A., Gridelli, C., Reck, M., Kerr, K., & Felip, E. (2012). Metastatic non-small-cell lung cancer (NSCLC): ESMO Clinical Practice Guidelines for diagnosis, treatment and follow-up. *Ann Oncol*, 23 Suppl 7, vii56-64. doi:10.1093/annonc/mds226
- Picon-Ruiz, M., Pan, C., Drews-Elger, K., Jang, K., Besser, A. H., Zhao, D., . . . Slingerland, J. M. (2016). Interactions between Adipocytes and Breast Cancer Cells Stimulate Cytokine Production and Drive Src/Sox2/miR-302b-Mediated Malignant Progression. *Cancer Res*, 76(2), 491-504. doi:10.1158/0008-5472.Can-15-0927
- Prabavathy, D., Swarnalatha, Y., & Ramadoss, N. (2018). Lung cancer stem cells—origin, characteristics and therapy. *Stem Cell Investigation*, 5, 6. doi:10.21037/sci.2018.02.01
- Rafiemanesh, H., Mehtarpour, M., Khani, F., Hesami, S. M., Shamlou, R., Towhidi, F., . . . Moini, A. (2016). Epidemiology, incidence and mortality of lung cancer and their relationship with the development index in the world. *Journal of thoracic disease*, 8(6), 1094-1102. doi:10.21037/jtd.2016.03.91
- Rappa, G., Fodstad, O., & Lorico, A. (2008). The stem cell-associated antigen CD133 (Prominin-1) is a molecular therapeutic target for metastatic melanoma. *Stem Cells*, 26(12), 3008-3017. doi:10.1634/stemcells.2008-0601

- Ren, F., Sheng, W.-Q., & Du, X. (2013). CD133: A cancer stem cells marker, is used in colorectal cancers. *World Journal of Gastroenterology : WJG*, *19*(17), 2603-2611. doi:10.3748/wjg.v19.i17.2603
- Reya, T., Morrison, S. J., Clarke, M. F., & Weissman, I. L. (2001). Stem cells, cancer, and cancer stem cells. *Nature*, *414*(6859), 105-111. doi:10.1038/35102167
- Robinson, S. D., Reynolds, L. E., Wyder, L., Hicklin, D. J., & Hodivala-Dilke, K. M. (2004). Beta3-integrin regulates vascular endothelial growth factor-A-dependent permeability. *Arterioscler Thromb Vasc Biol*, *24*(11), 2108-2114. doi:10.1161/01.ATV.0000143857.27408.de
- Sarin, N., Engel, F., Kalayda, G. V., Mannewitz, M., Cinatl, J., Jr., Rothweiler, F., . . . Frotschl, R. (2017). Cisplatin resistance in non-small cell lung cancer cells is associated with an abrogation of cisplatin-induced G2/M cell cycle arrest. *PLoS One*, *12*(7), e0181081. doi:10.1371/journal.pone.0181081
- Sasaki, T., Hiroki, K., & Yamashita, Y. (2013). The role of epidermal growth factor receptor in cancer metastasis and microenvironment. *BioMed research international*, *2013*, 546318-546318. doi:10.1155/2013/546318
- Satelli, A., & Li, S. (2011). Vimentin in cancer and its potential as a molecular target for cancer therapy. *Cell Mol Life Sci*, *68*(18), 3033-3046. doi:10.1007/s00018-011-0735-



- Seguin, L., Desgrosellier, J. S., Weis, S. M., & Cheresh, D. A. (2015). Integrins and cancer: regulators of cancer stemness, metastasis, and drug resistance. *Trends Cell Biol*, 25(4), 234-240. doi:10.1016/j.tcb.2014.12.006
- Sen, B., & Johnson, F. M. (2011). Regulation of SRC family kinases in human cancers. *Journal of signal transduction*, 2011, 865819-865819. doi:10.1155/2011/865819
- Seshacharyulu, P., Ponnusamy, M. P., Haridas, D., Jain, M., Ganti, A. K., & Batra, S. K. (2012). Targeting the EGFR signaling pathway in cancer therapy. *Expert opinion on therapeutic targets*, 16(1), 15-31. doi:10.1517/14728222.2011.648617
- Shafee, N., Smith, C. R., Wei, S., Kim, Y., Mills, G. B., Hortobagyi, G. N., . . . Lee, E. Y. H. P. (2008). Cancer stem cells contribute to cisplatin resistance in Brca1/p53-mediated mouse mammary tumors. *Cancer Res*, 68(9), 3243-3250. doi:10.1158/0008-5472.CAN-07-5480
- Shanker, M., Willcutts, D., Roth, J. A., & Ramesh, R. (2010). Drug resistance in lung cancer. *Lung Cancer (Auckland, N.Z.)*, 1, 23-36.
- Shibue, T., & Weinberg, R. A. (2017). EMT, CSCs, and drug resistance: the mechanistic link and clinical implications. *Nature reviews. Clinical oncology*, 14(10), 611-629. doi:10.1038/nrclinonc.2017.44
- Shih, J. Y., & Yang, P. C. (2011). The EMT regulator slug and lung carcinogenesis. *Carcinogenesis*, 32(9), 1299-1304. doi:10.1093/carcin/bgr110

- Sia, D., Alsinet, C., Newell, P., & Villanueva, A. (2014). VEGF signaling in cancer treatment. *Curr Pharm Des*, 20(17), 2834-2842.
- Siegel, R. L., Miller, K. D., & Jemal, A. (2018). Cancer statistics, 2018. *CA Cancer J Clin*, 68(1), 7-30. doi:10.3322/caac.21442
- Singh, C. K., George, J., & Ahmad, N. (2013). Resveratrol-based combinatorial strategies for cancer management. *Annals of the New York Academy of Sciences*, 1290(1), 113-121. doi:10.1111/nyas.12160
- Singh, S., Trevino, J., Bora-Singhal, N., Coppola, D., Haura, E., Altiok, S., & Chellappan, S. P. (2012). EGFR/Src/Akt signaling modulates Sox2 expression and self-renewal of stem-like side-population cells in non-small cell lung cancer. *Mol Cancer*, 11, 73. doi:10.1186/1476-4598-11-73
- Son, H., & Moon, A. (2010). Epithelial-mesenchymal Transition and Cell Invasion. *Toxicological Research*, 26(4), 245-252. doi:10.5487/TR.2010.26.4.245
- Song, J.-X., Shaw, P.-C., Wong, N.-S., Sze, C.-W., Yao, X.-S., Tang, C.-W., . . . Zhang, Y.-B. (2012). Chrysotoxine, a novel bibenzyl compound selectively antagonizes MPP+, but not rotenone, neurotoxicity in dopaminergic SH-SY5Y cells. *Neuroscience Letters*, 521(1), 76-81. doi:<https://doi.org/10.1016/j.neulet.2012.05.063>
- Song, J. X., Shaw, P. C., Sze, C. W., Tong, Y., Yao, X. S., Ng, T. B., & Zhang, Y. B. (2010). Chrysotoxine, a novel bibenzyl compound, inhibits 6-hydroxydopamine induced

- apoptosis in SH-SY5Y cells via mitochondria protection and NF-kappaB modulation. *Neurochem Int*, 57(6), 676-689. doi:10.1016/j.neuint.2010.08.007
- Suzuki, E., Chiba, T., Zen, Y., Miyagi, S., Tada, M., Kanai, F., . . . Yokosuka, O. (2012). Aldehyde dehydrogenase 1 is associated with recurrence-free survival but not stem cell-like properties in hepatocellular carcinoma. *Hepatol Res*, 42(11), 1100-1111. doi:10.1111/j.1872-034X.2012.01028.x
- Taddei, M. L., Giannoni, E., Fiaschi, T., & Chiarugi, P. (2012). Anoikis: an emerging hallmark in health and diseases. *J Pathol*, 226(2), 380-393. doi:10.1002/path.3000
- Templeton, A. K., Miyamoto, S., Babu, A., Munshi, A., & Ramesh, R. (2014). Cancer stem cells: progress and challenges in lung cancer. *Stem Cell Investig*, 1, 9. doi:10.3978/j.issn.2306-9759.2014.03.06
- Thakur, B., & Ray, P. (2017). Cisplatin triggers cancer stem cell enrichment in platinum-resistant cells through NF-kappaB-TNFalpha-PIK3CA loop. *J Exp Clin Cancer Res*, 36(1), 164. doi:10.1186/s13046-017-0636-8
- Thomas, S. M., & Brugge, J. S. (1997). Cellular functions regulated by Src family kinases. *Annu Rev Cell Dev Biol*, 13, 513-609. doi:10.1146/annurev.cellbio.13.1.513
- Tian, Y., Jia, X., Wang, S., Li, Y., Zhao, P., Cai, D., . . . Dong, M. (2014). SOX2 oncogenes amplified and operate to activate AKT signaling in gastric cancer and predict immunotherapy responsiveness. *J Cancer Res Clin Oncol*, 140(7), 1117-1124. doi:10.1007/s00432-014-1660-0

- Turkson, J., Bowman, T., Garcia, R., Caldenhoven, E., De Groot, R. P., & Jove, R. (1998). Stat3 activation by Src induces specific gene regulation and is required for cell transformation. *Mol Cell Biol*, 18(5), 2545-2552. doi:10.1128/mcb.18.5.2545
- Tyryshkin, A., Gorgun, F. M., Abdel Fattah, E., Mazumdar, T., Pandit, L., Zeng, S., & Eissa, N. T. (2010). Src kinase-mediated phosphorylation stabilizes inducible nitric-oxide synthase in normal cells and cancer cells. *J Biol Chem*, 285(1), 784-792. doi:10.1074/jbc.M109.055038
- Vachon, P. H. (2011). Integrin signaling, cell survival, and anoikis: distinctions, differences, and differentiation. *Journal of signal transduction*, 2011, 738137-738137. doi:10.1155/2011/738137
- Vinogradov, S., & Wei, X. (2012). Cancer stem cells and drug resistance: the potential of nanomedicine. *Nanomedicine (Lond)*, 7(4), 597-615. doi:10.2217/nnm.12.22
- Voulgari, A., & Pintzas, A. (2009). Epithelial-mesenchymal transition in cancer metastasis: mechanisms, markers and strategies to overcome drug resistance in the clinic. *Biochim Biophys Acta*, 1796(2), 75-90. doi:10.1016/j.bbcan.2009.03.002
- Wang, L., Liu, X., Ren, Y., Zhang, J., Chen, J., Zhou, W., . . . Wu, C. (2017). Cisplatin-enriching cancer stem cells confer multidrug resistance in non-small cell lung cancer via enhancing TRIB1/HDAC activity. *Cell Death Dis*, 8(4), e2746. doi:10.1038/cddis.2016.409

- Wang, Y., Shi, J., Chai, K., Ying, X., & Zhou, B. P. (2013). The Role of Snail in EMT and Tumorigenesis. *Curr Cancer Drug Targets*, 13(9), 963-972.
- Wee, B., Pietras, A., Ozawa, T., Bazzoli, E., Podlaha, O., Antczak, C., . . . Holland, E. C. (2016). ABCG2 regulates self-renewal and stem cell marker expression but not tumorigenicity or radiation resistance of glioma cells. 6, 25956. doi:10.1038/srep25956  
<https://www.nature.com/articles/srep25956#supplementary-information>
- Weina, K., & Utikal, J. (2014). SOX2 and cancer: current research and its implications in the clinic. *Clinical and Translational Medicine*, 3, 19-19. doi:10.1186/2001-1326-3-19
- Xu, Y., So, C., Lam, H. M., Fung, M. C., & Tsang, S. Y. (2018). Apoptosis Reversal Promotes Cancer Stem Cell-Like Cell Formation. *Neoplasia*, 20(3), 295-303. doi:10.1016/j.neo.2018.01.005
- Yewale, C., Baradia, D., Vhora, I., Patil, S., & Misra, A. (2013). Epidermal growth factor receptor targeting in cancer: A review of trends and strategies. *Biomaterials*, 34(34), 8690-8707. doi:<https://doi.org/10.1016/j.biomaterials.2013.07.100>
- Yilmaz, M., & Christofori, G. (2009). EMT, the cytoskeleton, and cancer cell invasion. *Cancer Metastasis Rev*, 28(1-2), 15-33. doi:10.1007/s10555-008-9169-0
- Yu, Y., Ramena, G., & Elble, R. C. (2012). The role of cancer stem cells in relapse of solid tumors. *Front Biosci (Elite Ed)*, 4, 1528-1541.

- Zakaria, N., Satar, N. A., Abu Halim, N. H., Ngalim, S. H., Yusoff, N. M., Lin, J., & Yahaya, B. H. (2017). Targeting Lung Cancer Stem Cells: Research and Clinical Impacts. *Frontiers in oncology*, 7, 80-80. doi:10.3389/fonc.2017.00080
- Zhang, J., Kalyankrishna, S., Wislez, M., Thilaganathan, N., Saigal, B., Wei, W., . . . Kurie, J. M. (2007). SRC-family kinases are activated in non-small cell lung cancer and promote the survival of epidermal growth factor receptor-dependent cell lines. *Am J Pathol*, 170(1), 366-376. doi:10.2353/ajpath.2007.060706
- Zhang, S., Wang, Y., Chen, Z., Kim, S., Iqbal, S., Chi, A., . . . Wu, D. (2013). Genistein enhances the efficacy of cabazitaxel chemotherapy in metastatic castration-resistant prostate cancer cells. *Prostate*, 73(15), 1681-1689. doi:10.1002/pros.22705
- Zhang, Y., Wang, Z., Yu, J., Shi, J., Wang, C., Fu, W., . . . Yang, J. (2012). Cancer stem-like cells contribute to cisplatin resistance and progression in bladder cancer. *Cancer Lett*, 322(1), 70-77. doi:10.1016/j.canlet.2012.02.010



จุฬาลงกรณ์มหาวิทยาลัย  
**CHULALONGKORN UNIVERSITY**

## VITA

NAME	นฤมล ภูมมาพันธุ์
DATE OF BIRTH	22 กันยายน 2529
PLACE OF BIRTH	จังหวัดสุโขทัย
INSTITUTIONS ATTENDED	<p>- 2015 – Present Ph.d. candidate of Philosophy Program in Biomedical Sciences (International Program), Graduate School, Chulalongkorn University, Bangkok, Thailand GPA: 4.00</p> <p>- 2009 - 2012 Master of Science (Toxicology) (International Program), Faculty of Science, Mahidol University, Bangkok, Thailand GPA: 3.54</p> <p>- 2004 - 2008 Bachelor of Science (Medical Technology), Thammasat University, Pathumthani, Thailand GPA: 2.89</p> <p>- 2000 - 2003 High School Diploma, Sawanananwittaya School, Sukhothai, Thailand Major: Science - Mathematics GPA: 3.7</p>
HOME ADDRESS	5/32 คอนโดชาโตว์อินทาวน์ 14-2 ซอยพหลโยธิน 14 ถนนพหลโยธิน แขวงสามเสนใน เขตพญาไท กรุงเทพมหานคร 10400
PUBLICATION	<ol style="list-style-type: none"><li>1. Bhummaphan N, Chanvorachote P. Gigantol Suppresses Cancer Stem Cell-Like Phenotypes in Lung Cancer Cells %J Evidence-Based Complementary and Alternative Medicine. 2015;2015:10.</li><li>2. Bhummaphan N, Pongrakhananon V, Sritularak B, Chanvorachote P. Cancer Stem Cell-Suppressing Activity of Chrysotoxine, a Bibenzyl from Dendrobium pulchellum. The Journal of pharmacology and experimental therapeutics. 2018;364(2):332-46.</li><li>3. Petpiroon N, Bhummaphan N, Tungsukruthai S, Pinkhien T, Maiuthed A, Sritularak B, et al. Chrysotobibenzyl inhibition of lung cancer cell migration through Caveolin-1-dependent mediation of the integrin switch and the sensitization of lung cancer cells to cisplatin-mediated apoptosis. Phytomedicine : international journal of phytotherapy and phytopharmacology. 2019;58:152888.</li></ol>



4. Bhummaphan N, Petpiroon N, Prakhongcheep O, Sritularak B, Chanvorachote P. Lusianthridin targeting of lung cancer stem cells via Src-STAT3 suppression. *Phytomedicine : international journal of phytotherapy and phytopharmacology*. 2019;62:152932.
5. Maiuthed A, Bhummaphan N, Luanpitpong S, Mutirangura A, Apornawan C, Meeprasert A, et al. Nitric oxide promotes cancer cell dedifferentiation by disrupting an Oct4:caveolin-1 complex: A new regulatory mechanism for cancer stem cell formation. *J Biol Chem*. 2018;293(35):13534-52.
6. Pin-On P, Apornawan C, Siriluksana J, Bhummaphan N, Chanvorachote P, Mutirangura A. Targeting high transcriptional control activity of long mononucleotide A-T repeats in cancer by Argonaute 1. *Gene*. 2019;699:54-61.
7. Petpiroon N, Bhummaphan N, Soonnarong R, Chantarawong W, Maluangnont T, Pongrakhananon V, et al. TiO<sub>2</sub> Nanosheets Inhibit Lung Cancer Stem Cells by Inducing Production of Superoxide Anion. *Molecular pharmacology*. 2019;95(4):418-32.
8. Bhukhai K, Suksen K, Bhummaphan N, Janjorn K, Thongon N, Tantikanlayaporn D, et al. A phytoestrogen diarylheptanoid mediates estrogen receptor/Akt/glycogen synthase kinase 3beta protein-dependent activation of the Wnt/beta-catenin signaling pathway. *J Biol Chem*. 2012;287(43):36168-78.

AWARD RECEIVED

Award of Excellent prize outstanding Oral Presentation: The Honorable  
Mention of Merck Young Scientist Award, 2015, Thailand

จุฬาลงกรณ์มหาวิทยาลัย  
CHULALONGKORN UNIVERSITY